UNITED STATES DEPARTMENT OF THE INTERIOR

GEOLOGICAL SURVEY

Geotechnical characterization and mass-movement potential of the United States Mid-Atlantic Continental Slope and Rise

by

James S. Booth[1], Ronald C. Circé[1], and Alfred G. Dahl[1]

Open-File Report 85-351

Prepared in cooperation with the
U.S. Bureau of Land Management
under Memorandum of Understanding
AA851-MU0-18
and Interagency Agreements
AA851-IA1-17 and AA851-IA2-26

1. Woods Hole, Massachusetts 02543

1985

Contents

Illustrations

Tables

INTRODUCTION

Mapping of the United States continental margin by geophysical means has revealed diverse and widespread evidence of mass movement. However, the spatial distribution of these slope failures, as well as their frequencies, types, and magnitudes, varies considerably. Questions thus arise concerning future mass movements on different parts of the margin, particularly the slope and rise, and on the causes of these events. These questions can be addressed by determining the properties of the sediments and the stresses which are acting on or within them. This report represents an initial attempt at such an investigation: it presents the results of geotechnical studies and slope-stability analysis of a portion of the Mid-Atlantic Continental Slope and Rise (fig. 1). Specifically, our objective was to (1) establish the current stability of the slope and rise, and (2) establish the geologic conditions which may promote slope failures in this general setting.

Because knowledge of the geotechnical properties of sediments is one of the chief prerequisites for understanding the various aspects of mass movement, these properties formed the primary data base for the investigation. Because the geotechnical data also serve to describe the engineering characteristics of the sediment, such a description is also included in this report.

Present geologic setting

Surficial geologic processes, such as mass movement, are closely associated with geologic setting. And from both regional and localized studies the geologic setting has been examined thoroughly (e.g., Emery and Uchupi, 1972; Embley and Jacobi, 1977; McGregor, 1977; Knebel and Carson, 1979; McGregor and others, 1979). In particular, Robb and others (1981) have described the area shown in figure 1 in detail. The description which follows is largely taken from their work.

The study area is morphologically complex. From Carteret Canyon to South Toms Canyon it is highly dissected by numerous canyons and similar, often related features; southwest of Carteret Canyon the slope is likewise dissected, but to a much lesser degree. Regional gradients can be relatively high (~7°), and slope angles of 10°–25° are common in canyon areas. Some parts of the Quaternary section are 450 m thick near the top of the slope, but the section, which is most conspicuous as a part of lobate intercanyon ridges, thins rapidly downslope and is often absent in the lower reaches of canyon axes. Tertiary material crops out on the lower slope and in some canyons, but Quaternary sediments generally blanket the upper Continental Rise.

The Holocene/Pleistocene surface sediments are predominantly clastic silty clays and clayey silts (Doyle and others, 1979; Keller and others, 1979), although some parts of the upper slope are covered with a thin layer of sand derived from the adjacent shelf. Vertical variations in sand percentages and discrete sand lenses have been found in some cores (Doyle and others, 1979), however, implying a complex depositional history. Hathaway and others (1979) report that silty clays and clayey silts predominate most of the Quaternary section, as determined from Atlantic Margin Coring Project (AMCOR) borings in the upper 300 m of sediment. Sedimentation rates for the Pleistocene/Holocene probably average a few tens of centimeters per 1,000 years (Emery and Uchupi, 1972; Poag, 1980).

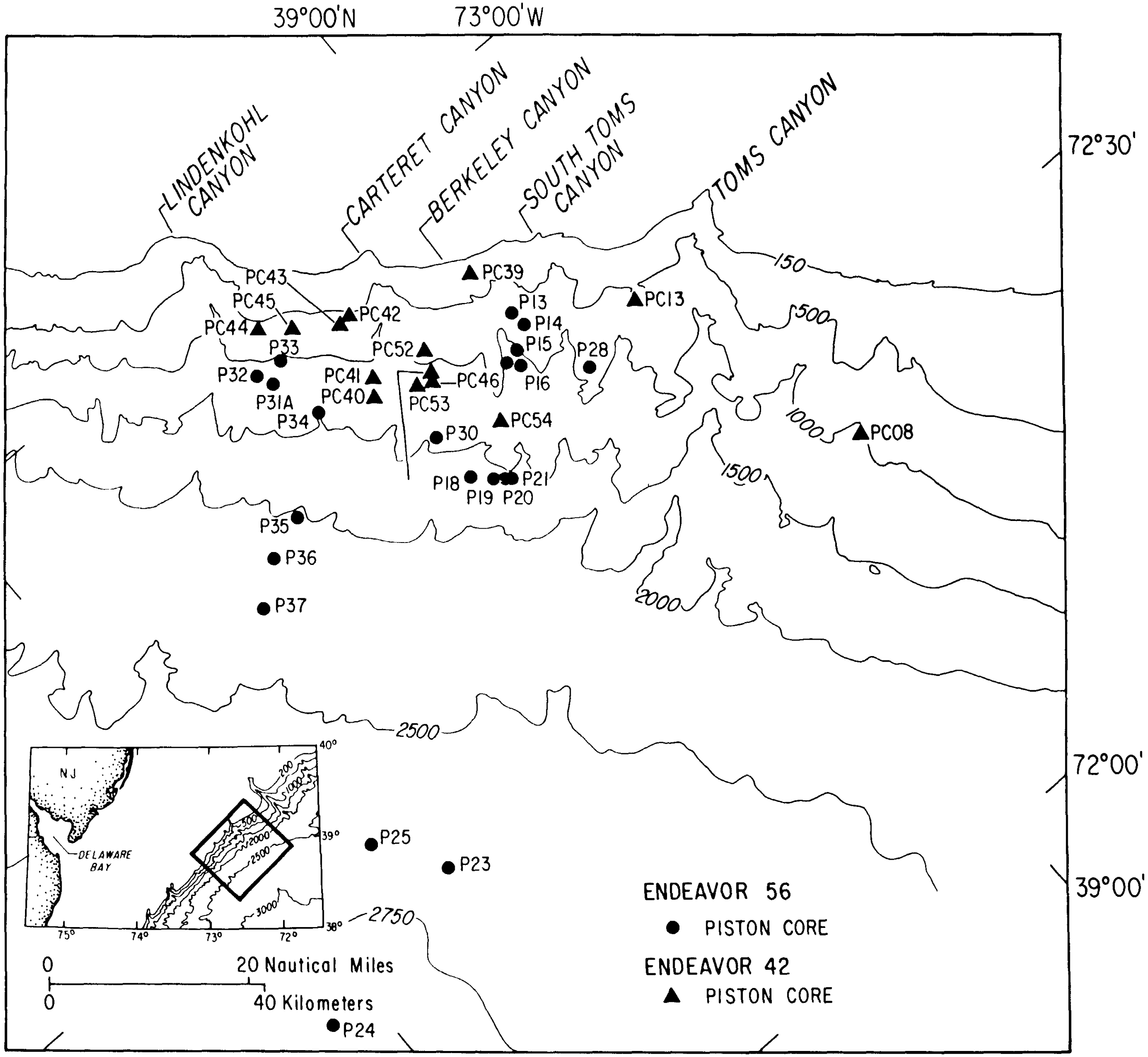

Figure 1. Piston-core station locations.

Few current measurements have been made on the slope or rise in the Mid-Atlantic region. The Western Boundary Undercurrent is known to impinge on the margin, however. A measurement made by Keller and Shepard (1978) at midslope between Washington and Baltimore Canyons (i.e., southwest of the study area) indicates that currents in that area may be below the threshold of grain movement. These authors also suggest that currents generated by tides or internal waves may be responsible for some of the oscillatory currents measured in canyons.

The area of investigation may experience the effects of an occasional earthquake, although seismic activity is generally low on the U.S. east coast. Emery and Uchupi (1972) state that most of the continental margin appears to be aseismic. A summary of historical data by Sykes (1978) shows that several minor earthquakes have occurred onshore, but that none of significant magnitude has occurred proximal to the study area. Recently emplaced seismic nets in the northeastern United States are showing, however, that earthquake activity does occur on the margin and that magnitudes (m_b) of 2 to 4 are common (Yang and Aggarwal, 1981).

Also a part of the geologic setting are the agents or properties that exist within a sediment section which may influence the mechanical stability. Gas, artesian pressure, and organic matter are examples. On the upper part of the Mid-Atlantic slope, high-resolution seismic-reflection profiles indicate that some sediment may be gas charged (Hall and Ensminger, 1979), and significant quantities of methane were measured in AMCOR Hole 6021 (Hathaway and others, 1979), which was drilled in the northeast corner of the study area. It is not known if artesian pressure exists in the area. Robb and others (1984) have demonstrated, however, that the possibility should be investigated. A relatively high organic content can influence slope stability, and the oxygen (O_2) minimum layer, which promotes anomalously high organic content in sediment, intercepts the slope at approximately 300 m (Emery and Uchupi, 1972). Assuming the bathymetric position of the O_2 minimum fluctuated in accordance with sea level, then the slope sediments laid down in recent geologic time between the 300- and 500-m isobaths were or may be organic rich.

Evidence of past movement

Evidence of mass movement within the study area (fig. 1) is sparse. Robb and others (1981) have determined that only 1.3% of the Continental Slope surface has identifiable slide deposits. The addition of other evidence, such as rubble fields, possible debris flows, and possible scarps (but eliminating the numerous canyons and similar features *per se* from consideration in order to be consistent with Robb and others (1981)), would only increase the figure by a few percent. In contrast, a massive slide has been identified to the southwest near Wilmington Canyon by McGregor (1977), and other investigators (e.g., Embley and Jacobi, 1977; Knebel and Carson, 1979; Malahoff and others, 1980) have reported evidence of other mass movements to the southwest. To the northeast of the study area, Keer and Cardinell (1981) have identified what may be *en echelon* slumping near Hudson Canyon.

Previous slope-stability analyses and geotechnical investigations

Previous geotechnical investigations have addressed the slope-stability question and, as research continues, are providing an increasingly accurate description of the engineering properties of the slope and rise sediments. As a part of the first stage of this overall study, Booth and others (1981a) applied the infinite-slope model of stability analysis (drained, static case) and determined that the sediments were generally stable on that basis. On a set of cores collected on the upper slope, Olsen and others (1982) applied a similar analysis, but added undrained stability analysis to the evaluation. Their results indicated general stability for drained cases, but some sites, particularly those on valley walls, are unstable when classified in terms of undrained analysis. The infinite-slope model was also used by Keller and others (1979) in a more general investigation of the U.S. Atlantic Continental Slope. General stability was also implied by their results. Sangrey and Marks (1981) figured ground accelerations into the infinite-slope model and showed, using data from AMCOR 6021, that earthquakes may cause instability in the area. They also concluded, however, that the slope was generally stable. In an initial investigation of canyons in the study area, Booth and others (1981b) applied Bishop's Simplified Method of Slices and Wedge Analysis to assess mass-movement potential and determined that many sidewalls and headwalls of canyons in the study area may be metastable.

In addition to the slope-stability analyses, the aforementioned works provided data pertinent to a geotechnical description of the area. Studies by McGregor and others (1979) and Lambert and others (1981) have also added significantly to the geotechnical data base. In aggregate, these previous investigations have shown that the Quaternary sediments, particularly in the upper few meters, tend to be soft, highly plastic, and normally consolidated to lightly overconsolidated. Water contents typically exceed the liquid limit in the surface material, and sensitivities may be slightly greater than the norm. In general, the geotechnical properties of the slope sediment are in accord with those expected for fine-grained sediment.

This report will add to the geotechnical data base, particularly on the lower slope and upper rise, and will provide a more comprehensive view of slope stability within the study area.

METHODS

Shipboard

Sampling/analytical

The piston cores used for the geotechnical aspect of the study were collected aboard the R/V ENDEAVOR in August 1979 and October 1980. The coring system was modified from the conventional design in order to obtain cores with minimal mechanical disturbance because many geotechnical properties, especially those related to strength, are vulnerable to the effects of disturbance. Details of the modifications are presented in Booth and others (1981a). Thirty-three cores up to approximately 10-m long were recovered during the two cruises in the area. Figure 1 shows the locations of these cores and table I shows the station data.

Table I

Station Data

Mid-Atlantic Piston Cores

Core	Latitude (N.)	Longitude (W.)	Water depth (m)	Core length (m)
PC08	39°07.21'	72°24.82'	1,180	5.85
PC13	39°03.22'	72°40.83'	556	5.32
PC39	38°57.94'	72°49.40'	246	0.95
PC40	38°50.26'	72°48.08'	1,113	7.08
PC41	38°50.93'	72°48.08'	1,123	4.54
PC43	38°51.37'	72°52.18'	622	9.42
PC44	38°48.11'	72°55.42'	575	4.50
PC45	38°49.52'	72°54.03'	688	6.97
PC46	38°52.49'	72°46.53'	930	7.05
PC51	38°53.25'	72°46.13	1,103	0.30
PC52	38°53.25'	72°47.37'	813	6.73
PC53	38°52.32'	72°46.00'	1,035	10.06
PC54	38°54.13'	72°40.75'	1,145	8.58
P13	38°58.32'	72°45.98'	710	2.77
P14	38°58.39'	72°44.34'	685	6.30
P15	38°57.35'	72°43.71'	950	6.30
P16	38°56.95'	72°42.61'	1.045	6.06
P17	38°56.43'	72°43.15'	1,195	2.72
P18	38°51.35'	72°39.54'	1,600	5.64
P19	38°52.09'	72°38.45'	1,475	7.25
P20	38°52.49'	72°37.90'	1,500	5.63
P21	38°52.76'	72°26.04'	1,665	1.55
P24	38°28.99'	72°19.16'	2,815	2.19
P25	38°35.41'	72°26.04'	2,665	2.19
P28	38°59.36'	72°39.44'	860	10.68
P30	38°51.34'	72°42.70'	1,335	9.40
P31A	38°46.98'	72°52.11'	1,190	7.30
P32	38°46.65'	72°53.31'	1,090	4.14
P33	38°47.83'	72°52.84'	1,015	6.07
P34	38°47.51'	72°48.77'	1,400	4.22
P35	38°43.45'	72°44.71'	2,000	2.63
P36	38°41.17'	72°43.46'	2,185	6.31
P37	38°39.16'	72°41.80'	2,305	4.96

As was the case during sampling operations, avoiding disturbance was the prime consideration during core processing and storage. Once onboard, the cores were cut into 1.5-m sections by using a tube cutter to sever the liner and a wire saw to part the sediment. Up to three subsections were also cut for later triaxial and consolidation testing. All subsections, which were generally taken from near the bottom portions of the cores, were X-rayed in order to judge the condition of the sample; only apparently undisturbed samples were retained for later testing. Finally, the subsections were capped, taped, sealed with wax, and stored upright at $4^{o}C$ in specially fabricated boxes padded with foam rubber. The remaining core sections were split lengthwise: one part of each section served as the archive half, the other as a "working" half, which was taken to the shipboard laboratory for description, strength testing, and subsampling.

After a cursory description, "undisturbed" undrained shear strength was measured with a four-bladed, 12.7 mm-square laboratory vane at intervals of 0.50 m and at lithologic changes. Obvious sand layers, which are cohesionless and therefore inappropriate for this type of test, were avoided. The blade was inserted normal to the long direction of the core and buried at least 20 mm into the section to be tested. In order to guard against sample drainage during the application of torque, a rotation rate of 0.0262 radians/s (90^{o}/min) was used. This relatively high rate of speed also maximizes measured shear strength and, because of possible detrimental effects of ship motion and vibrations, allows a test to be completed quickly to minimize disturbance. Previous work (e.g., Booth, 1979) has shown that strength reduction due to the release of in situ stresses and mechanical disturbance may generally be kept to less than 30% if care is taken. Remolded strength (strength of thoroughly kneaded sample) was also determined with the vane apparatus. The precision of the vane shear measurements is ±0.30 kiloPascals (kPa).

Subsamples for index-property testing were taken at the points of strength measurements, placed in plastic bags, and sealed in cans for later laboratory testing. These subsamples and samples taken for triaxial and consolidation testing were transported to the laboratory in a refrigerated ($4^{o}C$) van.

Laboratory

Index Properties

The suite of geotechnical index property tests (water content, liquid and plastic limits, and grain-specific gravity) was conducted according to procedures recommended by The American Society for Testing and Materials (1982), with two exceptions; grain-specific gravity was measured with an air comparison pycnometer and all water-content data were corrected for salt content. Precisions were: water content ±3% (relative); liquid limit, ±3% (absolute); plastic limit, ±2% (absolute), and grain-specific gravity, ±1% (relative). Derived from this basic data set were plasticity index, liquidity index, bulk density, and porosity.

In addition, results of textural and mineralogical analyses were made available by L. J. Poppe (unpub. data, 1980, 1982).

Triaxial Testing

Consolidated undrained triaxial tests with pore-pressure measurements were conducted in accordance with procedures given by Bishop and Henkel (1957). For each set of tests, three or four specimens (depending on availability of suitable material) were cut from the prime core sample, trimmed to a right cylinder (50 mm D. x 100 mm), and placed in triaxial cells. After the specimens were saturated they were consolidated to 0.75 (only if a fourth specimen was available), 1.0, 2.0, and 4.0 times the assumed in situ overburden pressure. When consolidation was complete, the specimens were sheared, generally at a rate of 0.015 mm/min. Data from all phases of the tests, including axial force, specimen length, specimen volume, pore pressure, and time, were logged by an automatic data-acquisition system. From this basic data set, the angle of internal friction with respect to effective stress (ϕ'), cohesion with respect to effective stress (c'), percent strain at failure, and undrained strength to effective overburden stress ratio (S_u/σ'_{vo}) were determined.

Consolidation testing

The constant rate of strain (CRS) method was used for consolidation testing. In this method, a sediment disc 63.5 mm D. x 25-mm-thick is confined in a ring (one-dimensional test) and shortened (consolidated) at a constant rate. The increase in stress is monitored together with the change in length and pore pressure. The strain rate must be slow enough so that effective stress remains equal, or nearly so, to applied stress. Drainage is permitted. Wissa and others (1971) give details of the procedure. Derived from the test are preconsolidation pressure (P_c), which is the maximum past pressure experienced by a sample (Casagrande's (1936) method was used to determine P_c), the coefficient of consolidation (C_v), the compression index (C_c), and the coefficient of permeability (k).

GEOTECHNICAL CHARACTERIZATION

Cohesion

The modern depositional surface of the Mid-Atlantic Continental Slope generally has a very soft consistency: shear strength (S_u) is often less than 5 kilopascals (kPa) in the upper few meters of the sediment column. However, erosional areas, which expose some Pleistocene as well as Tertiary sediments, have strengths approaching 100 kPa. The mean S_u value is 9.5 kPa (table II). This is slightly greater than the reported range in mean S_u values for slope and rise sediments off the northeastern United States from previous studies (see Keller and others, 1979; McGregor and others, 1979; Lambert and others, 1981); however, the cores in this study were longer than those used in previous studies and some erosional areas, which are typified by much higher shear strengths, were purposely sampled. Also shown in table II is the range of cohesion values. Given the area's morphological complexity, the presence of erosional surfaces and other factors, it is obvious that although the mean value is useful for regional characterization, it is not necessarily representative of specific sites.

Based on core-averaged values, there is no apparent relationship between cohesion and water depth: a downslope trend in cohesion is not evident in our

Table II

Cohesion and index property data summary

Property	Number of measurements	Min.	Avg.	Max.
Natural shear strength (kPa)	316	1.0	9.5	90.0
Sensitivity	258	1.0	5.6*	13.8*
Water content (%)	377	26	65.5	131
Bulk density (g/cc)	351	1.41	1.71	2.05
Porosity (%)	350	41	63	78
Liquid limit (%)	370	21	58.1	110
Plastic limit (%)	371	15	23.8	41
Plasticity index (%)	368	6	34.5	76
Liquidity index	368	.4	1.3	4.8
Grain-specific gravity	233	2.59	2.72	2.89

*Because many samples were too weak to measure after remolding, these values are minimums.

data. The correlation coefficent (r) is -0.13 (n=27) (cores recovered from erosional surfaces were excluded from the analysis). It appears, therefore, that local variability in sediment strength may mask more subtle regional trends, if such trends exist. The range in cohesion data and the low r value reinforce the concept that this area has a complicated recent geologic history.

The erosional surfaces are shown clearly in profile, as are strength cutbacks and other cohesion information (figs. 2a-2ee). Cohesion values of cores wth a "PC" prefix represent corrections of previously released values (shear-strength data in Booth and others, 1981a. Abrupt increases in strength within a core (e.g., P20 in fig. 2t; P34 in fig. 2bb) as well as stiff sediment encountered at the top of a core (i.e., sediment surface) are indicative of erosional surfaces. In the latter case, the shortness of the core also reflects the high strength of the material (e.g., P13 in fig. 2m) (note that in some of the short cores shown in fig. 2 the presence of stiff material is not reflected in the profiles - this stiff material was removed and used in triaxial and/or consolidation tests). Relatively high cohesion is found at or near the top of several other cores, but this high strength does not continue downcore: reductions in strength to varying degrees are found beneath the anomalous surface values (e.g., P30, fig. 2x).

In general, the profiles show the expected increase in strength downcore. However, the profiles are not smooth. Significant fluctuations in strength are the norm in many cases. Changes in sand percentage and other lithologic inconsistencies probably contribute to the variability. Other factors, including changes in organic content, bioturbation, and disturbance, may also contribute.

As a final comment on the cohesion data, it must be pointed out that our attempts to characterize trends in the present depositional surface are, to a degree, biased - despite eliminating data from apparent erosional surfaces. Similarly, the mean cohesion value is, to a degree, biased. Obvious constraints are imposed on coring by topography and general sea-floor type, and additional bias is imposed by sample disturbance. Less conspicuous, however, is the effect that corer design and operation have on the data. Any coring system will, as primarily a function of effective mass, impact velocity, cross-sectional area, and surface area of the barrel, be able to penetrate a finite distance in a sediment with a given resistance. Thus, excepting cases where some penetration is achieved even in extremely hard sea floors, the absolute shear strength would tend to be at or less than some fixed value for all material cored by a given coring system. Trend analysis based on resultant data will, of course, be biased to some degree, as will the mean cohesion value. Comparison between studies which used different types of cores must take this effect into account.

Sensitivity

The ratio of natural ("undisturbed") shear strength to remolded shear strength is defined as sensitivity (S_t); it is an indicator of the potential strength loss in a soil due to remolding. Sediments from this study area have a mean S_t of 5.6; their S_t values range from 1 to 13.8 (table II). According to the classification developed by Rosenqvist (1953), these sediments, on average, are very sensitive, and range from insensitive (S_t ~1) to slightly

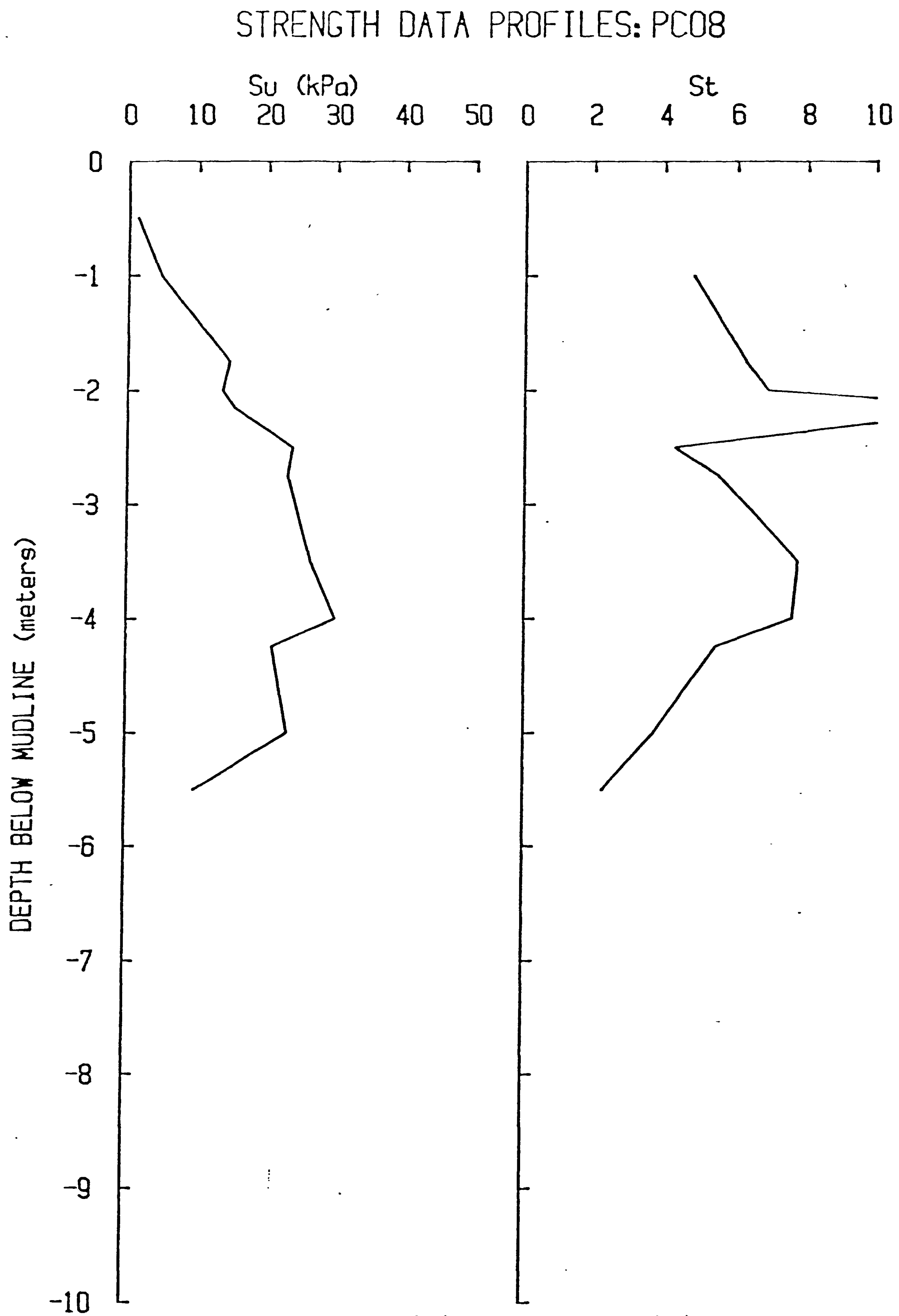

Figure 2a. Cohesion (S_u) and sensitivity (S_t) vs. depth in core.

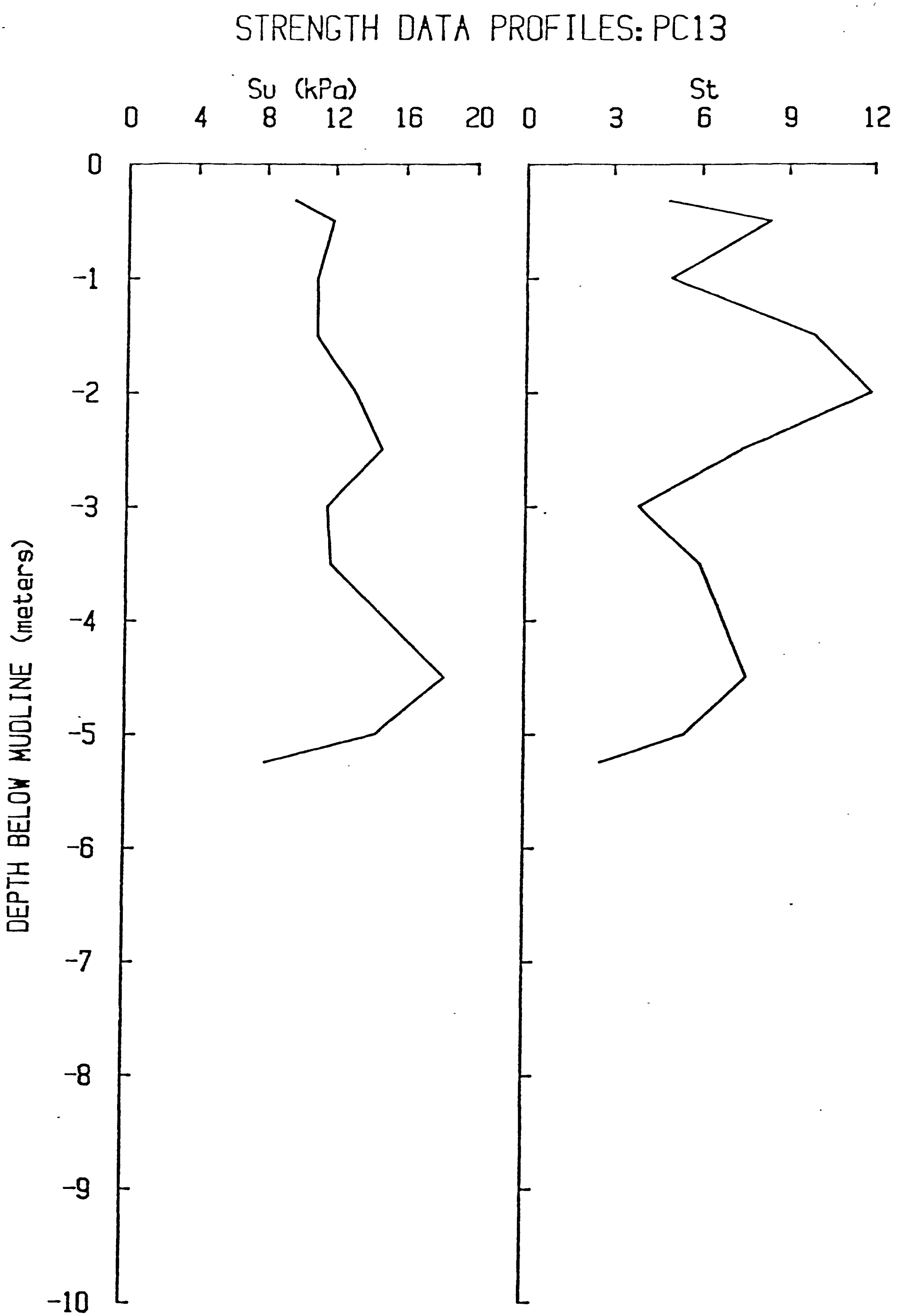

Figure 2b. Cohesion (S_u) and sensitivity (S_t) vs. depth in core.

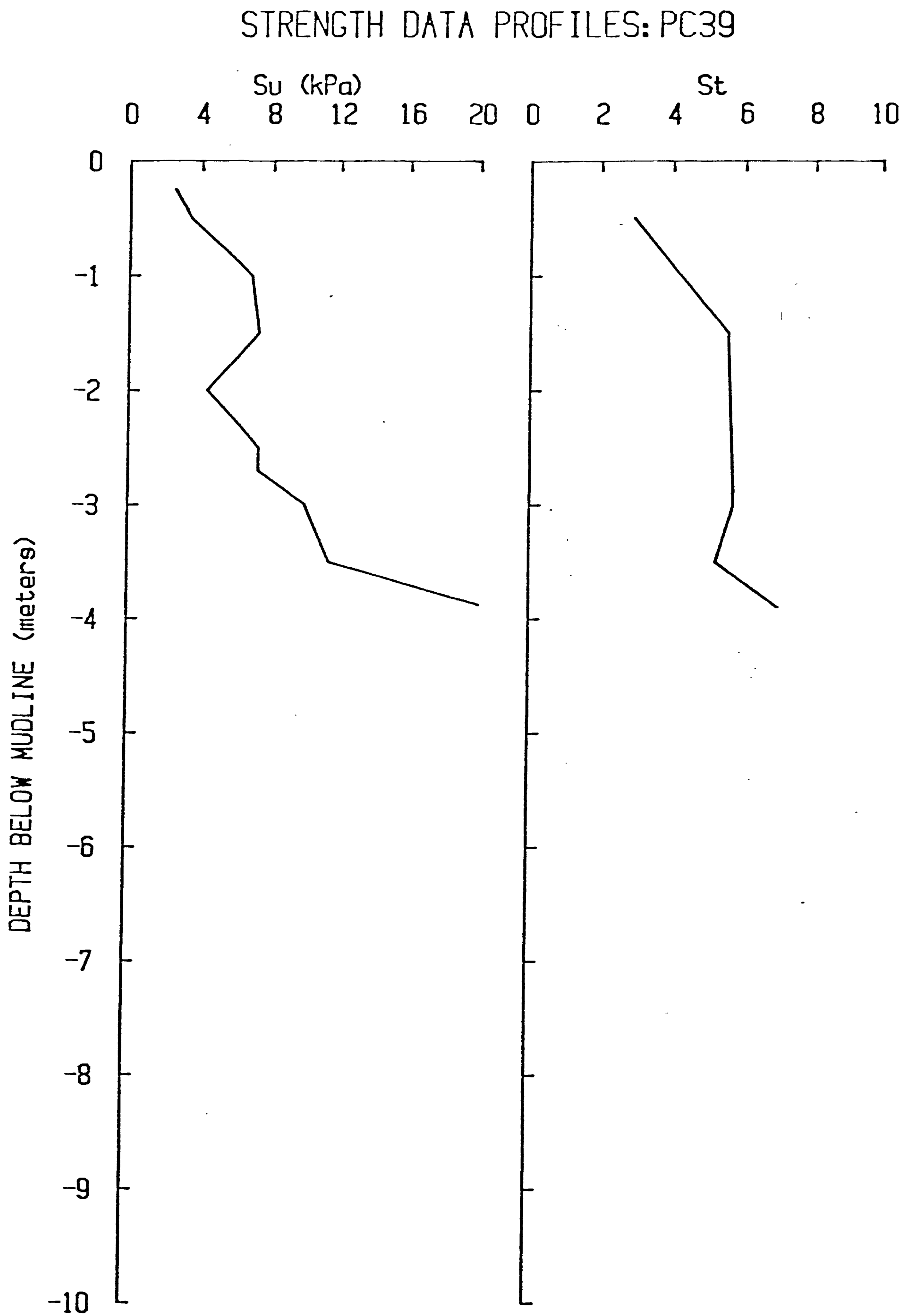

Figure 2c. Cohesion (S_u) and sensitivity (S_t) vs. depth in core.

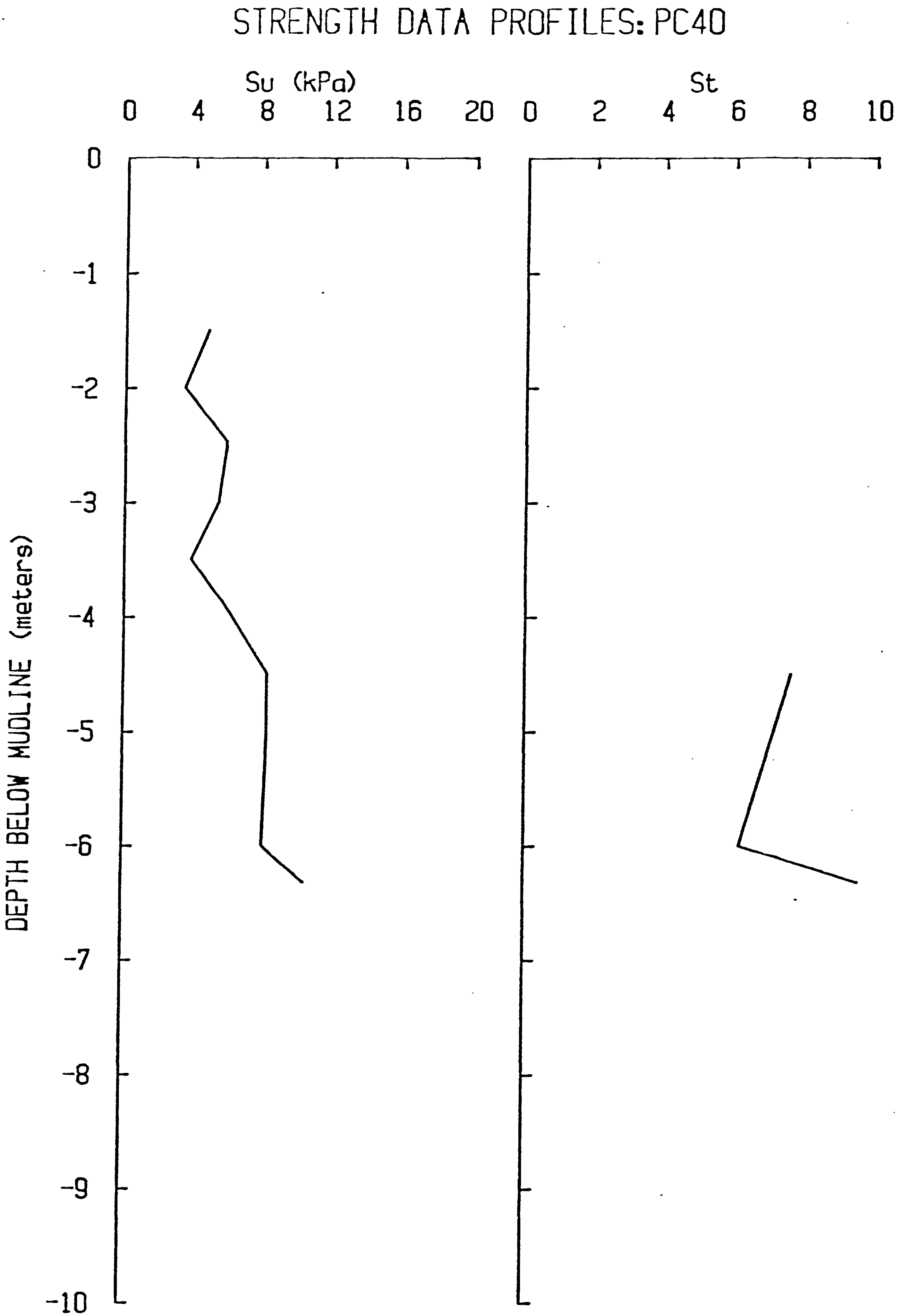

Figure 2d. Cohesion (S_u) and sensitivity (S_t) vs. depth in core.

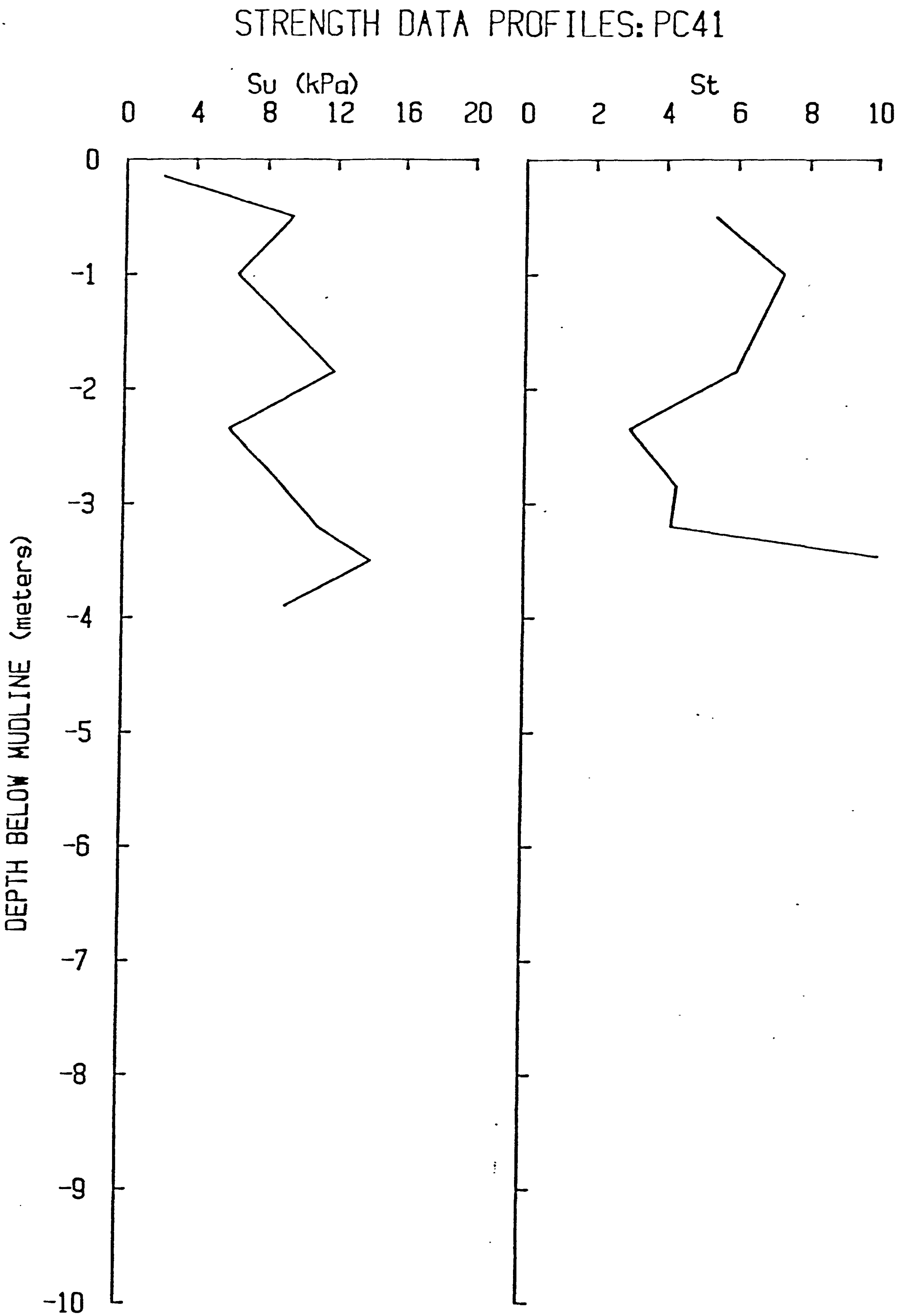

Figure 2e. Cohesion (S_u) and sensitivity (S_t) vs. depth in core.

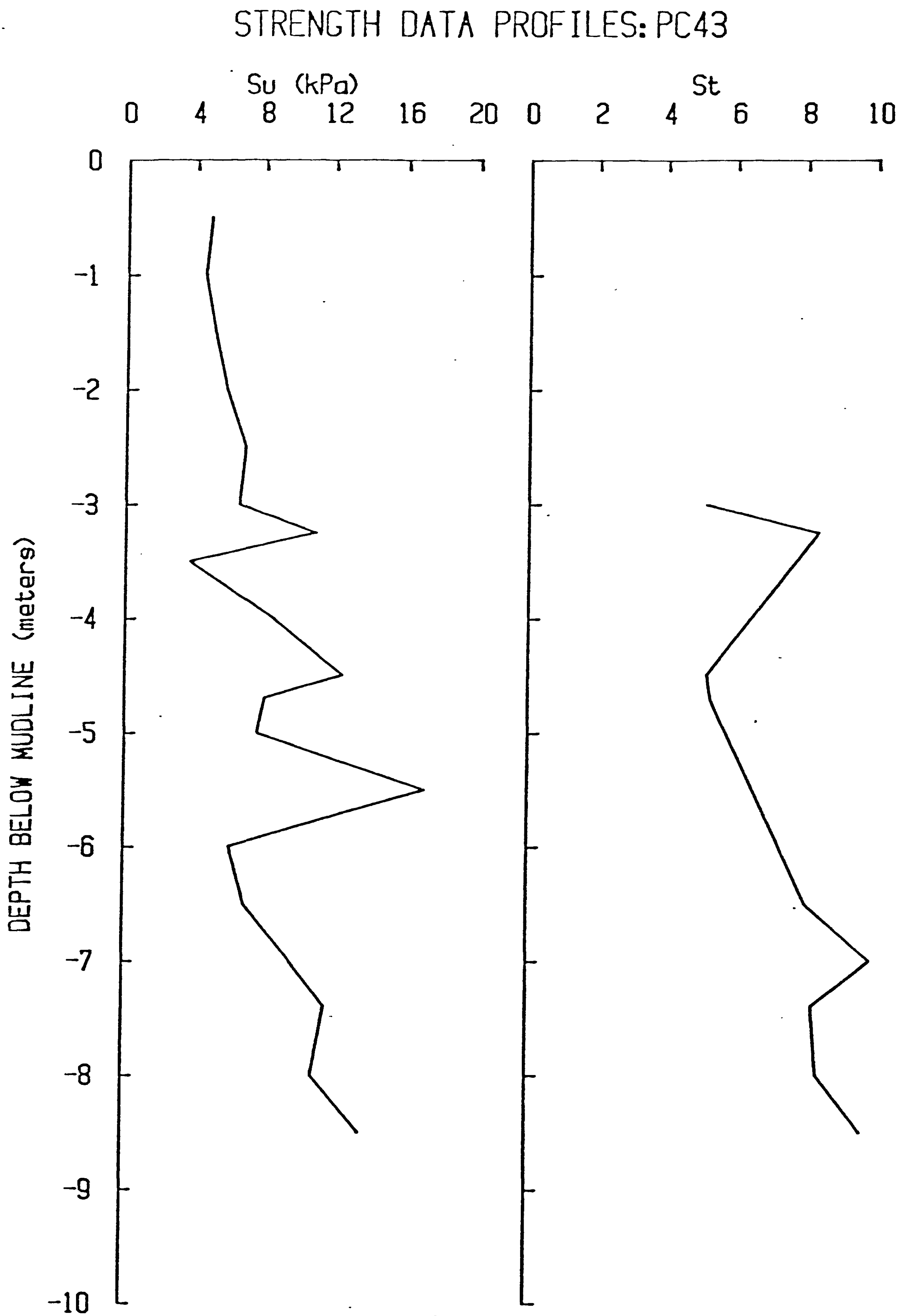

Figure 2f. Cohesion (S_u) and sensitivity (S_t) vs. depth in core.

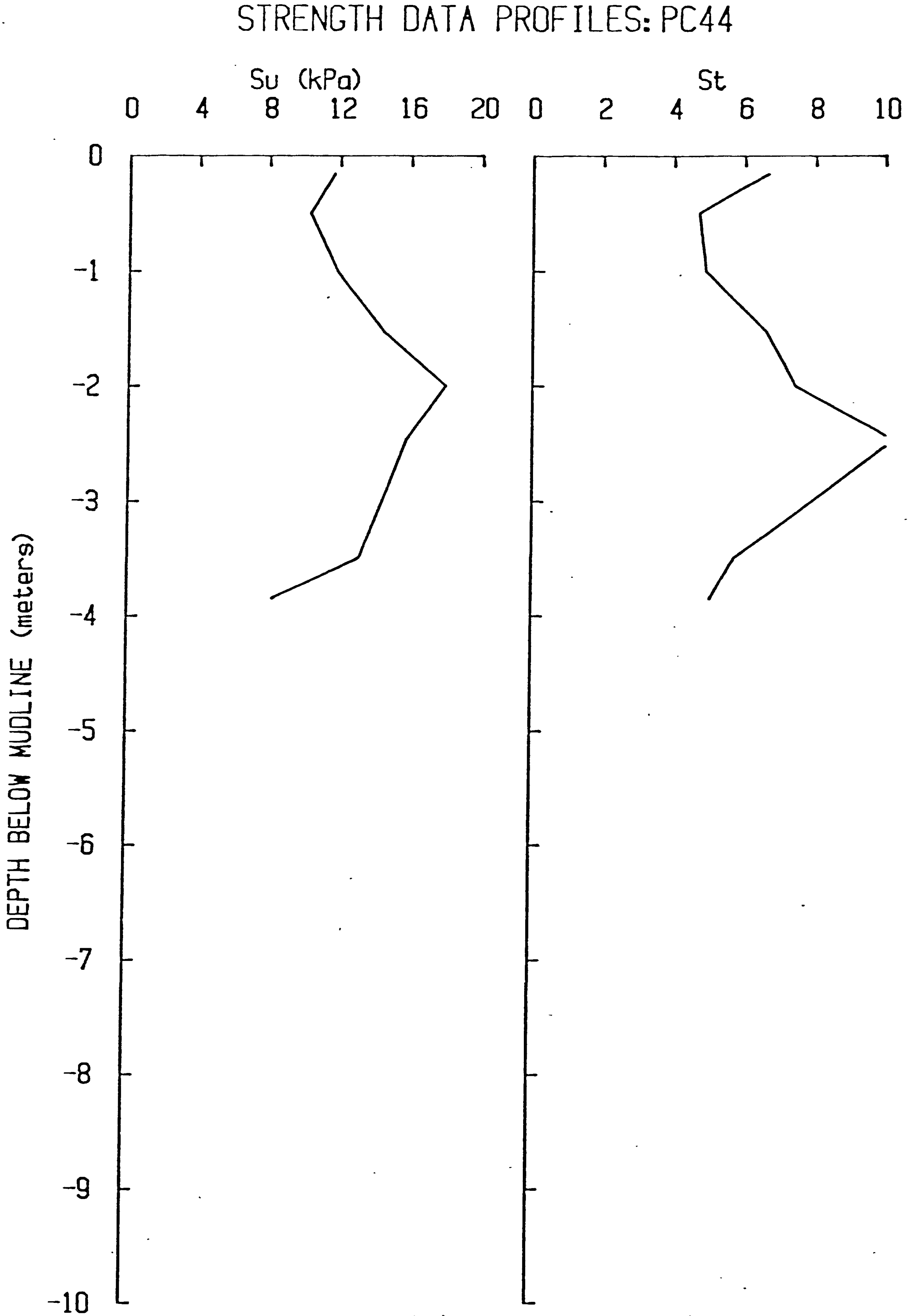

Figure 2g. Cohesion (S_u) and sensitivity (S_t) vs. depth in core.

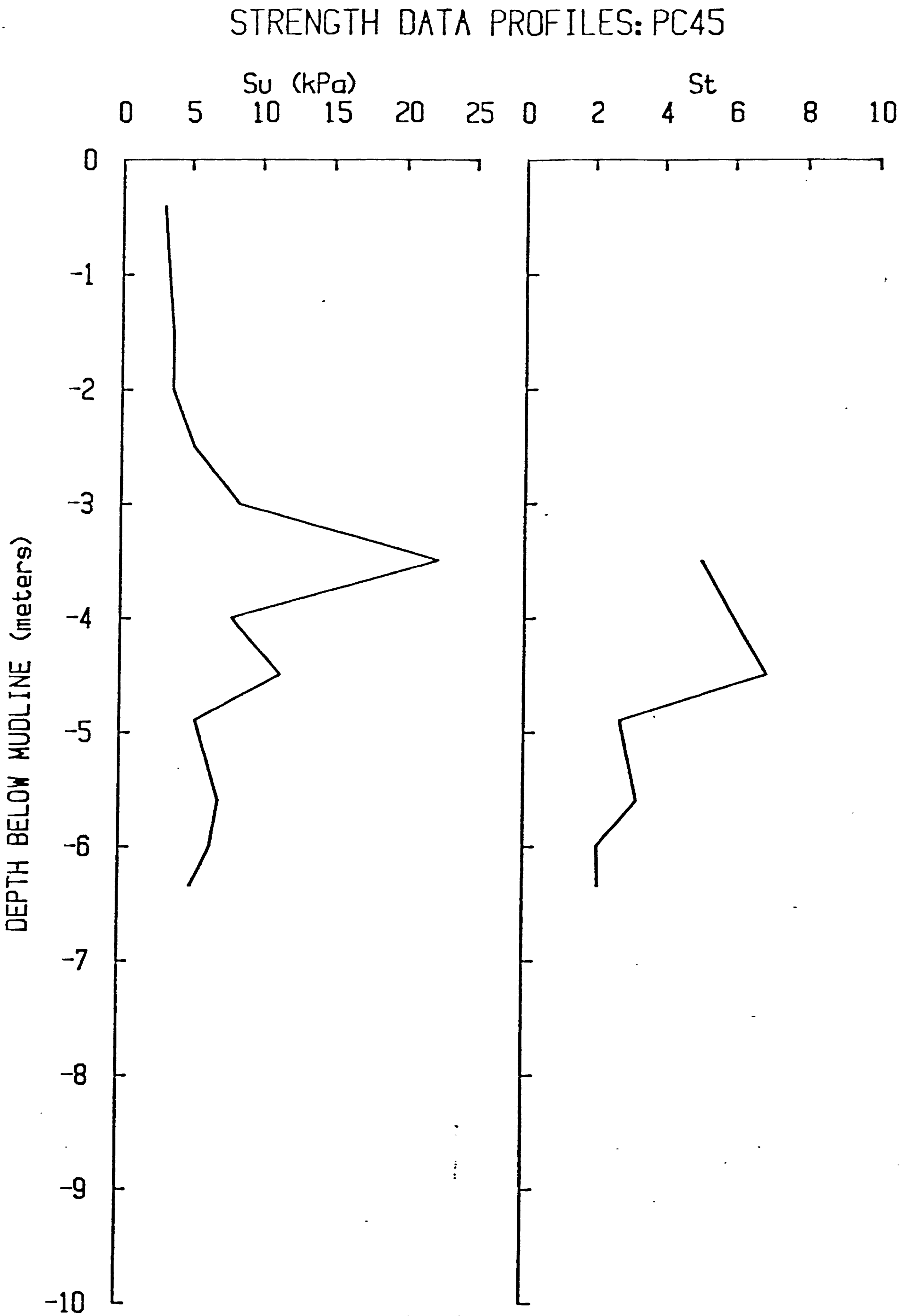

Figure 2h. Cohesion (S_u) and sensitivity (S_t) vs. depth in core.

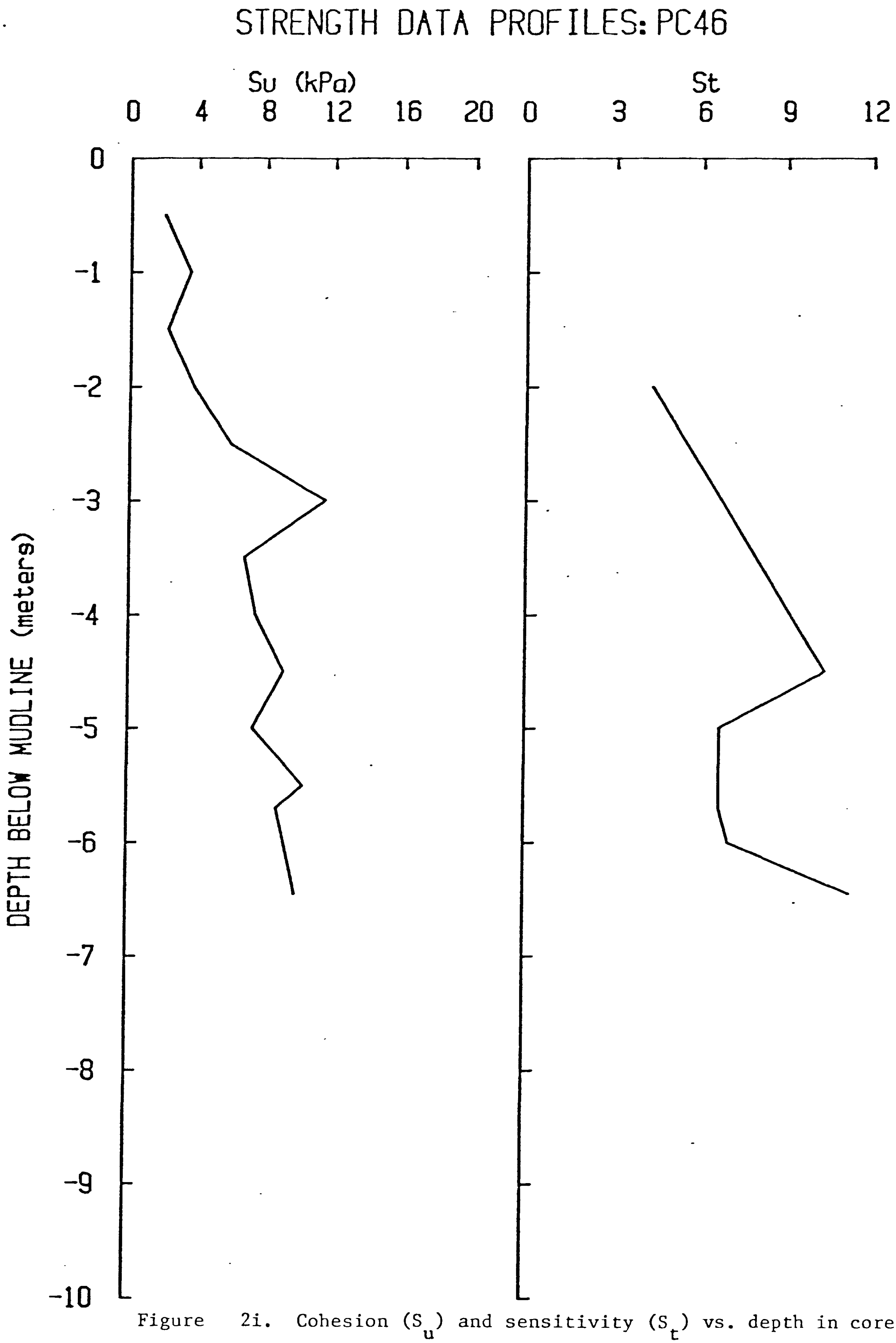

Figure 2i. Cohesion (S_u) and sensitivity (S_t) vs. depth in core.

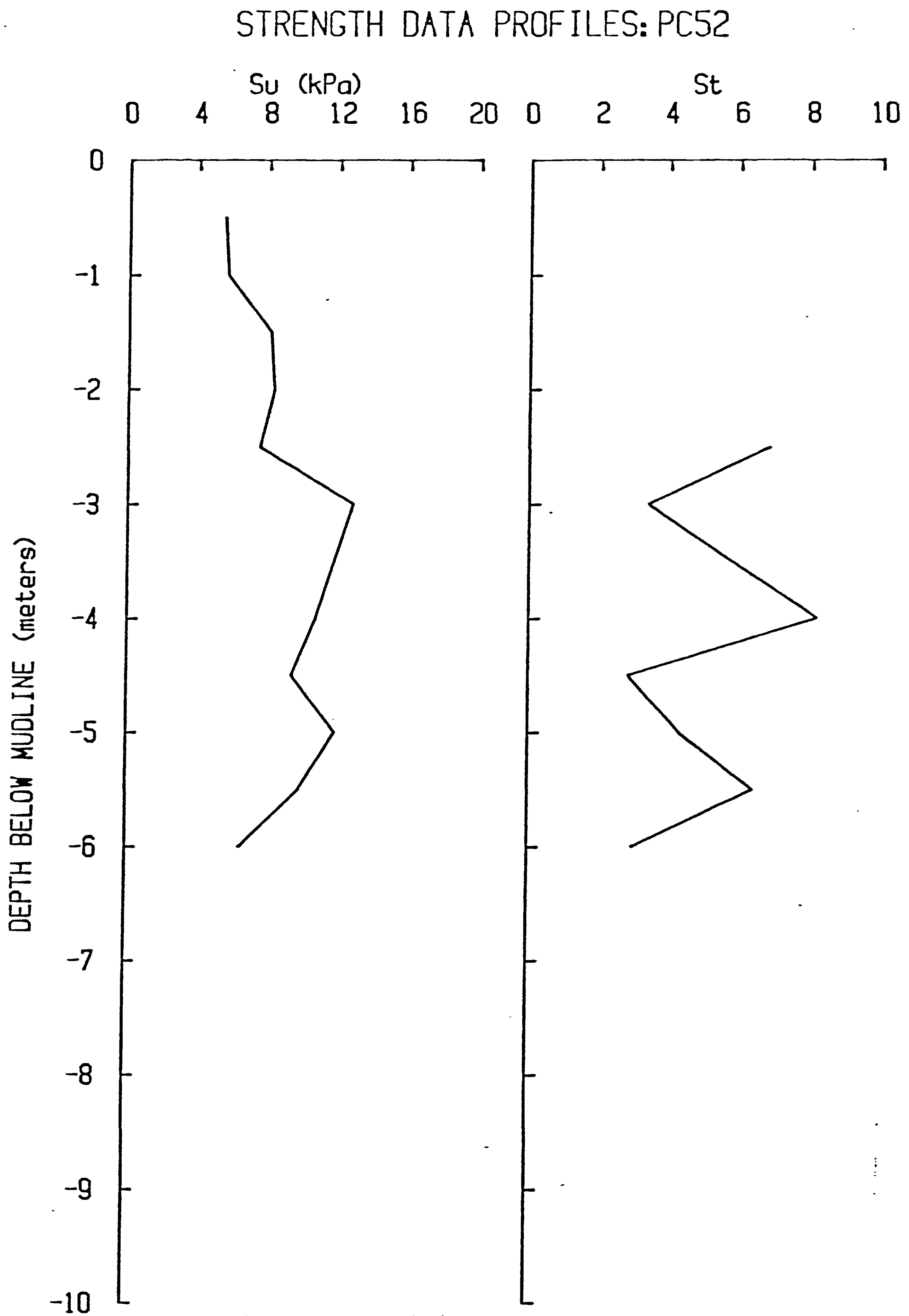

Figure 2j. Cohesion (S_u) and sensitivity (S_t) vs. depth in core.

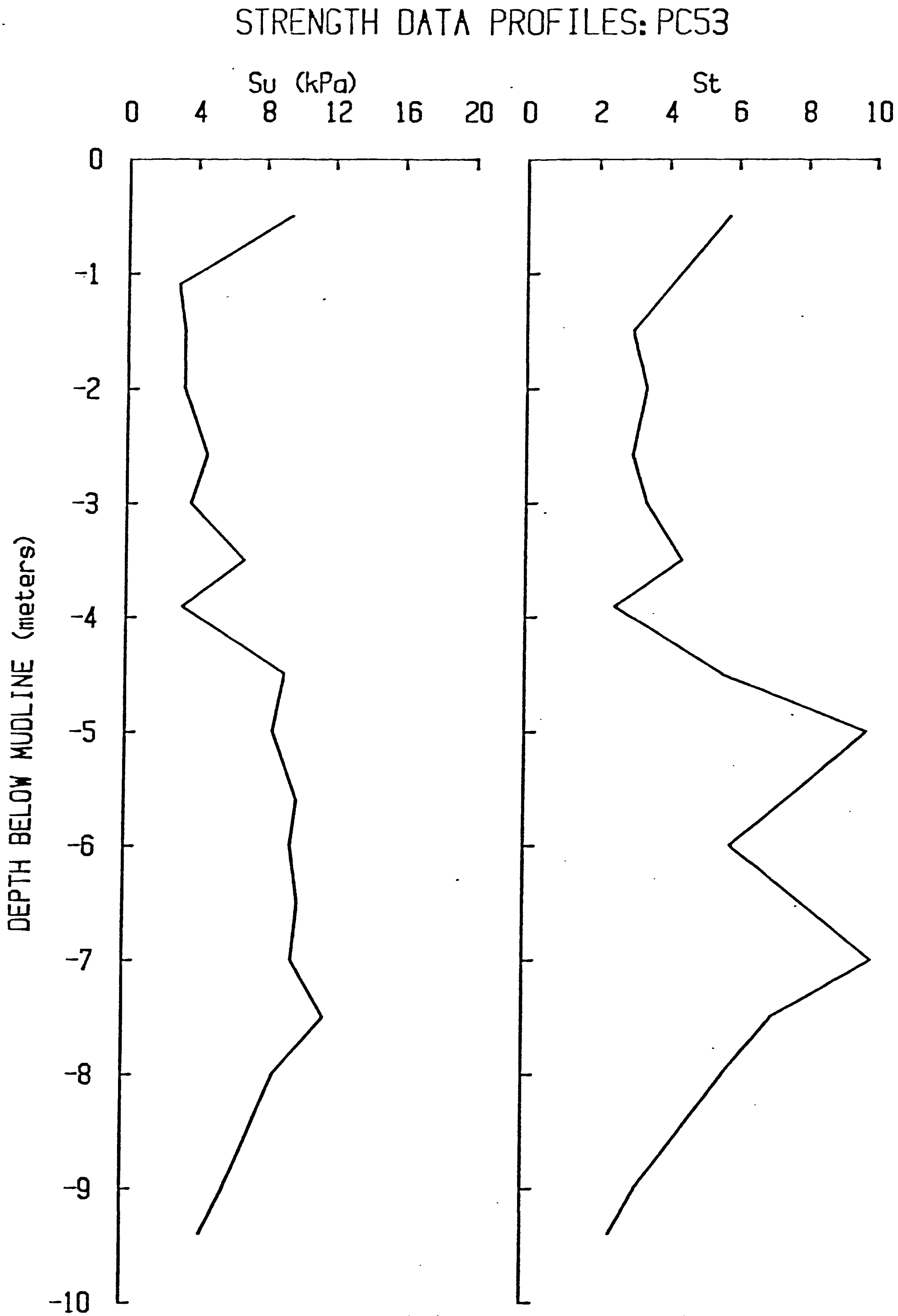

Figure 2k. Cohesion (S_u) and sensitivity (S_t) vs. depth in core.

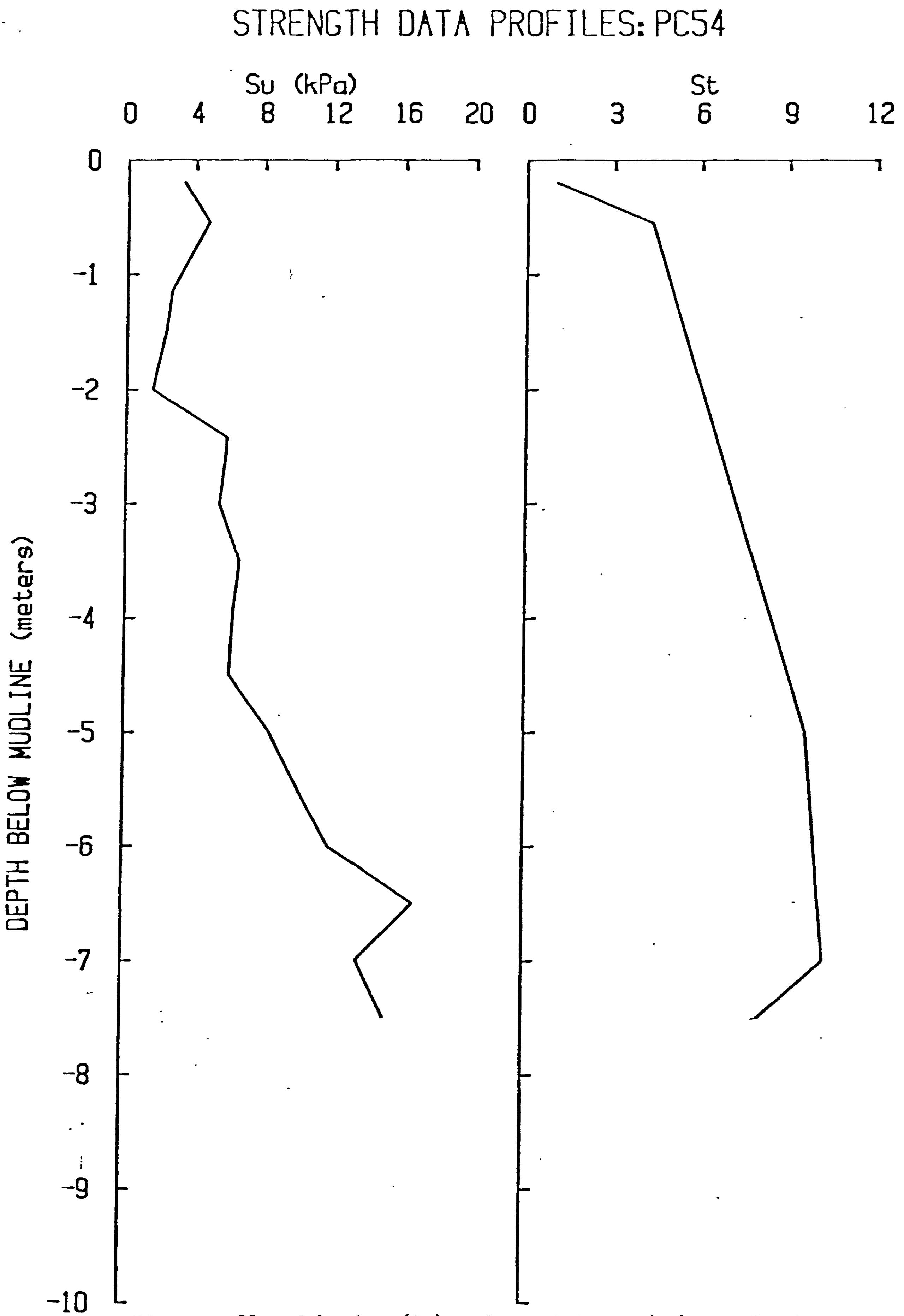

Figure 21. Cohesion (S_u) and sensitivity (S_t) vs. depth in core.

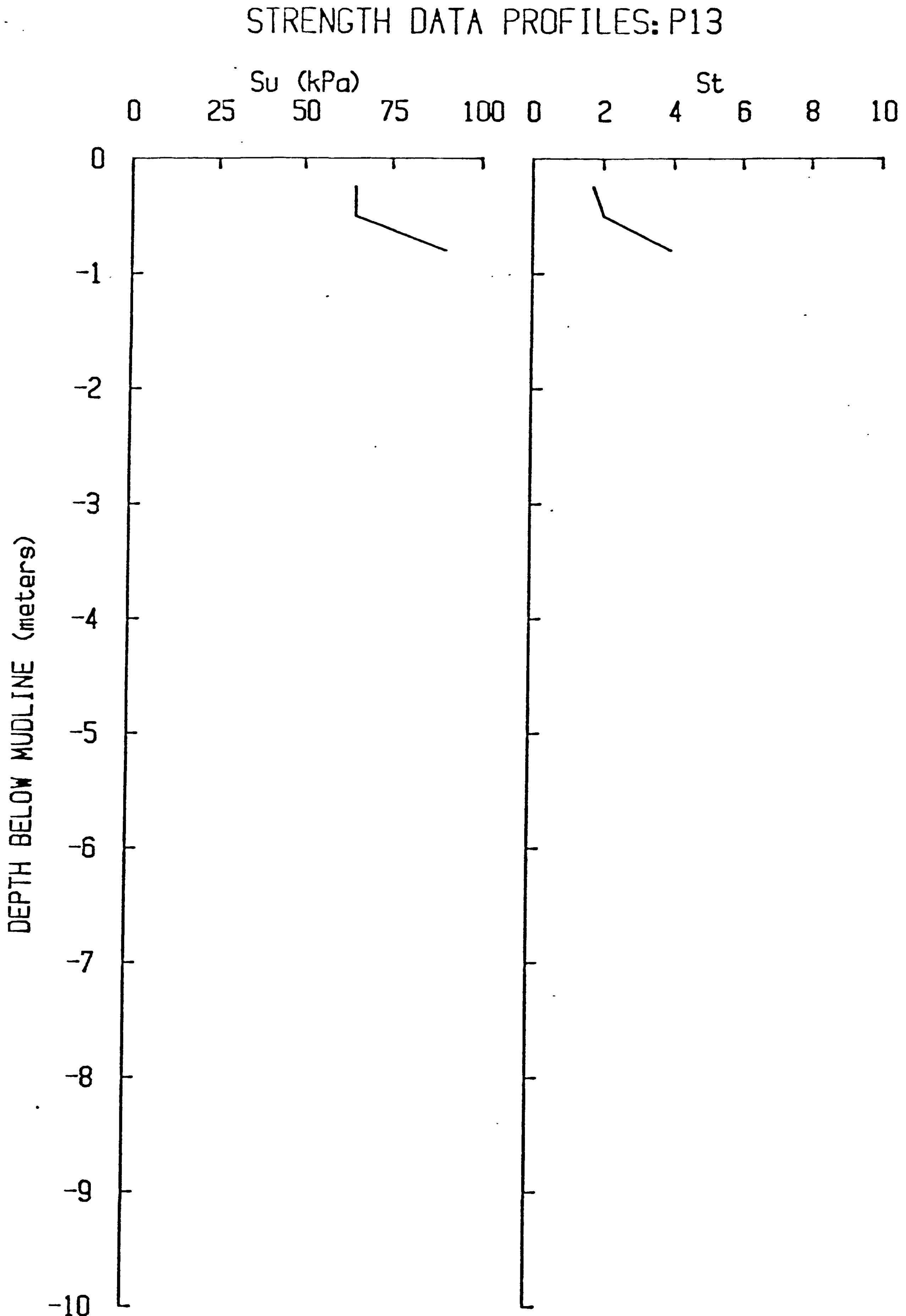

Figure 2m. Cohesion (S_u) and sensitivity (S_t) vs. depth in core.

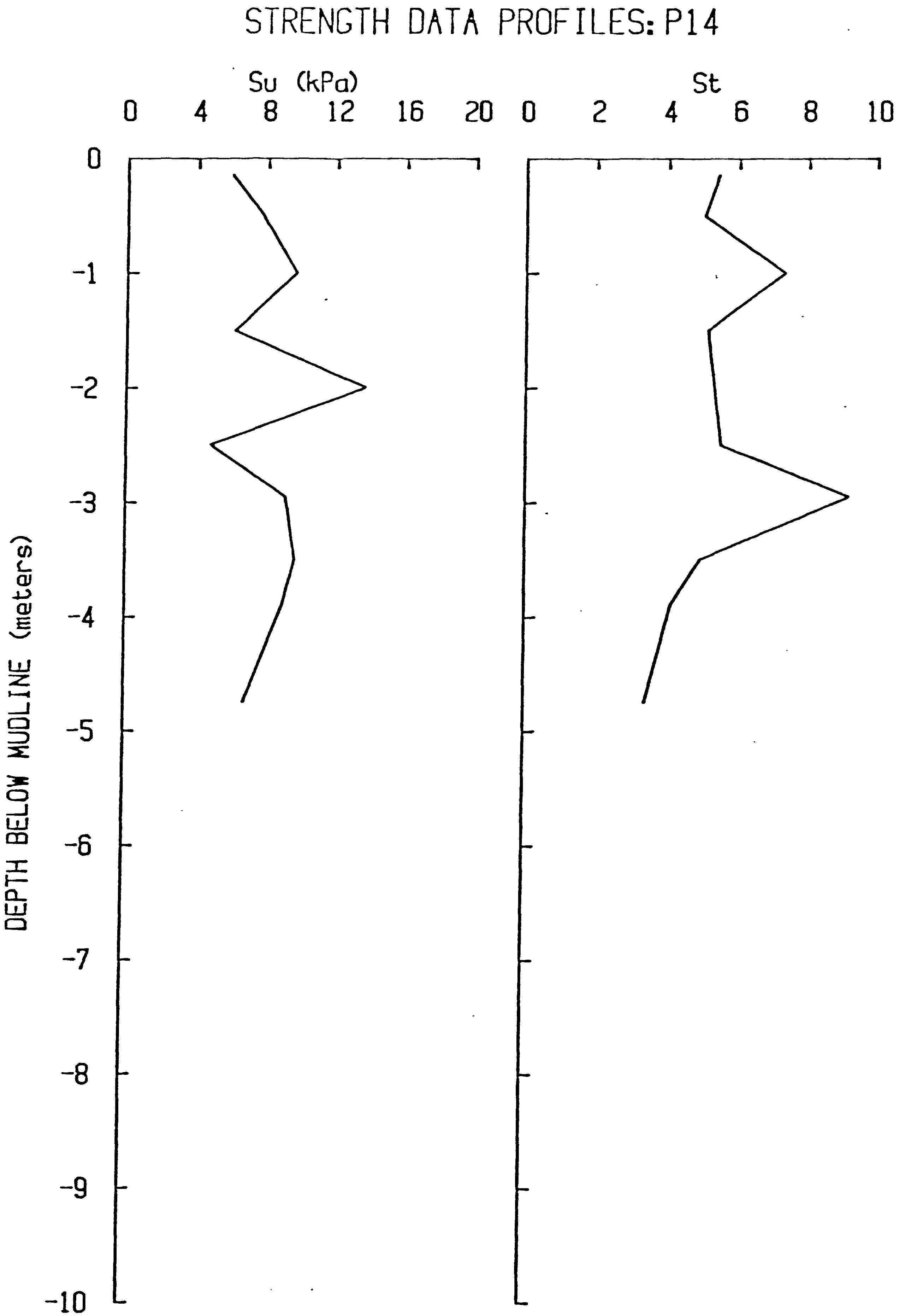

Figure 2n. Cohesion (S_u) and sensitivity (S_t) vs. depth in core.

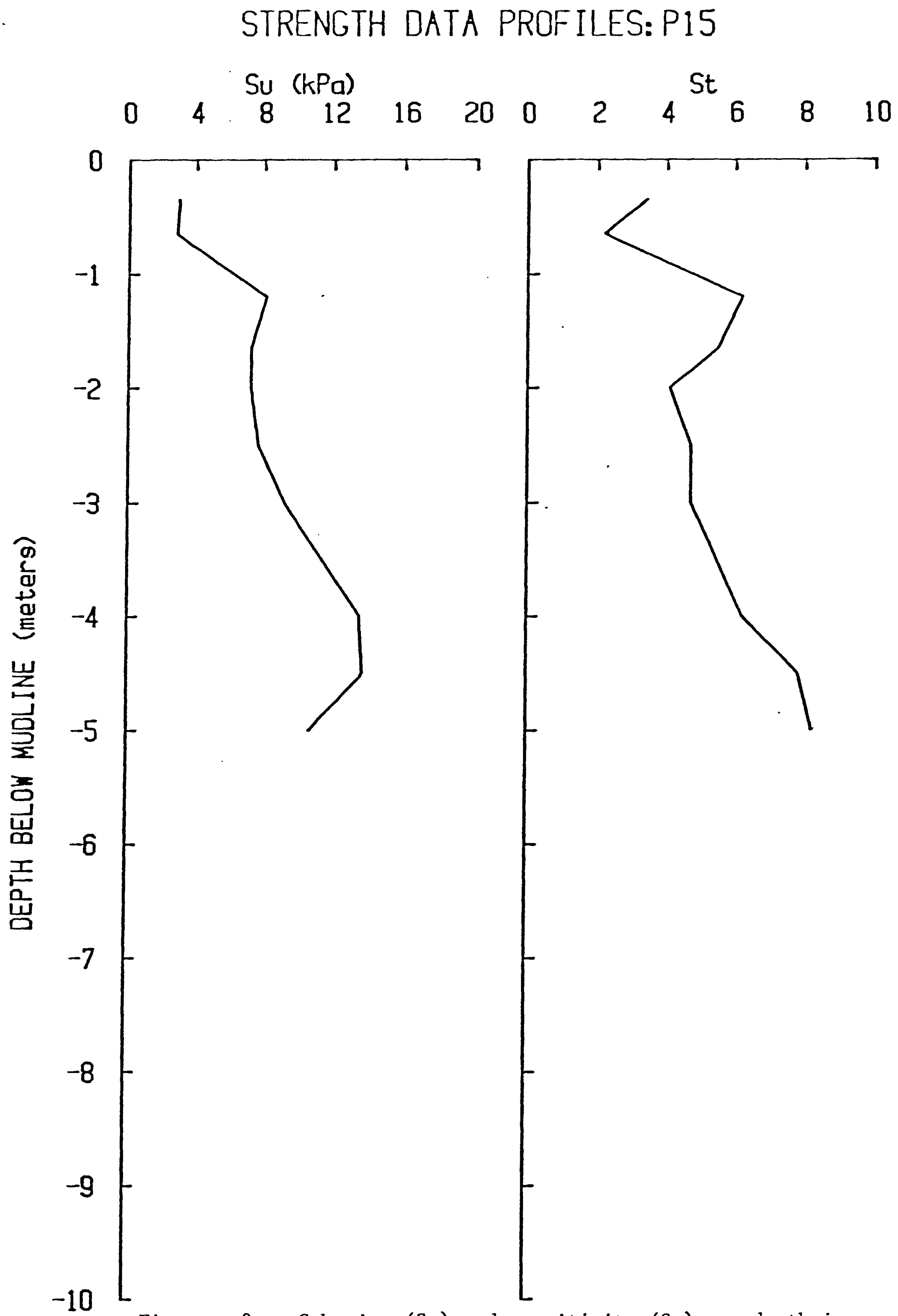

Figure 2o. Cohesion (S_u) and sensitivity (S_t) vs. depth in core.

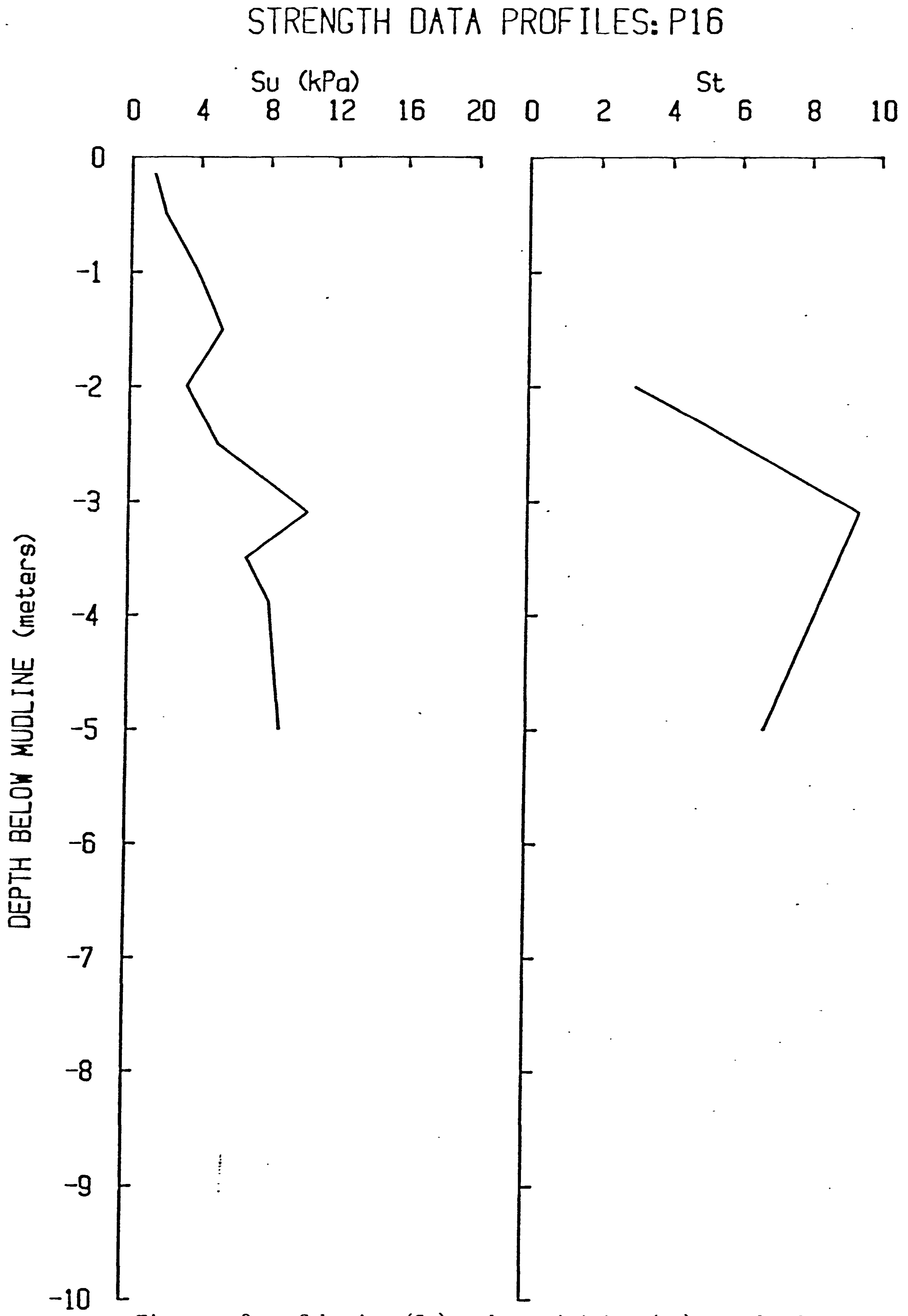

Figure 2p. Cohesion (S_u) and sensitivity (S_t) vs. depth in core.

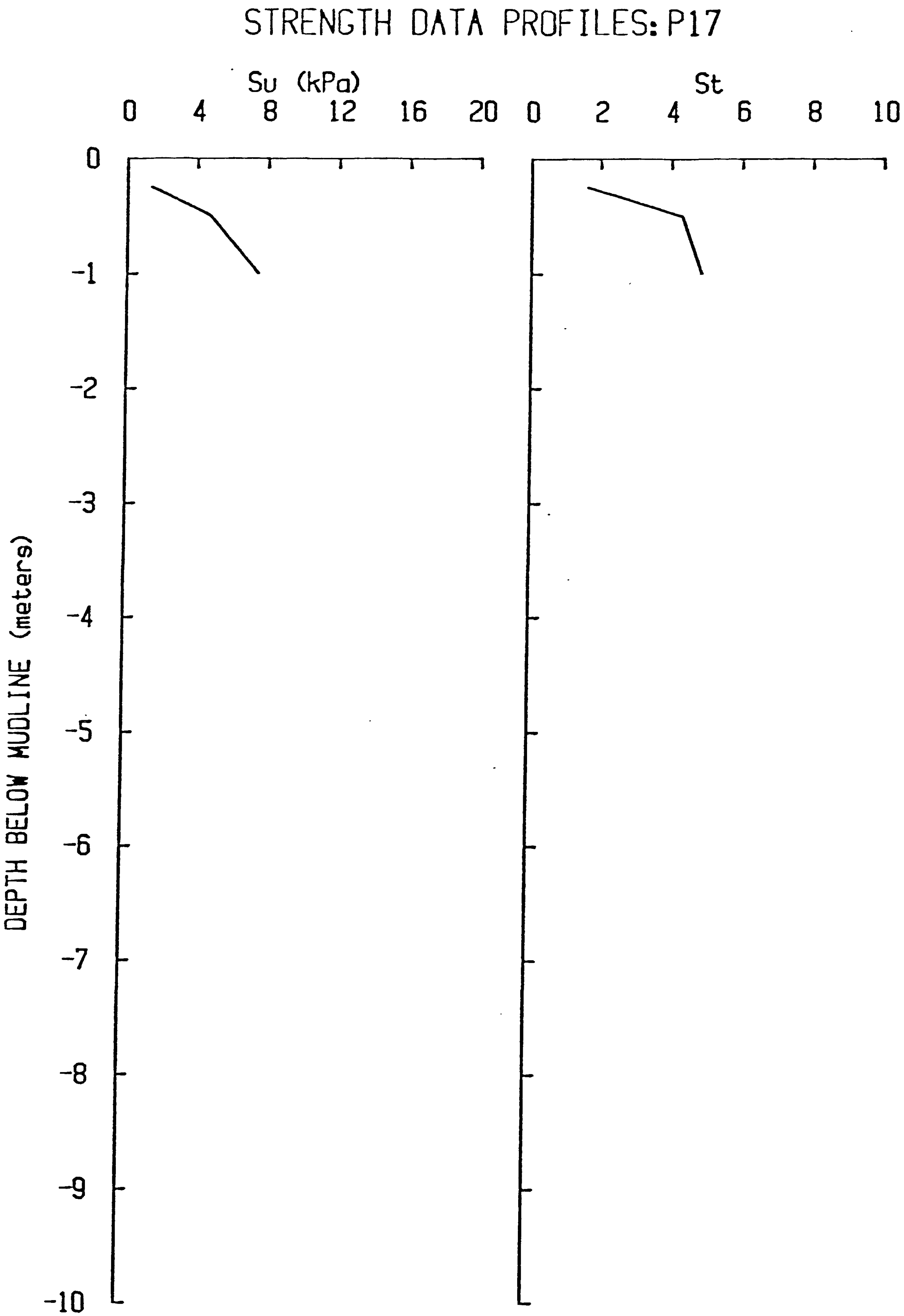

Figure 2q. Cohesion (S_u) and sensitivity (S_t) vs. depth in core.

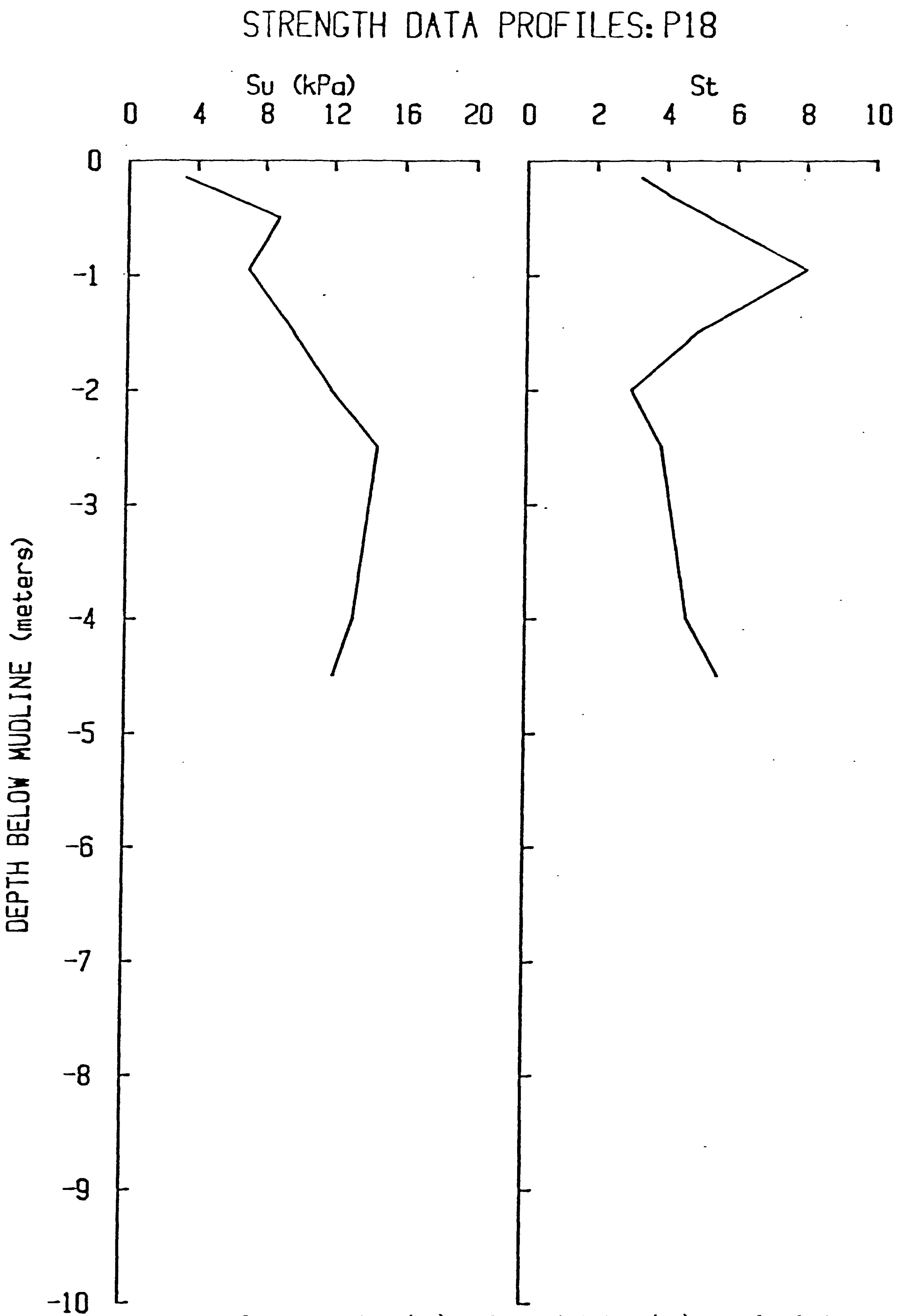

Figure 2r. Cohesion (S_u) and sensitivity (S_t) vs. depth in core.

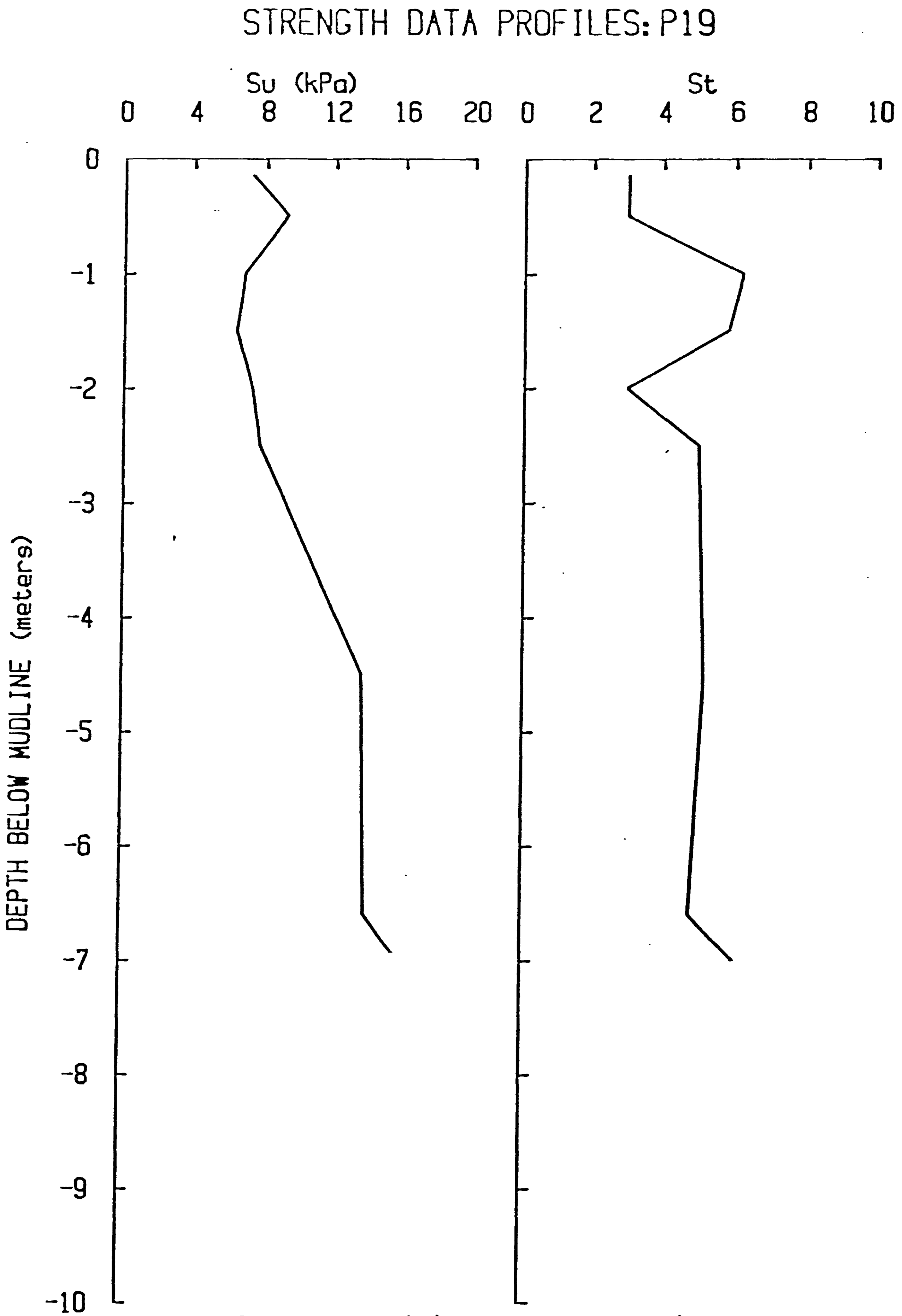

Figure 2s. Cohesion (S_u) and sensitivity (S_t) vs. depth in core.

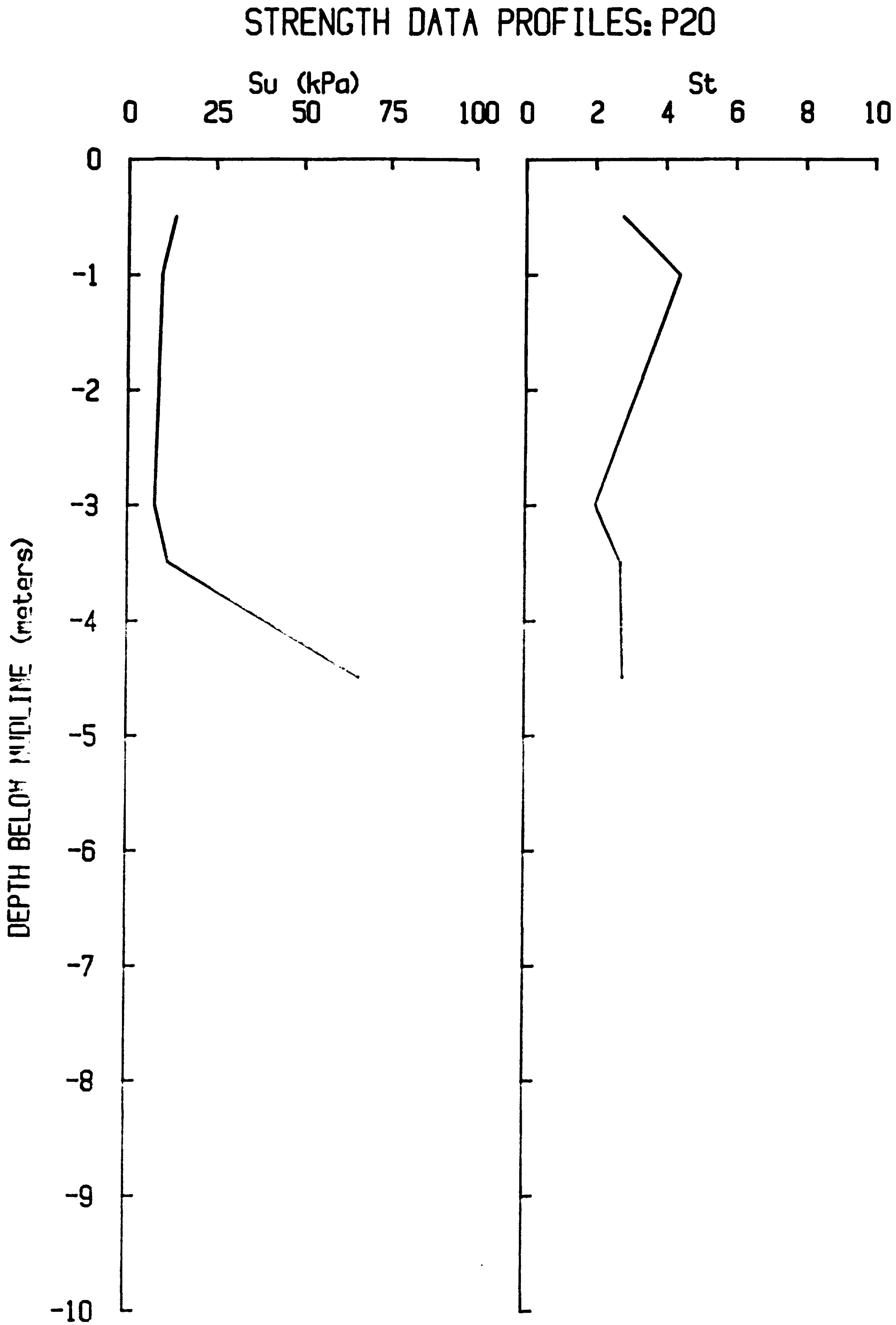

Figure 2t. Cohesion (S_u) and sensitivity (S_t) vs. depth in core.

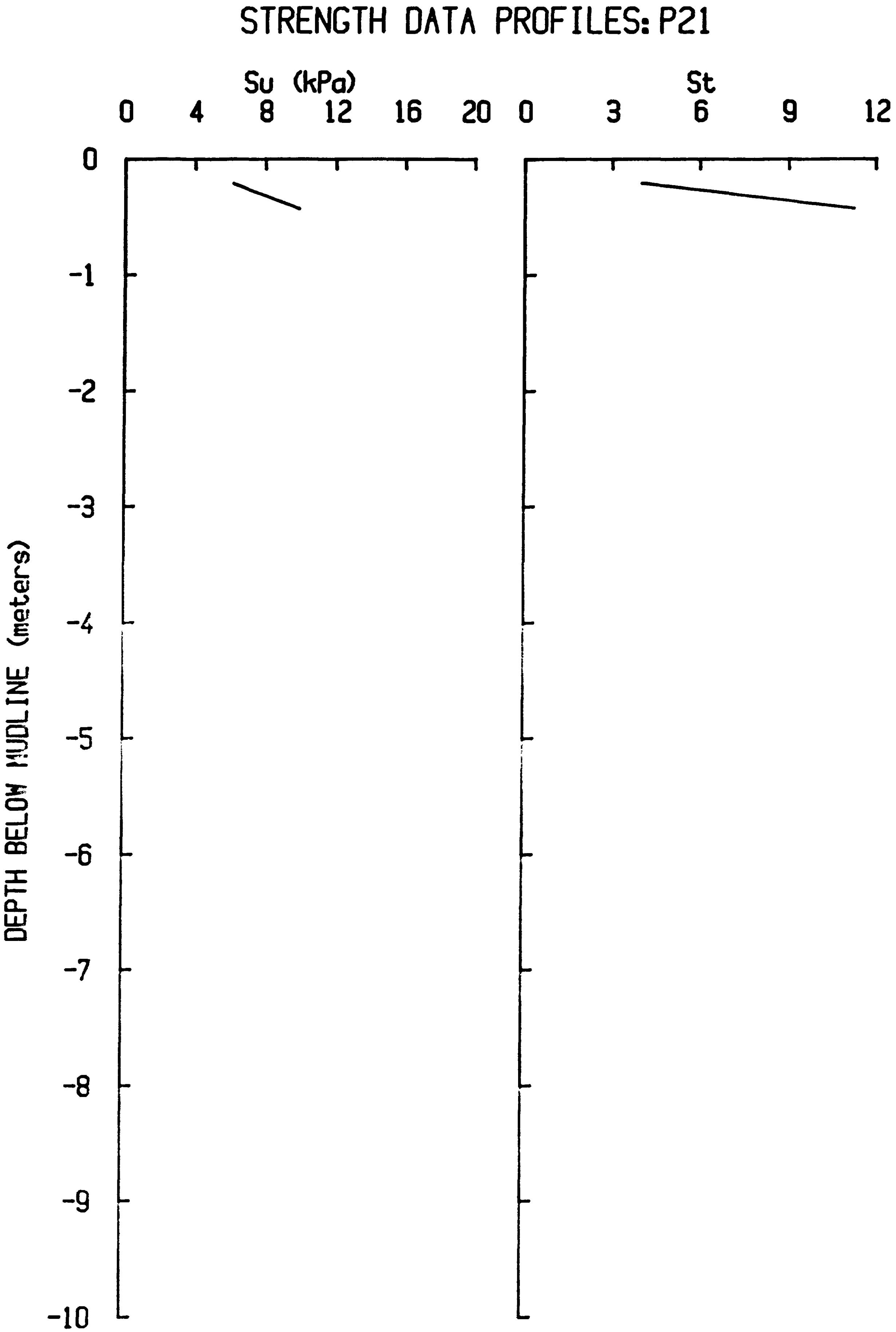

Figure 2u. Cohesion (S_u) and sensitivity (S_t) vs. depth in core.

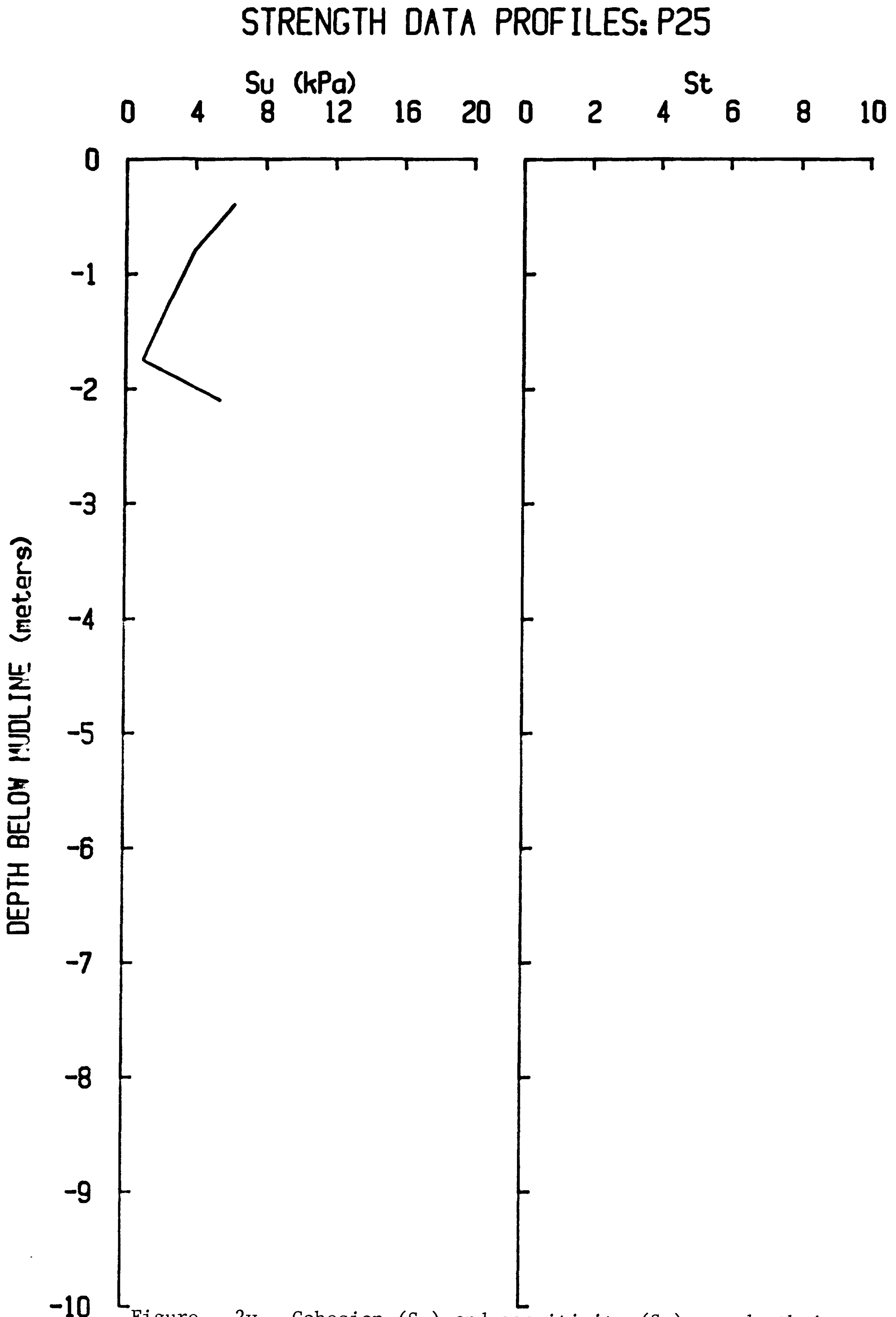

Figure 2v. Cohesion (S_u) and sensitivity (S_t) vs. depth in core.

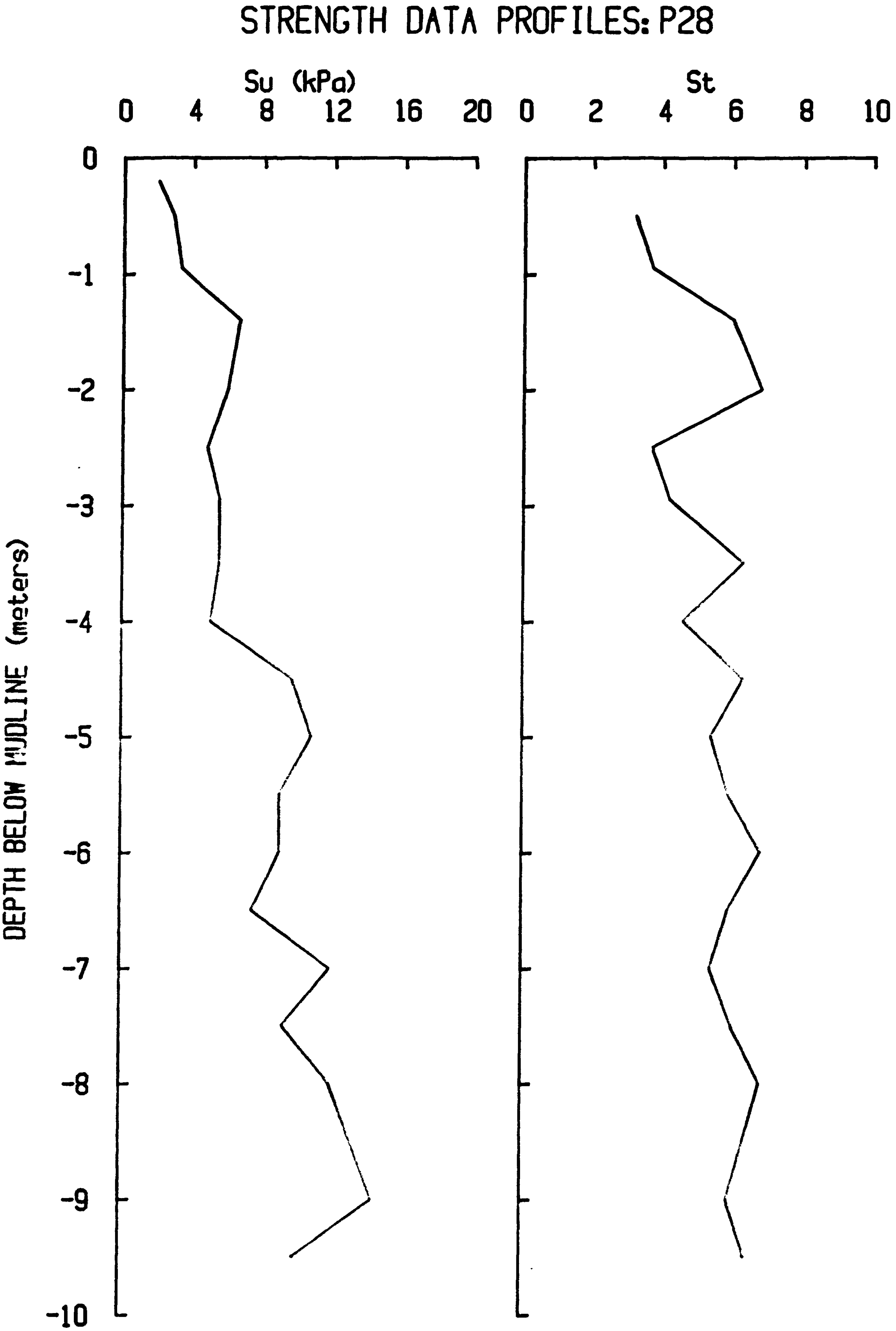

Figure 2w. Cohesion (S_u) and sensitivity (S_t) vs. depth in core.

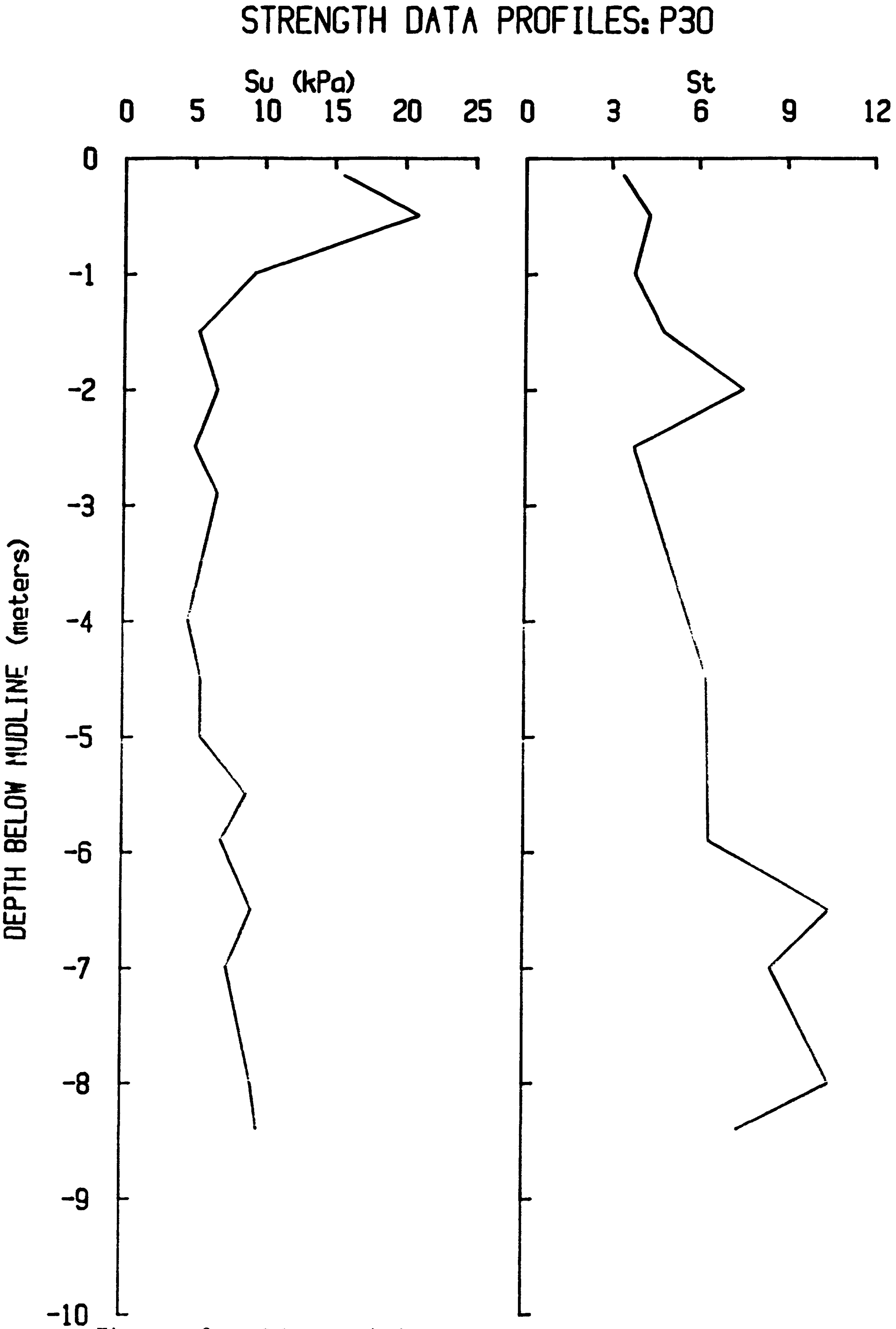

Figure 2x. Cohesion (S_u) and sensitivity (S_t) vs. depth in core.

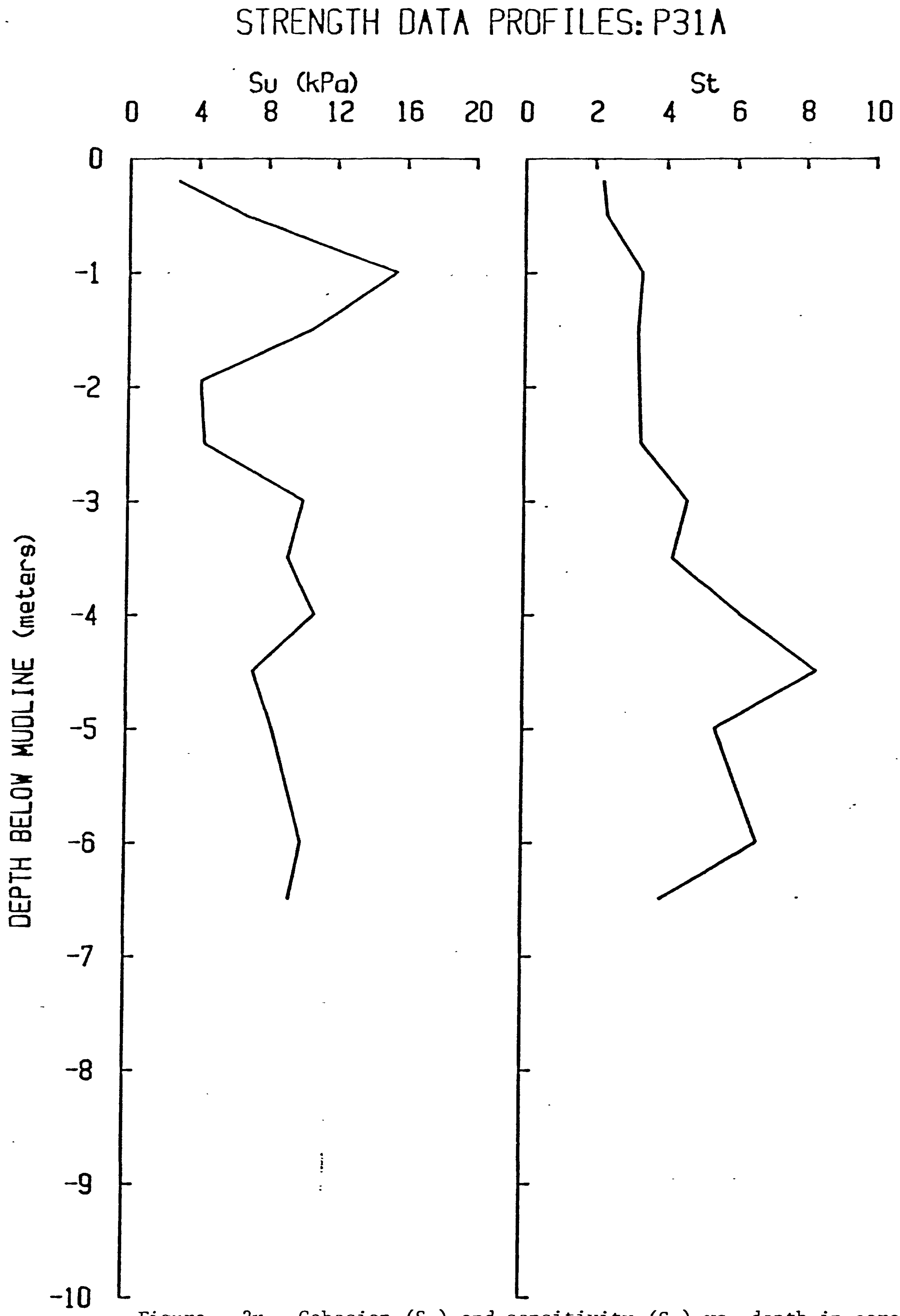

Figure 2y. Cohesion (S_u) and sensitivity (S_t) vs. depth in core.

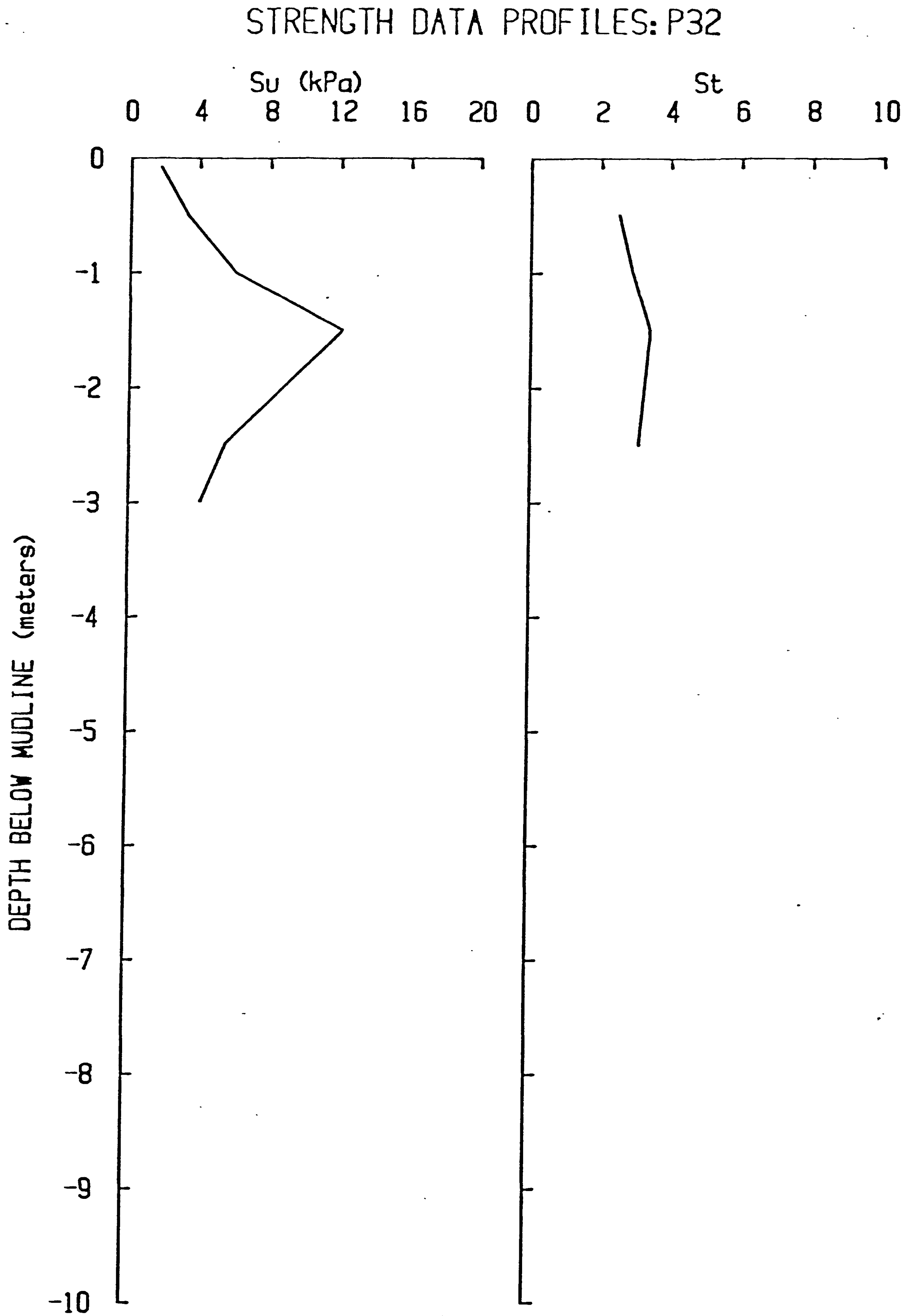

Figure 2z. Cohesion (S_u) and sensitivity (S_t) vs. depth in core.

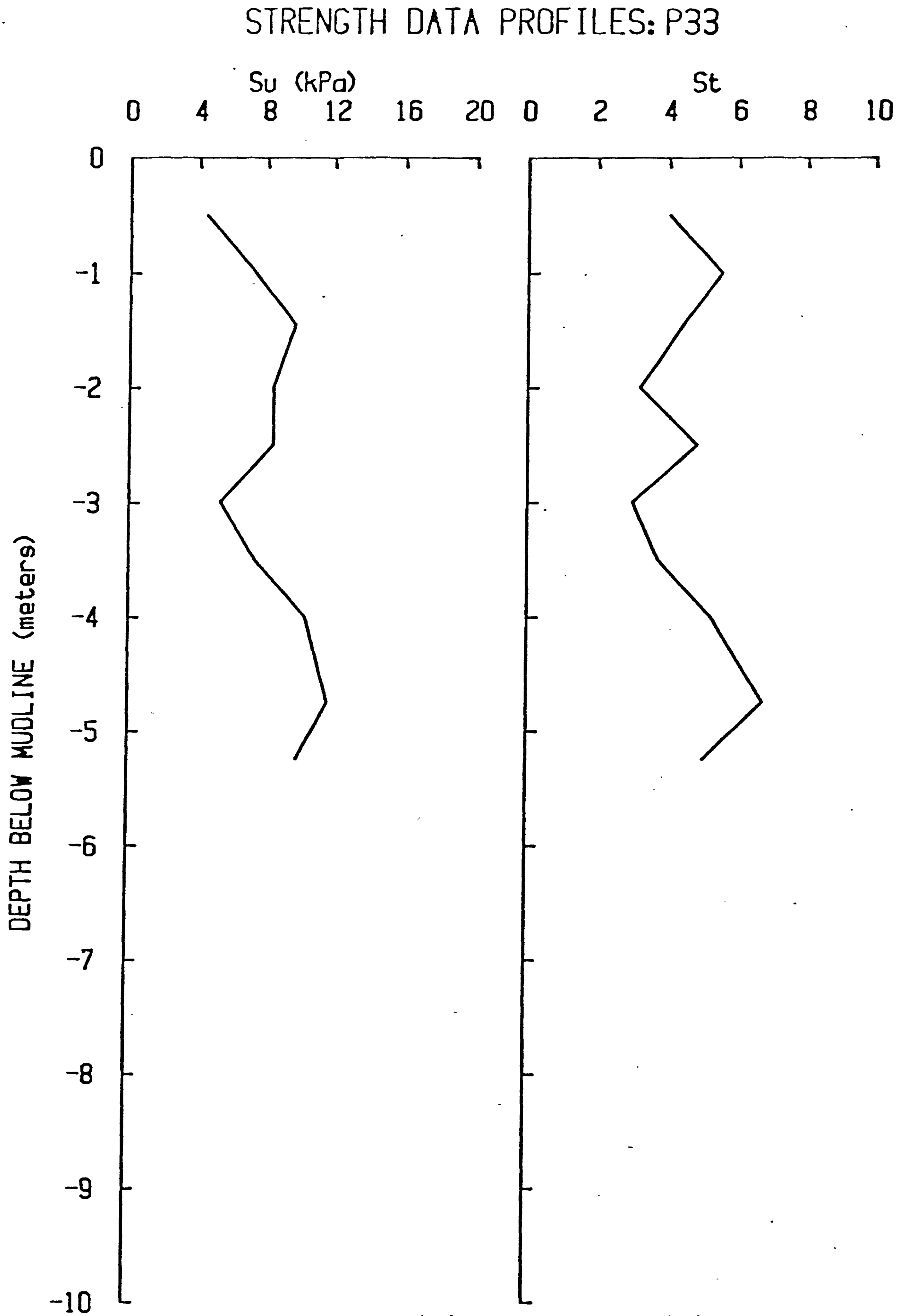

Figure 2aa. Cohesion (S_u) and sensitivity (S_t) vs. depth in core.

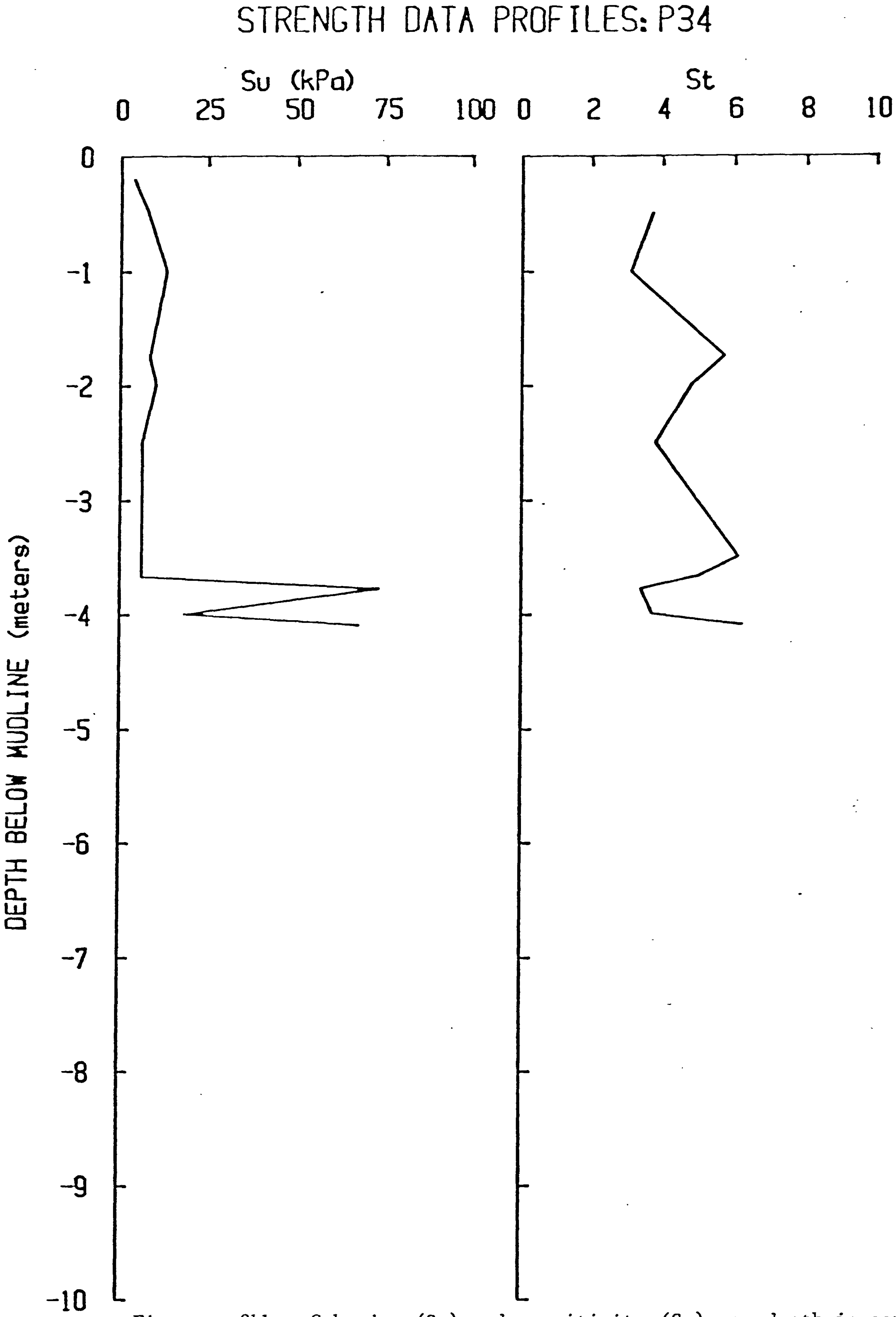

Figure 2bb. Cohesion (S_u) and sensitivity (S_t) vs. depth in core.

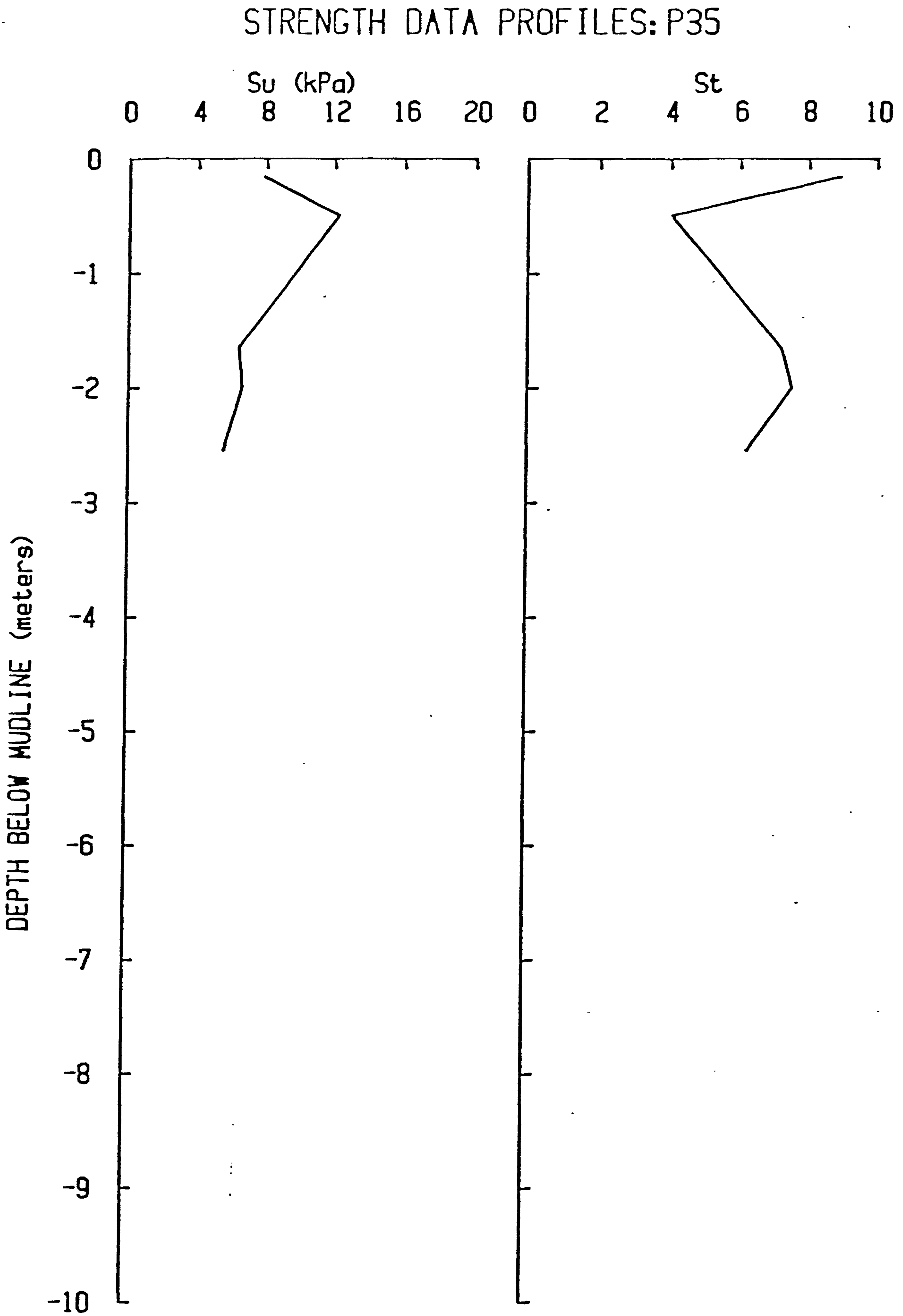

Figure 2cc. Cohesion (S_u) and sensitivity (S_t) vs. depth in core.

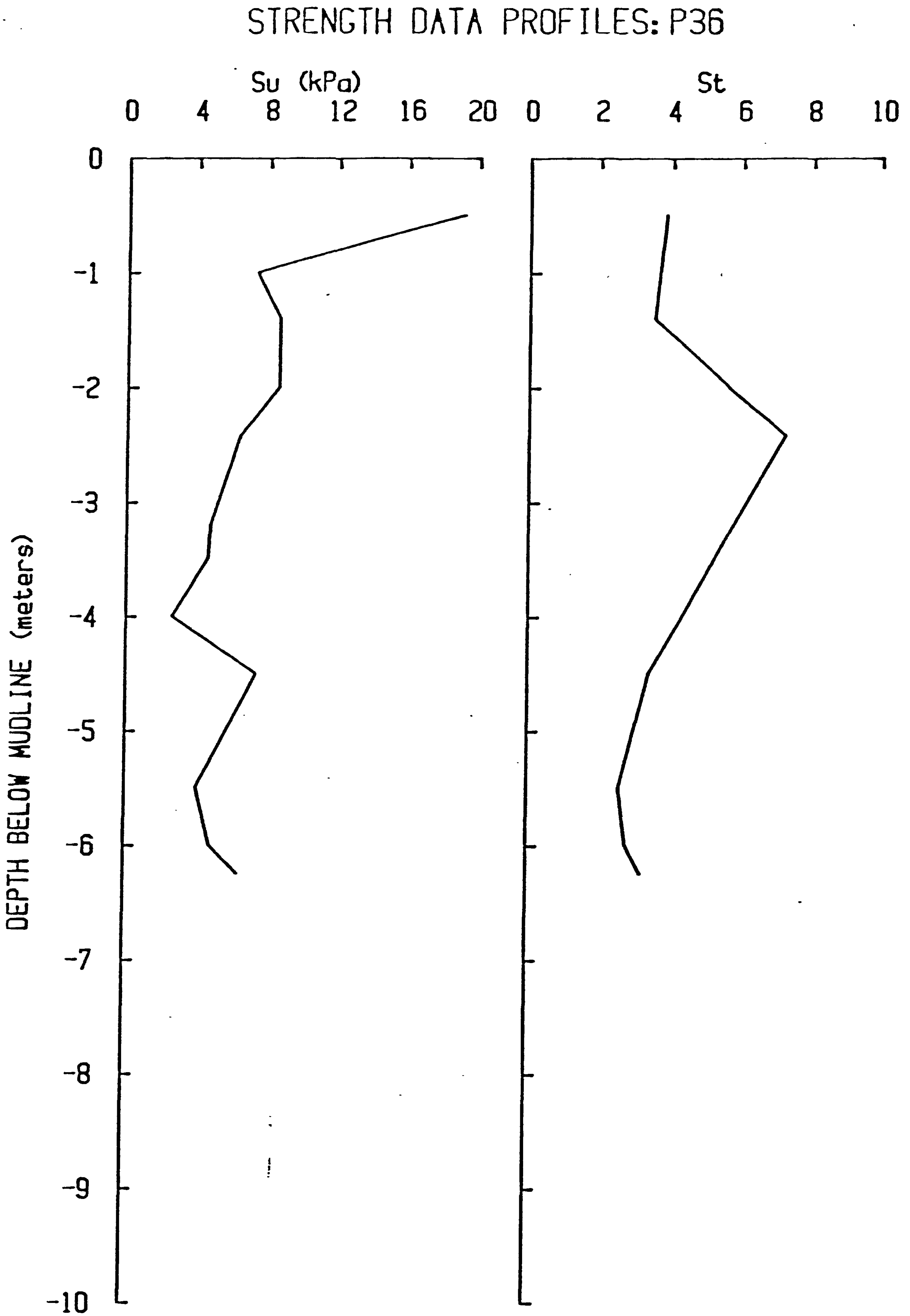

Figure 2dd. Cohesion (S_u) and sensitivity (S_t) vs. depth in core.

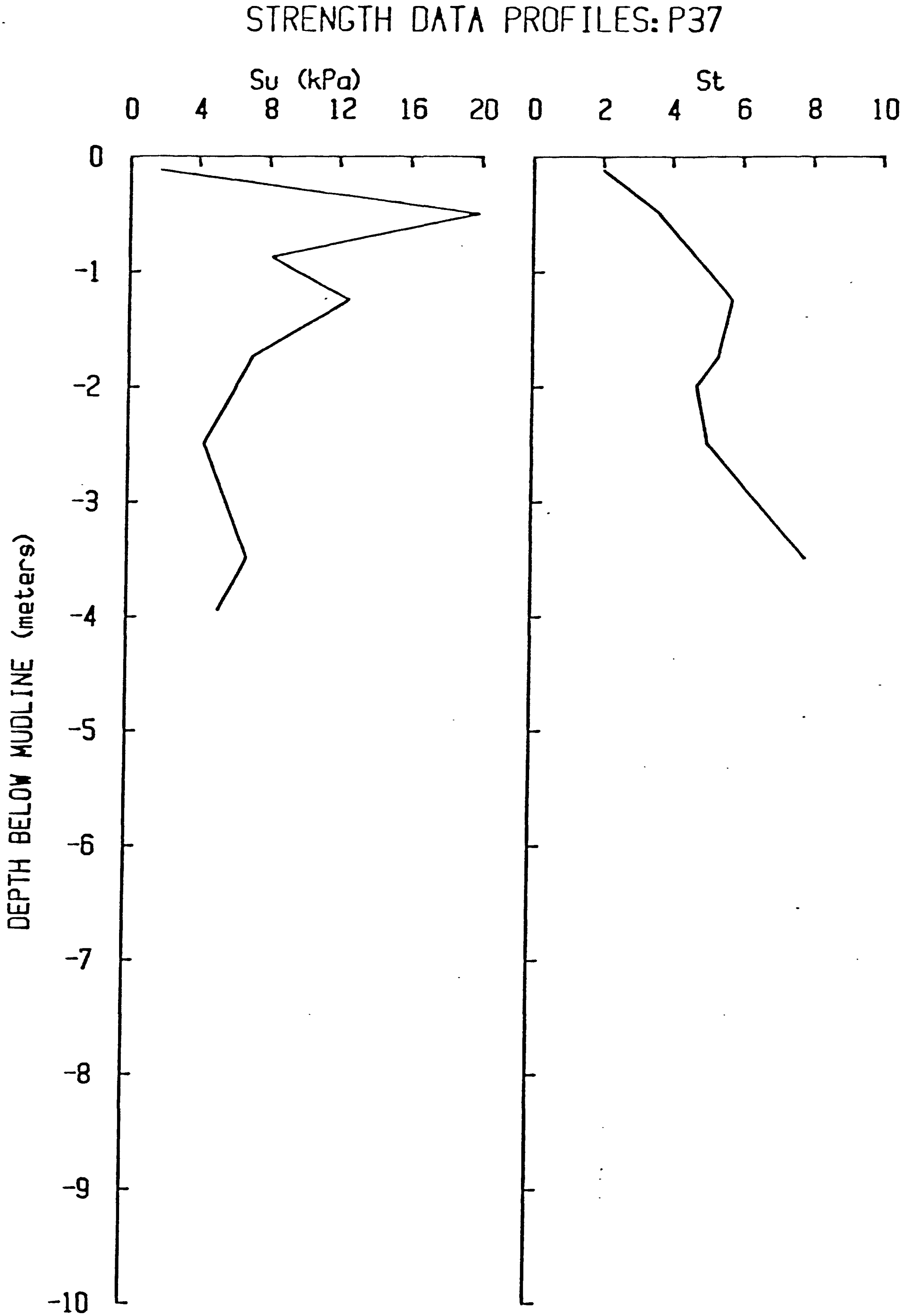

Figure 2ee. Cohesion (S_u) and sensitivity (S_t) vs. depth in core.

quick (S_t=8-16). In other terms, these sediments could lose as much as 93% of their strength through dynamic loading (e.g., earthquakes), strain softening, or other means; the average strength loss would be more than 85%.

A downslope trend in sediment sensitivity is not shown in our data (r=-0.19, n=27). As was the case for the cohesion data, the analysis was based on core-averaged values, and cores recovered from erosional surfaces were not used.

Profiles of sensitivity are shown in figures 2a-2ee. The profiles tend to be saw-toothed and there are no apparent downcore trends. In many cases, however, an immediate increase in sensitivity downcore is observed. This may indicate greater disturbance at the core tops or that sensitivities within the upper half meter of the core are partially controlled by small changes in overburden. Bioturbation, which tends to remold the sediment and hence decreases sensitivity, may also be a factor. The fact that sensitivity values less than the initial (top of core) value are commonly found elsewhere in the core profiles suggests that the effect may be of only minor importance. A few cores (e.g., PC13, fig. 2b) show parallel to subparallel cohesion and sensitivity profiles. This situation will be discussed at the end of this section.

The sensitivity values determined in this study are higher than the values reported in some studies in this and proximal slope areas (Keller and others, 1979; McGregor and others, 1979), although they are similar to those reported by Lambert and others (1981) and Booth and others (1985a). Marine fine-grained sediments typically have sensitivities of four or less; thus, these sediments are slightly more sensitive than normal. Factors which contribute to a high sensitivity are discussed by Mitchell (1976). Many of them, such as an open, metastable fabric, cements, thixotropic hardening, and the presence of dispersing agents (typically certain organic substances) may be causes in this particular environment. The high percentage of clay, which favors an open fabric, may be significant, particularly in light of the fact that Georges Bank slope sediments have a much higher silt content and a lower sensitivity (4.8 vs. 5.6) (Booth and others, 1985a) than the Mid-Atlantic slope sediments. However, the poor correlation between clay percentage ($<2\mu$) and sensitivity (r=-0.17, n=96) would argue against grain-size control of fabric and, hence, against its impacting sensitivity. Another factor which can cause elevated sensitivities, cementation, was not observed in these sediments; if present, it is not obvious. Further, criteria suggested by Nacci and others (1974) for identifying cements through geotechnical measurements generally are not met. The other sensitivity factors discussed by Mitchell (1976) have not been investigated.

Sensitivity may also be used as a crude indication of relative sample quality. In these sediments mechanical disturbance usually leads to a reduction in natural cohesion, but remolded strength remains the same. Accordingly, the sensitivity value (natural S_u/remolded S_u) decreases. Thus, although there are many factors which may influence the sensitivity value (as discussed previously), a strong positive correlation between natural cohesion and sensitivity may be an indication that systematic disturbance has occurred. The correlation coefficent determined in this regard was near zero (r=0.07; n=199) and is not statistically significant. The fact that our sensitivity values are equal or slightly greater than those reported from other studies conducted in this general area suggests, insofar as sensitivity may be used in this manner, that sample quality is relatively good.

Bulk-density group

Unit weight, water content, specific gravity, and porosity also vary over a wide range (table II). Of these properties, only grain-specific gravity is independent of the effects of the compaction process; the others tend to change in concert with relative compaction and, therefore, with one another.

The mean values shown in table II deviate from several other published values. Specifically, unit weight (1.67 g/cc) is higher, and water content (67%) and porosity (63%) are lower than values previously published for the general area by Keller and others (1979), McGregor and others (1979), and Lambert and others (1981). They are higher, however, than those published by Olsen and others (1982).

Specific gravity (table II) of solids is generally slightly lower than reported in these previous studies. The mean value (2.72) is also slightly less than the value typically reported for most terrigenous marine sediment.

Despite the shortness of some of the cores and the samples representing overconsolidated sediment, the properties in question do exhibit the expected downcore trends. The profiles shown in figures 3a-31 indicate, in general, that bulk density tends to increase, and water content and porosity tend to decrease, downcore. Specific gravity shows no trend. As with the cohesion and sensitivity profiles, a sawtooth pattern is present in these plots. Again, this suggests a complexity in depositional and postdepositional processes.

Significant downslope trends exist in this data set. Unit weight decreases, water content increases, and porosity increases with increasing water depth. Between 25% and 35% of the variability in these data (27 core-averaged values in each case) may be accounted for in this relationship. These trends are in accord with the findings of Keller and others (1979). Grain-specific gravity values are not significantly correlated with water depth.

Plasticity

Liquid limit (w_L), plastic limit (w_P), plasticity index (I_P), and liquidity index (I_L) provide a basis for classification, and indication of texture, mineralogy, and other inherent sediment properties, and some insight into stress behavior.

Classification is traditionally accomplished by using the plasticity chart devised by Casagrande (1948). The chart is divided into fields which represent different soil types. Figure 4 is a plot of samples from this study on such a chart. Although there is a scatter of data along and just above the "A-line", indicating a wide range in plasticity characteristics within the sediment, the dominant soil type is an inorganic clay of high plasticity. According to the Unified Soil Classification System, this soil is "CH". Soils in this category are considered relatively undesirable as foundation material (Wagner, 1957). It is, however, a common soil type on continental margins and is, in fact, a common terrestrial soil type as well.

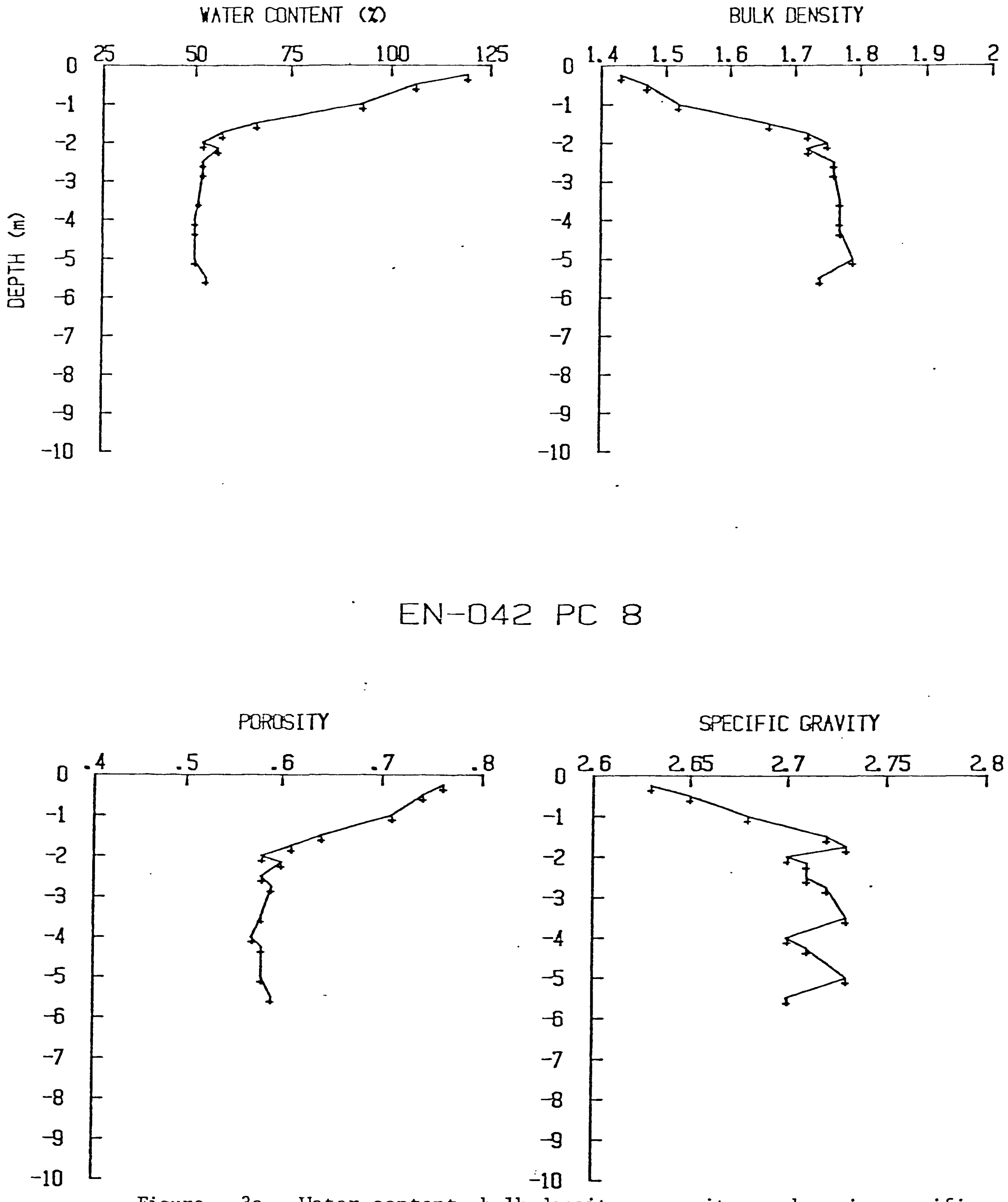

Figure 3a. Water content, bulk density, porosity, and grain-specific gravity vs. depth in core.

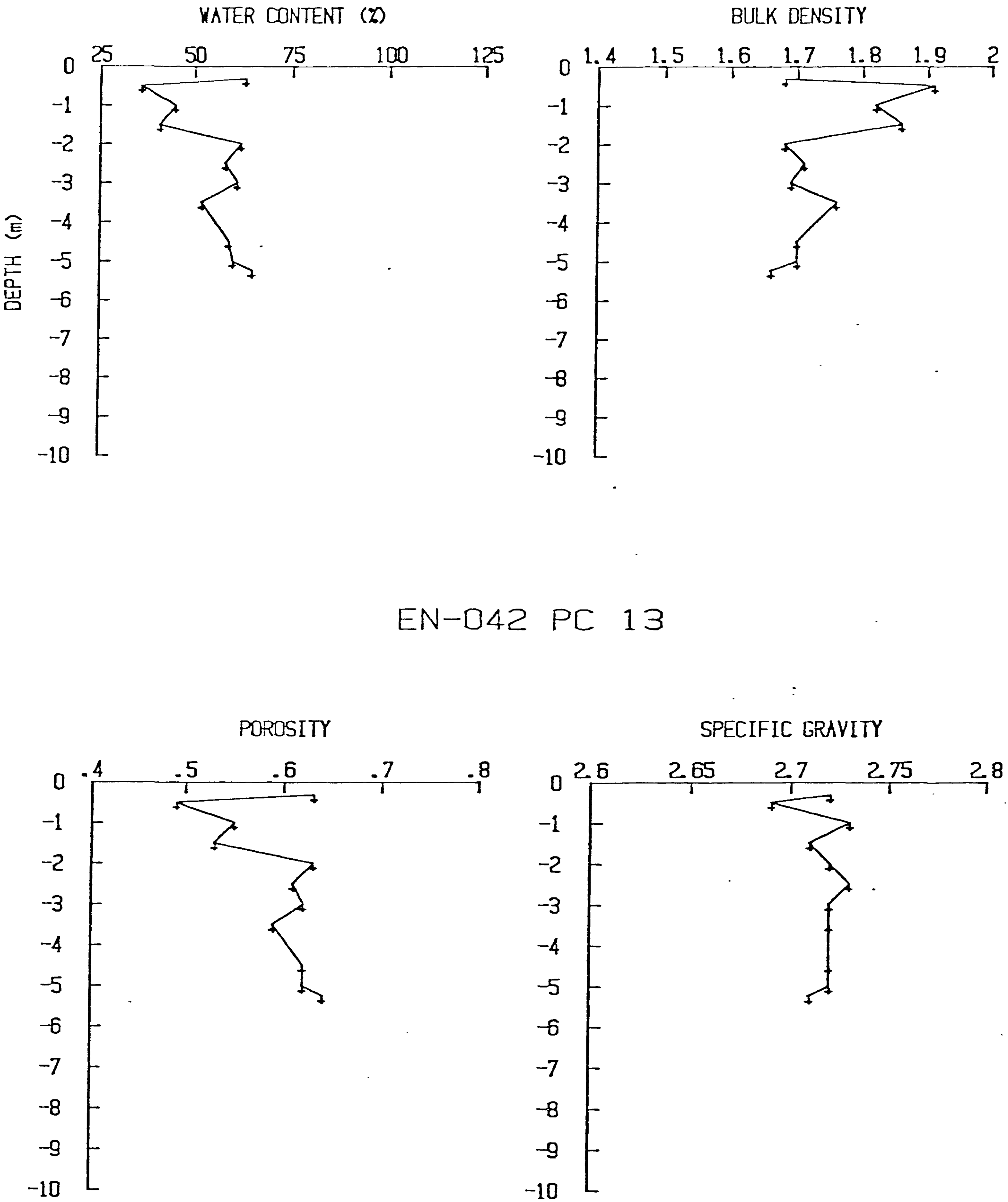

Figure 3b. Water content, bulk density, porosity, and grain-specific gravity vs. depth in core.

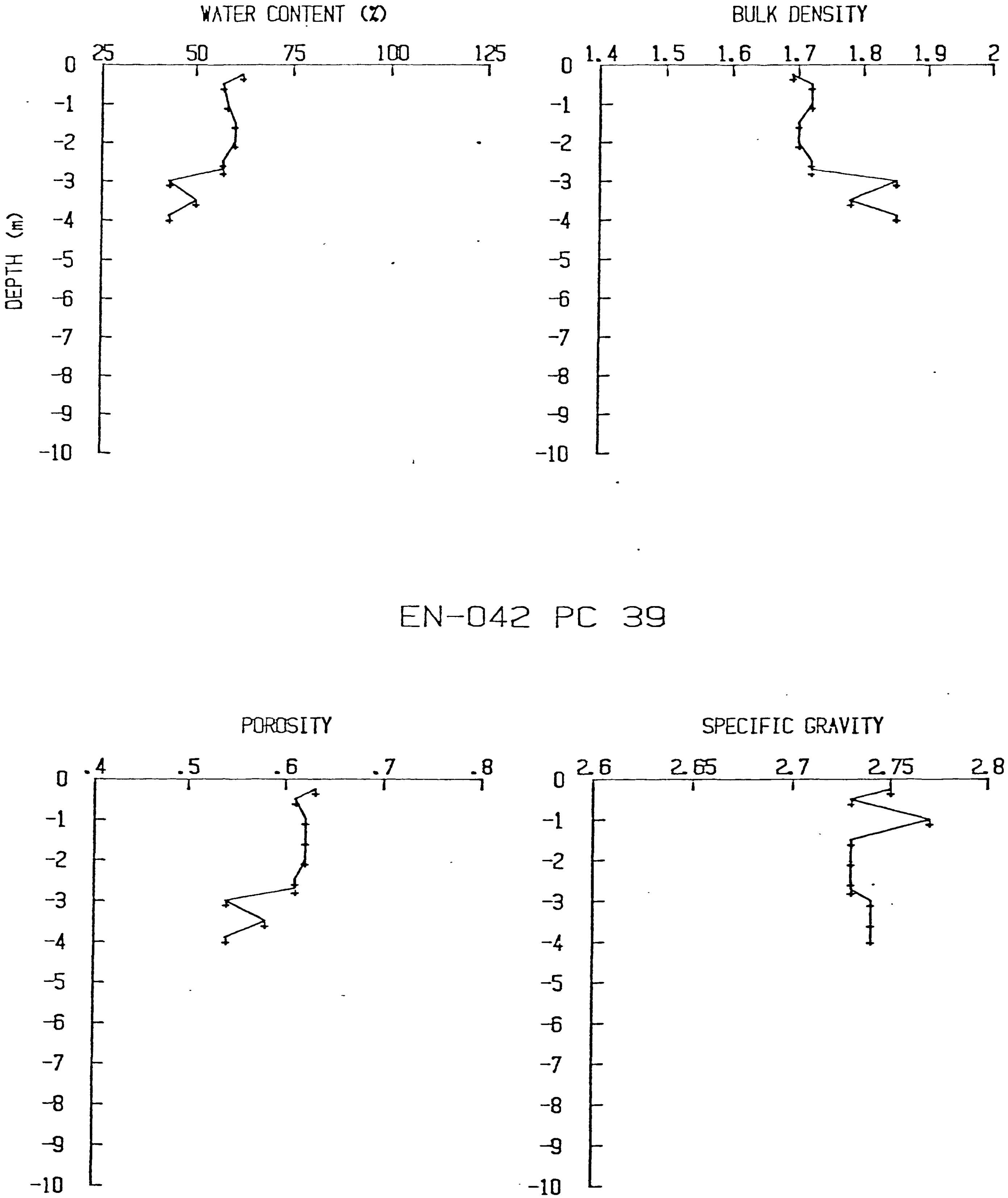

Figure 3c. Water content, bulk density, porosity, and grain-specific gravity vs. depth in core.

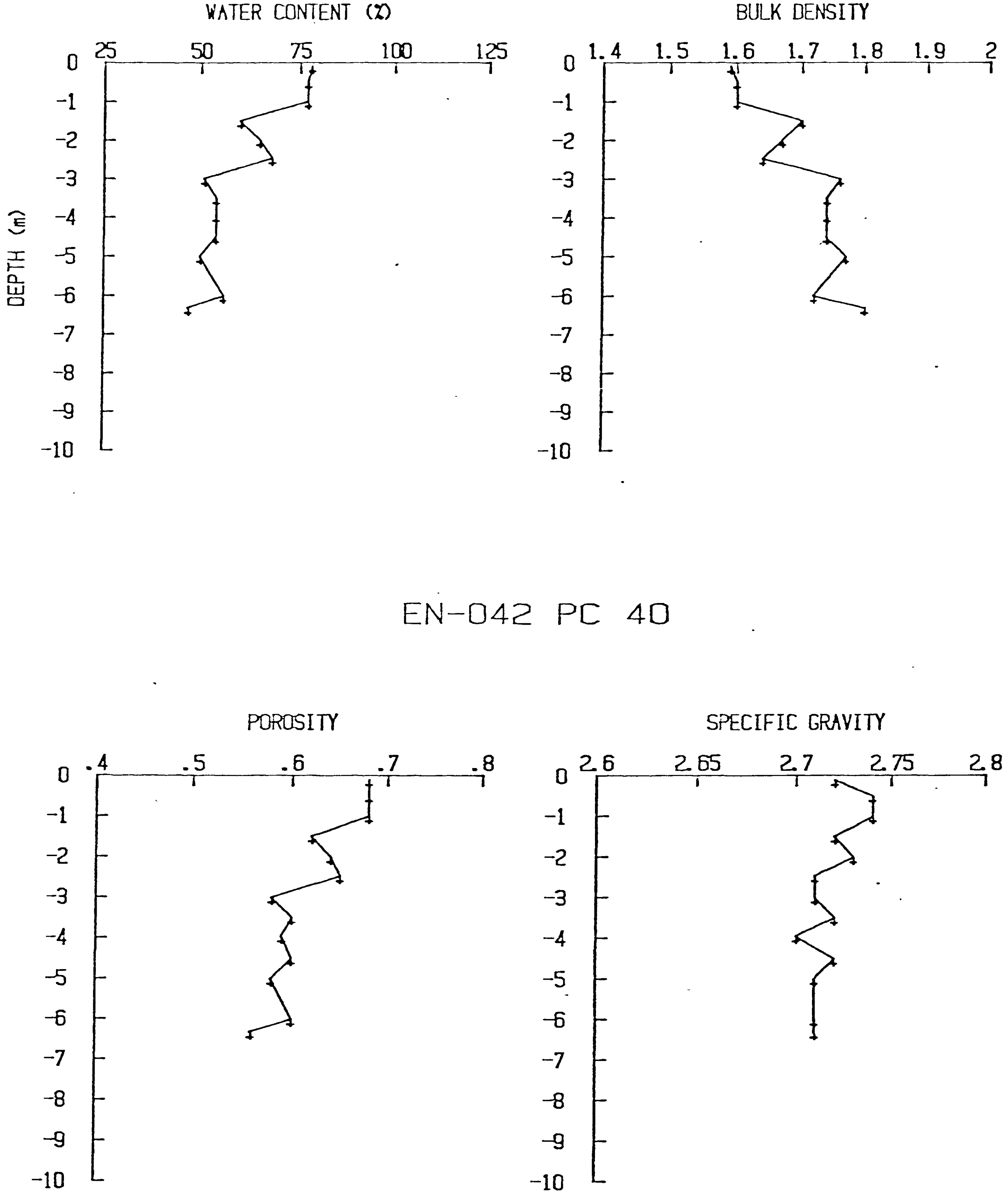

Figure 3d. Water content, bulk density, porosity, and grain-specific gravity vs. depth in core.

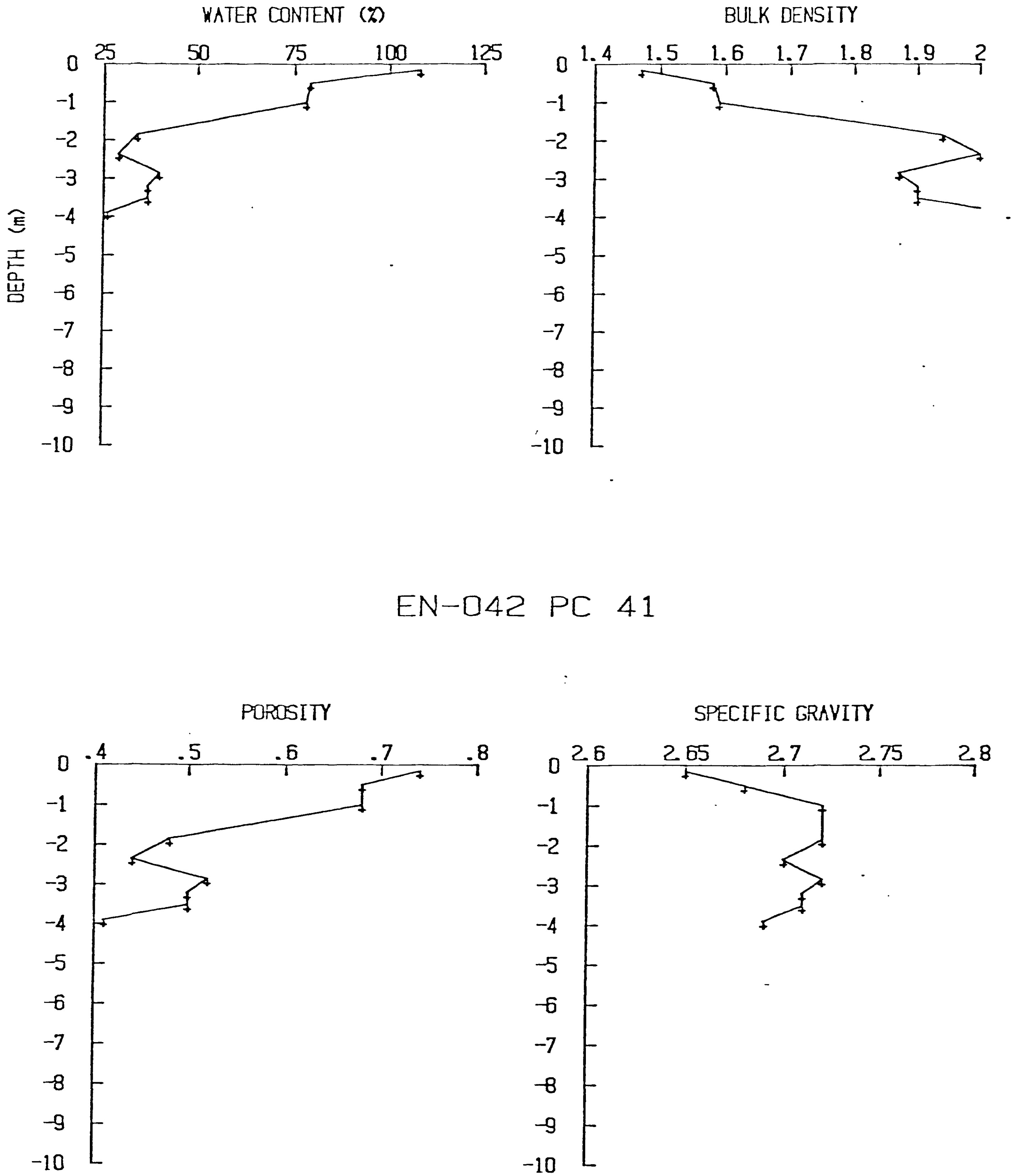

Figure 3e. Water content, bulk density, porosity, and grain-specific gravity vs. depth in core.

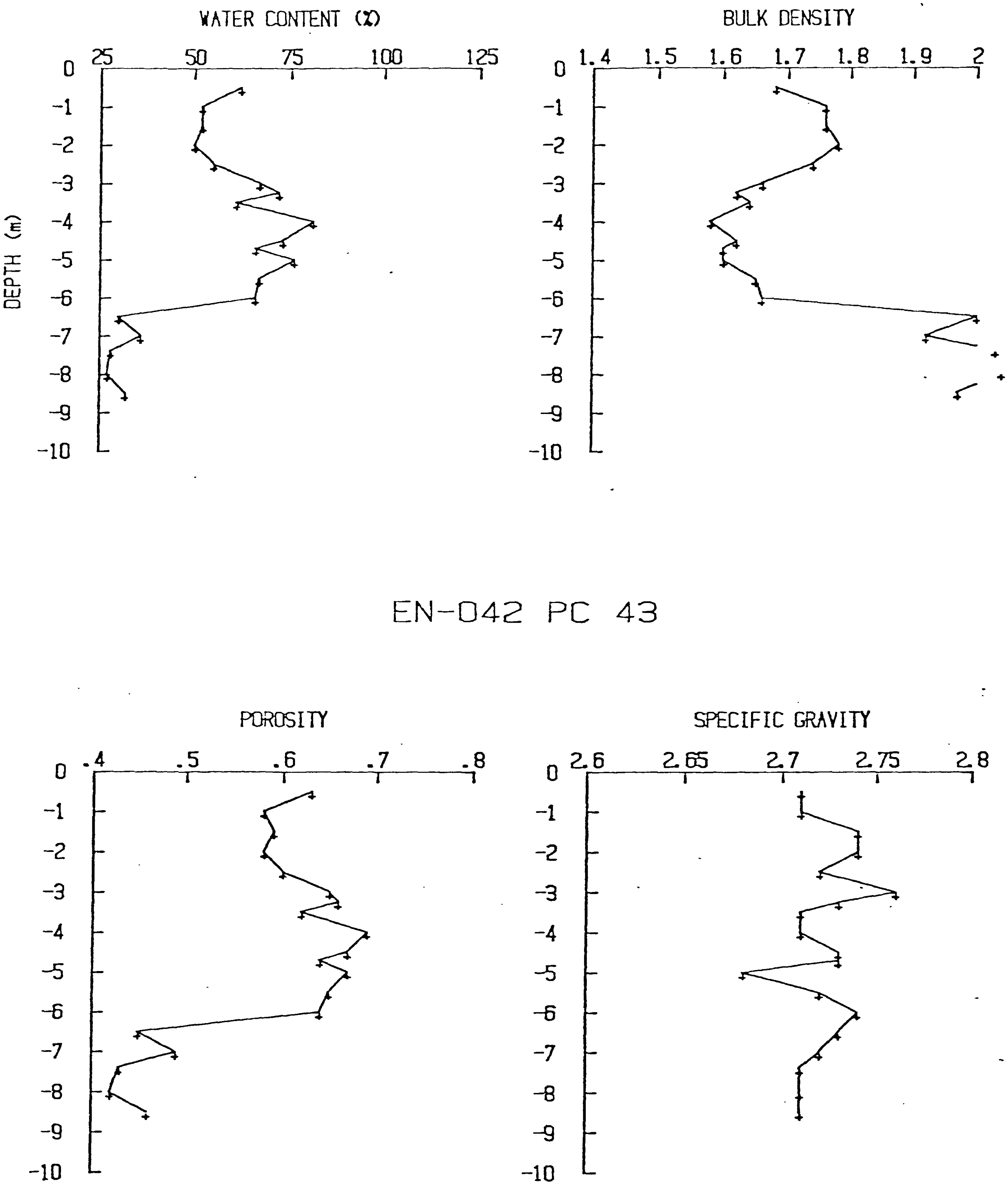

Figure 3f. Water content, bulk density, porosity, and grain-specific gravity vs. depth in core.

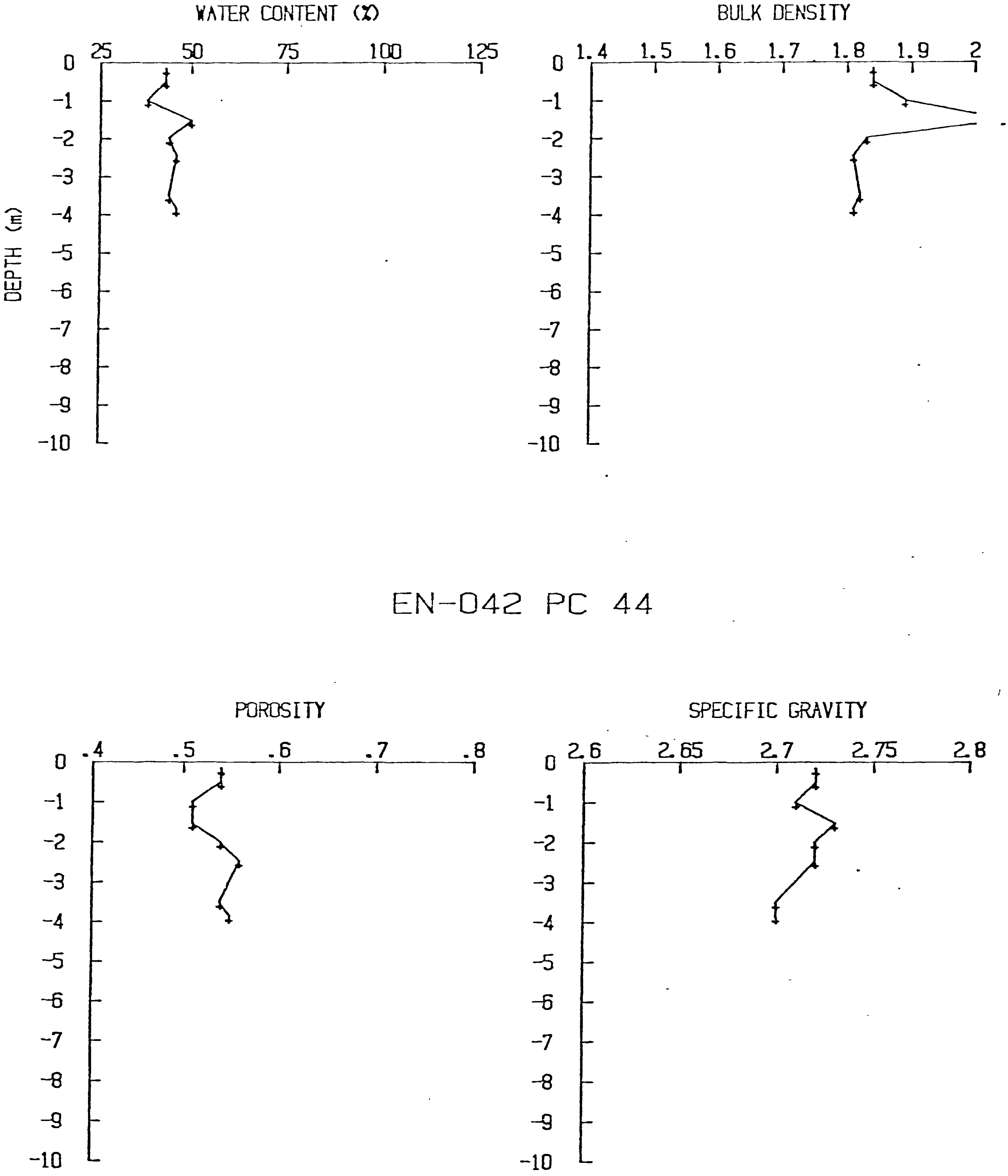

Figure 3g. Water content, bulk density, porosity, and grain-specific gravity vs. depth in core.

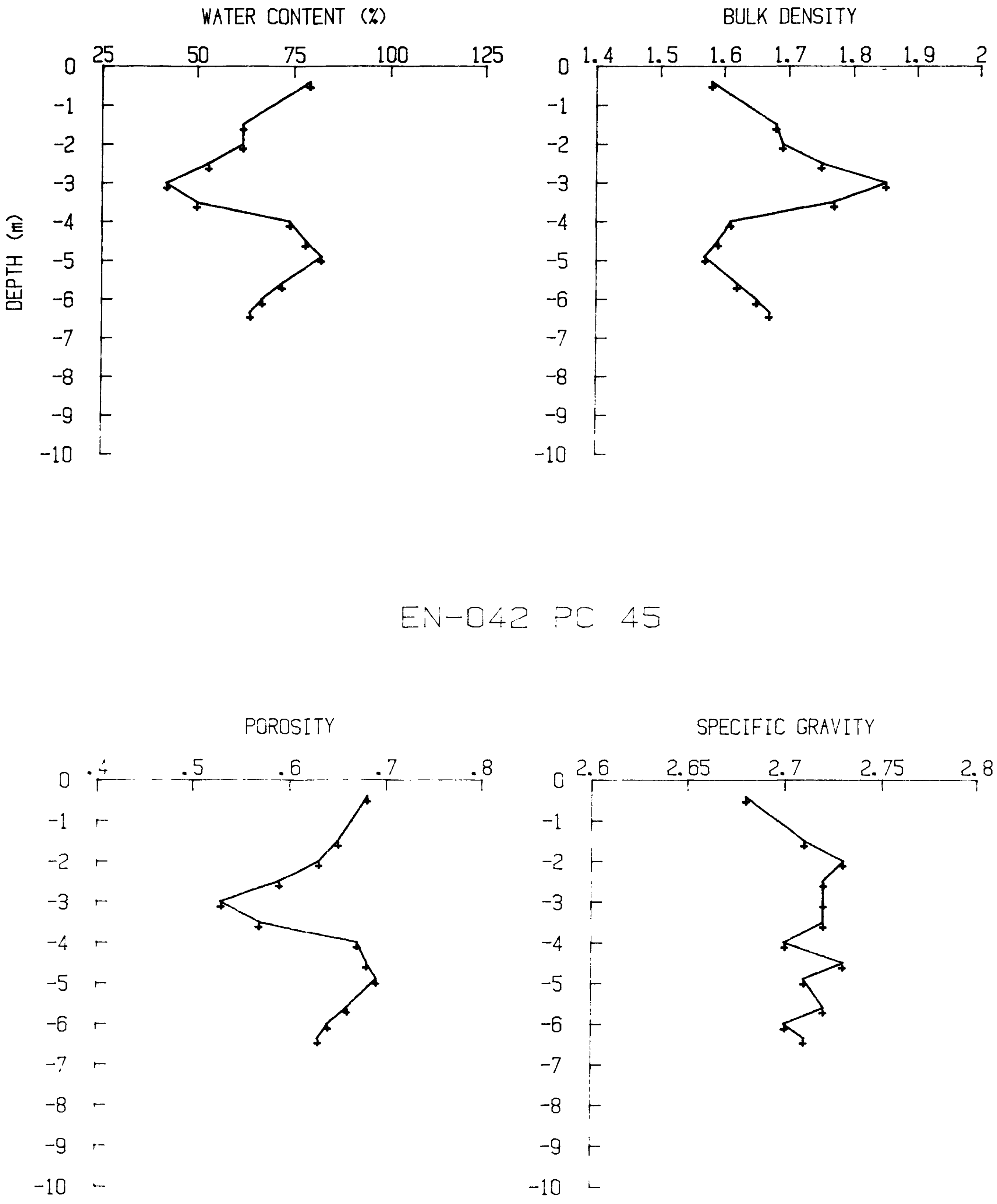

Figure 3h. Water content, bulk density, porosity, and grain-specific gravity vs. depth in core.

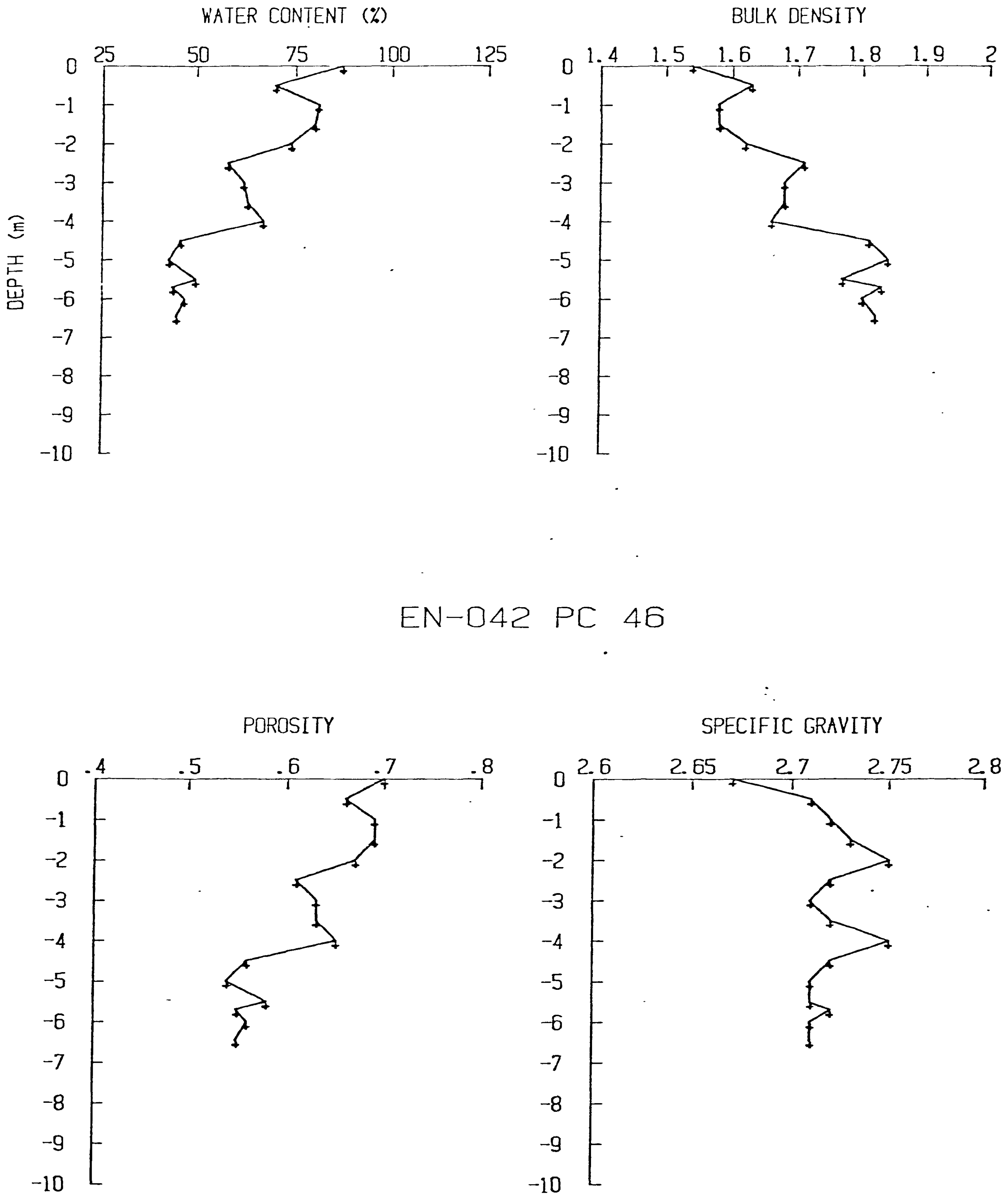

Figure 3i. Water content, bulk density, porosity, and grain-specific gravity vs. depth in core.

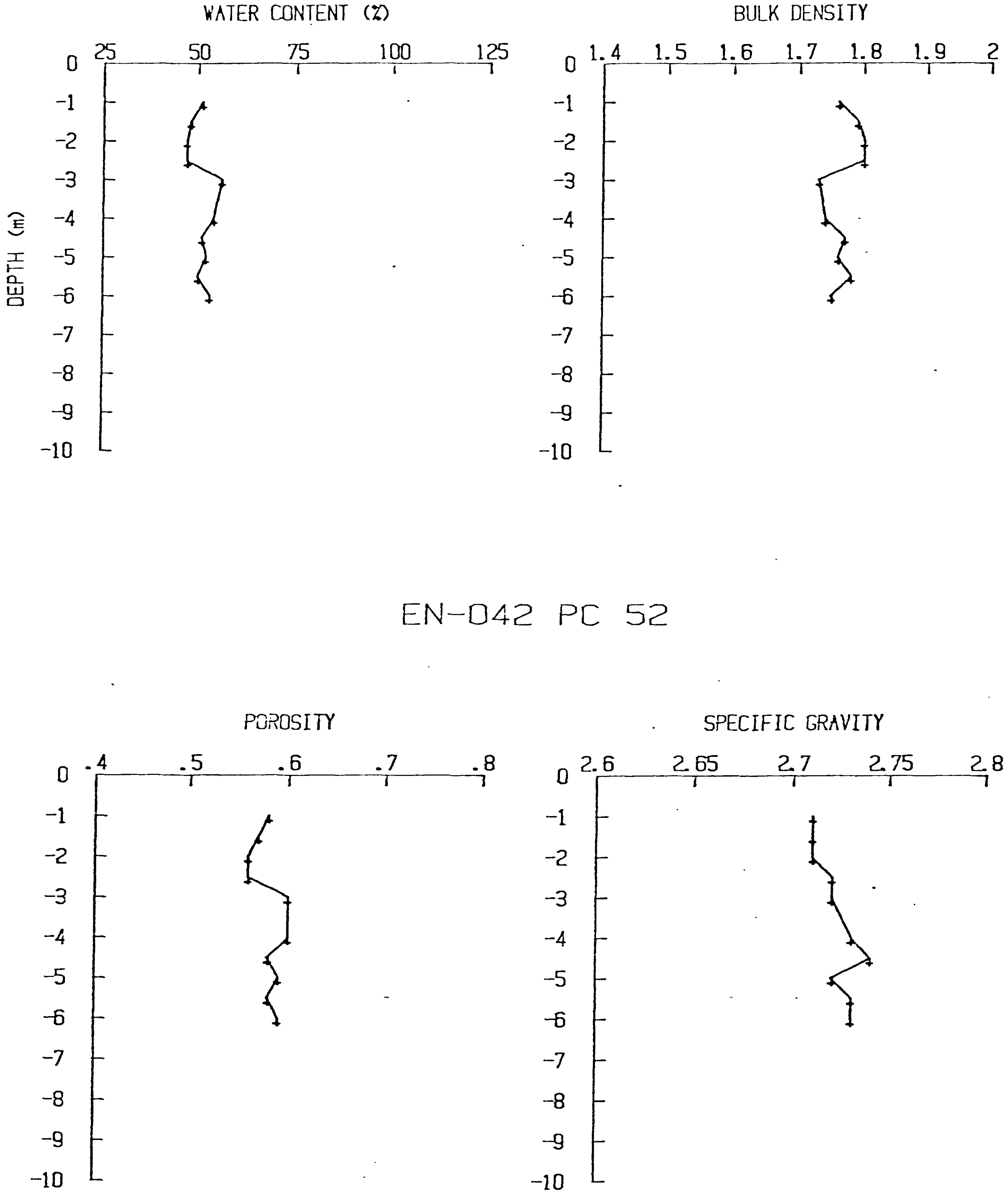

Figure 3j. Water content, bulk density, porosity, and grain-specific gravity vs. depth in core.

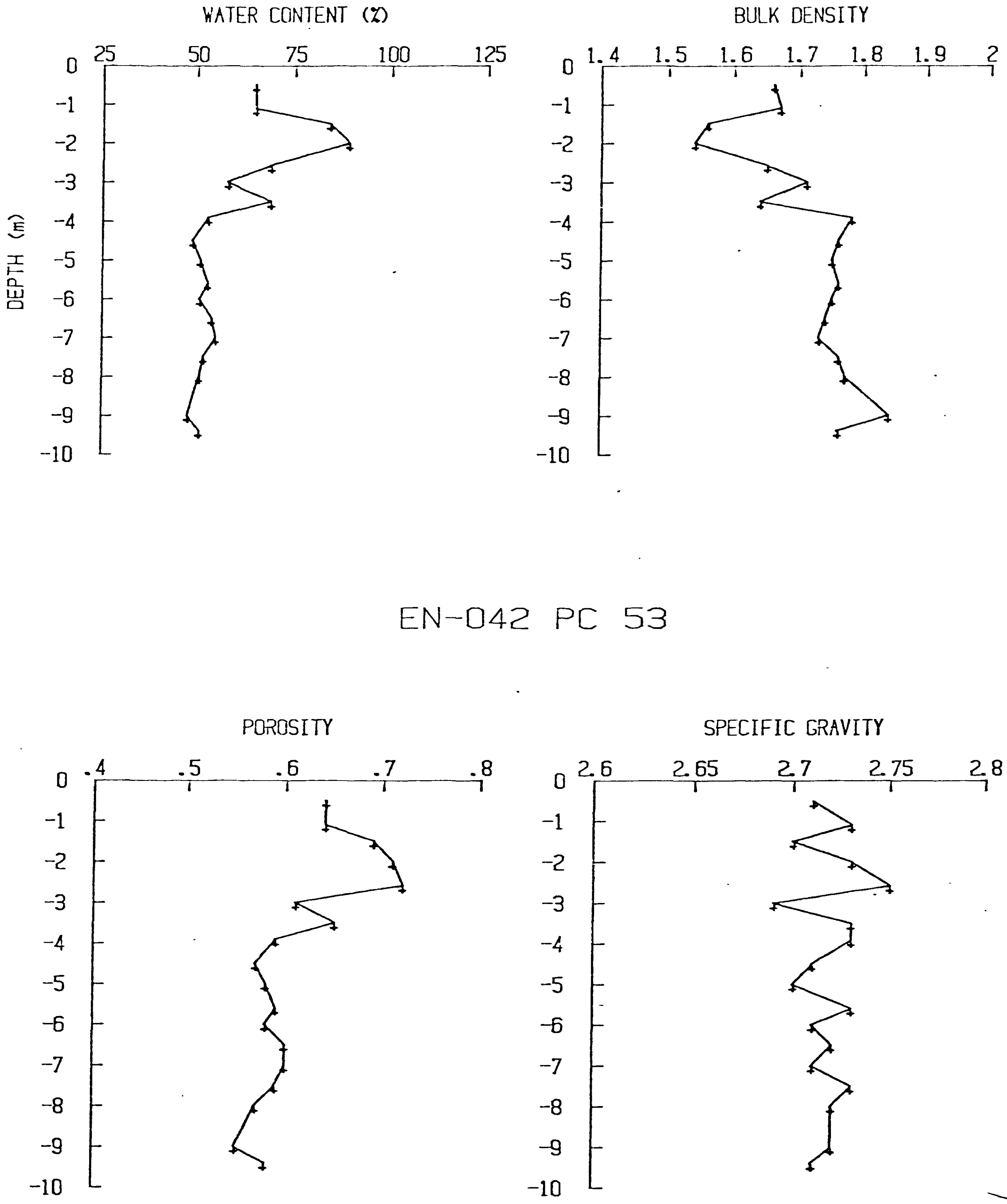

Figure 3k. Water content, bulk density, porosity, and grain-specific gravity vs. depth in core.

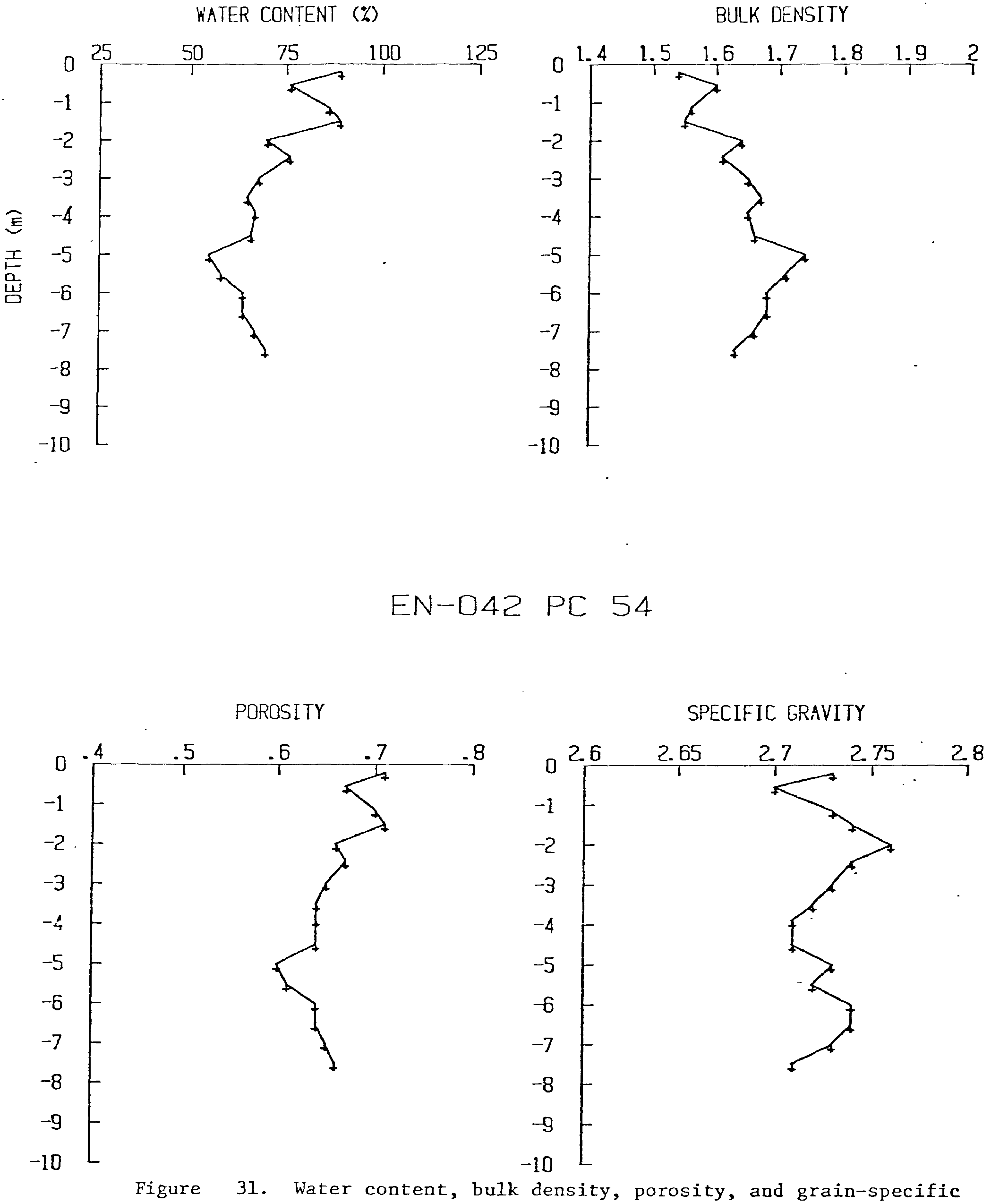

Figure 31. Water content, bulk density, porosity, and grain-specific gravity vs. depth in core.

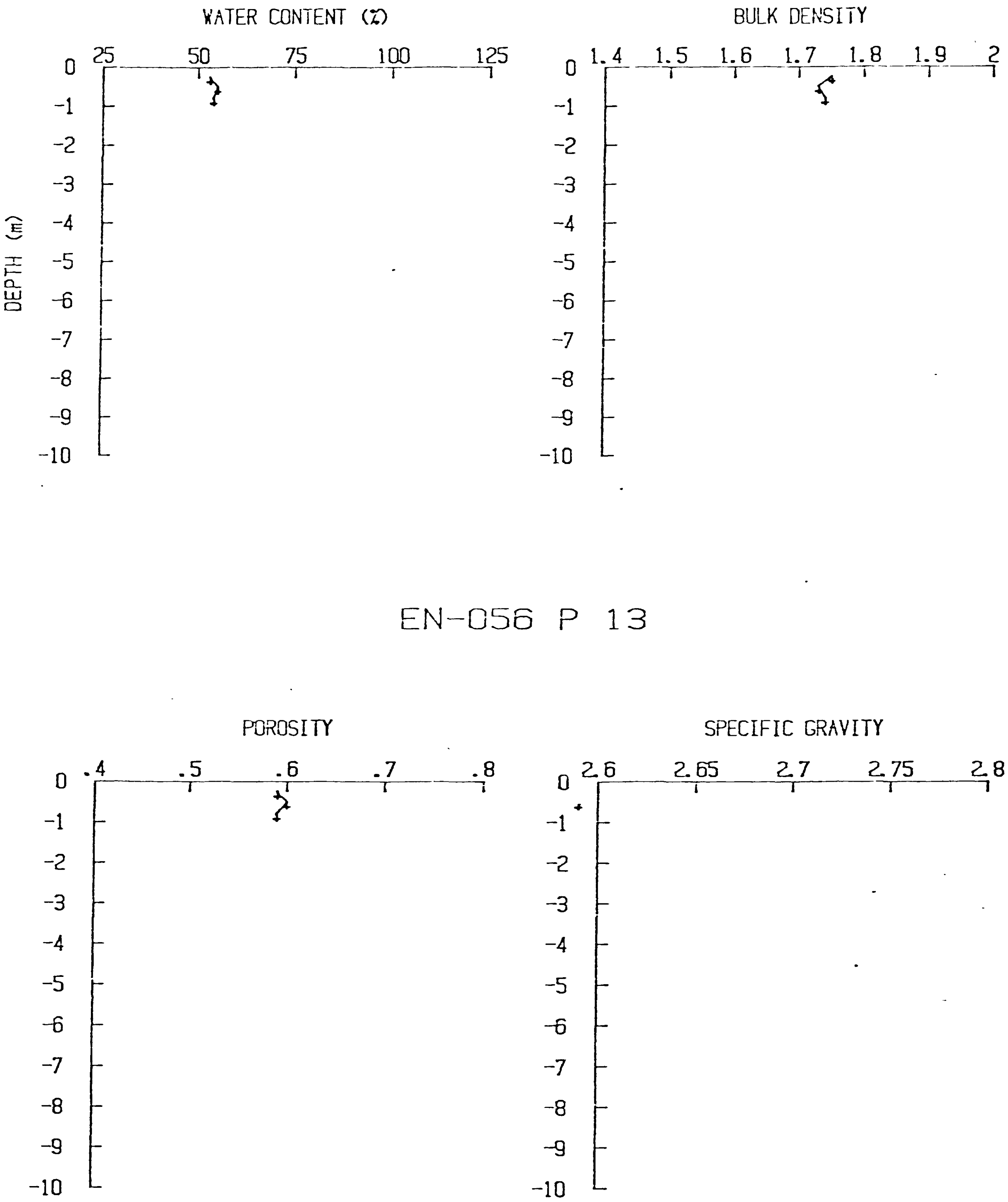

Figure 3m. Water content, bulk density, porosity, and grain-specific gravity vs. depth in core.

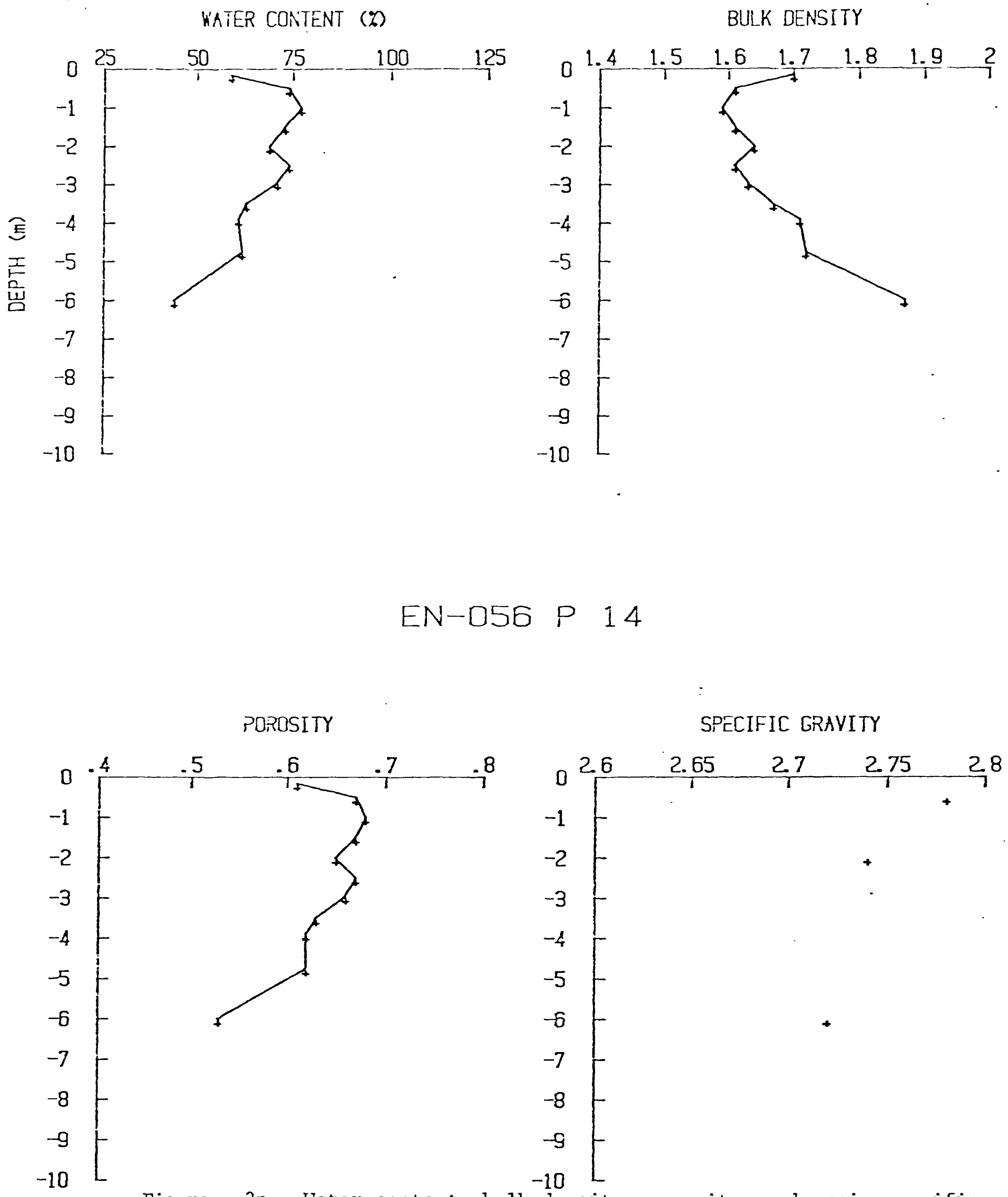

Figure 3n. Water content, bulk density, porosity, and grain-specific gravity vs. depth in core.

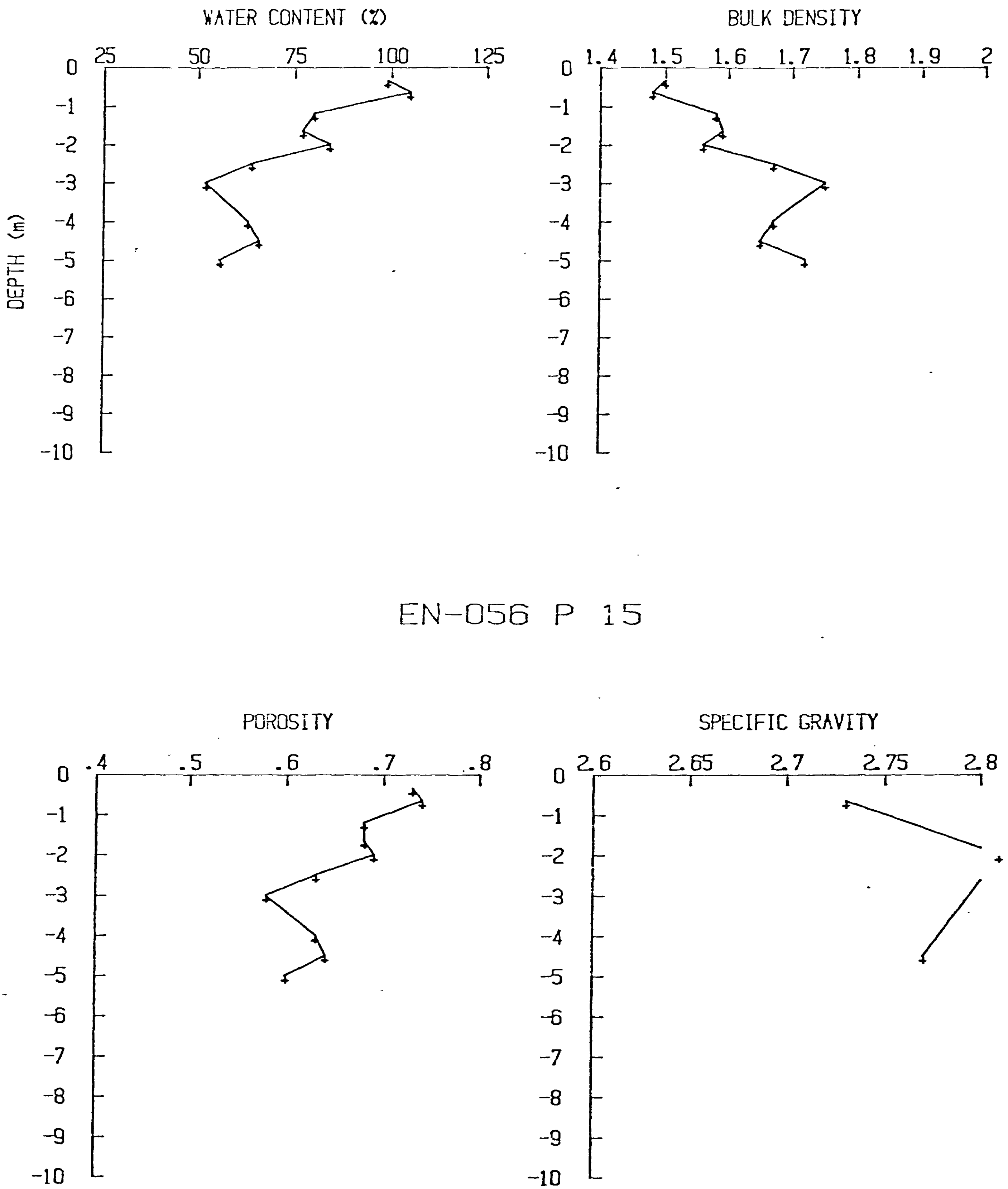

Figure 3o. Water content, bulk density, porosity, and grain-specific gravity vs. depth in core.

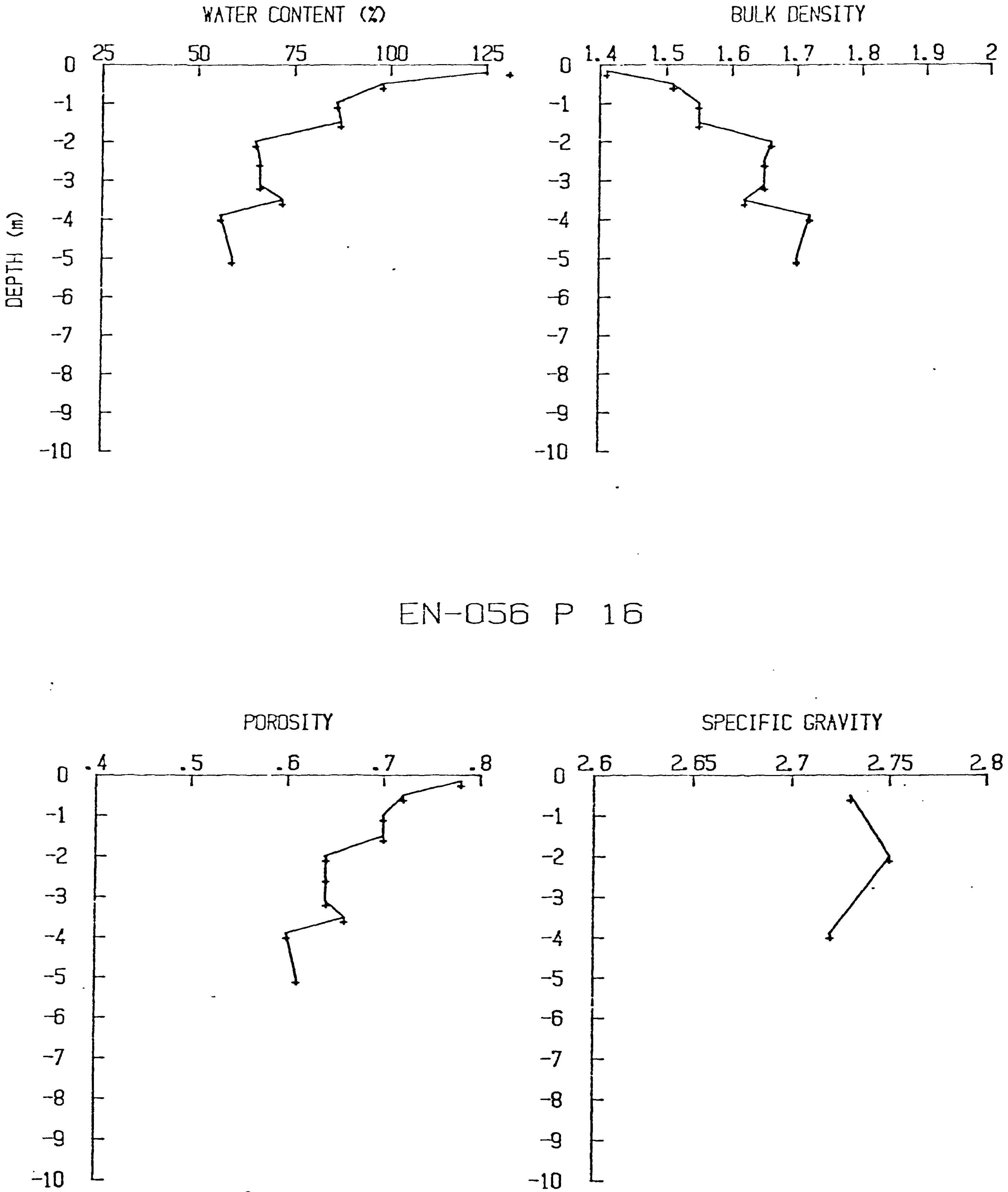

Figure 3p. Water content, bulk density, porosity, and grain-specific gravity vs. depth in core.

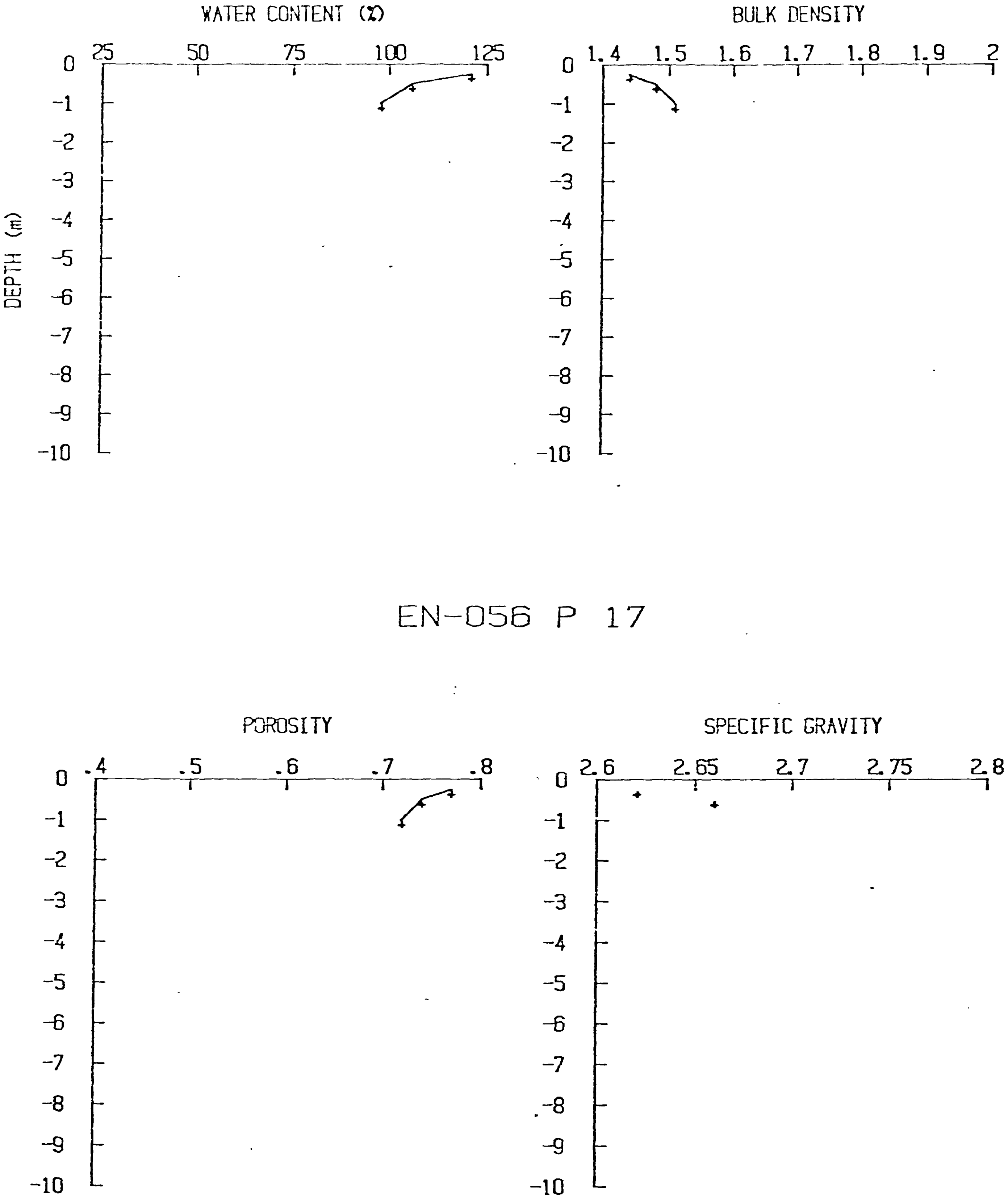

Figure 3q. Water content, bulk density, porosity, and grain-specific gravity vs. depth in core.

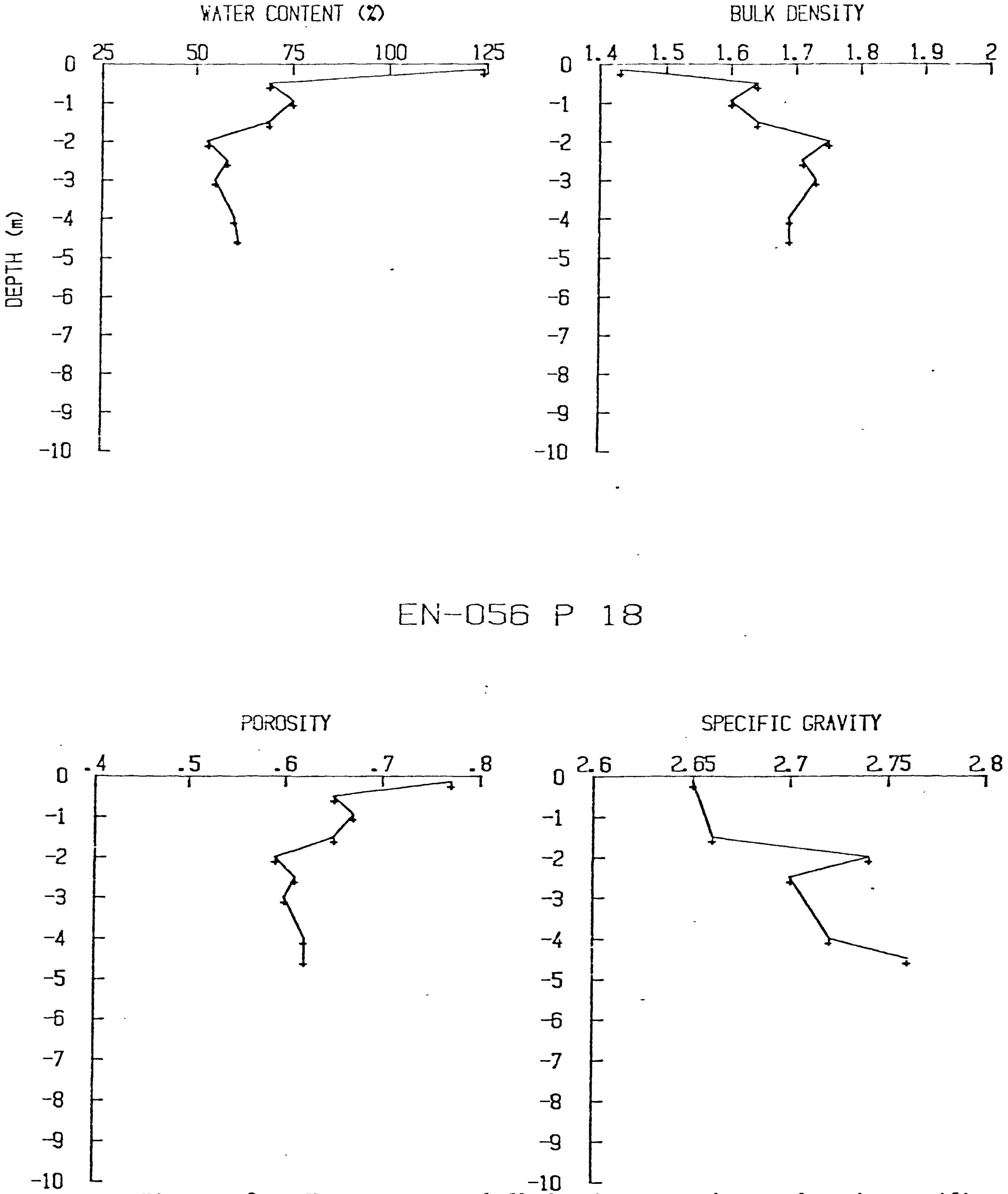

Figure 3r. Water content, bulk density, porosity, and grain-specific gravity vs. depth in core.

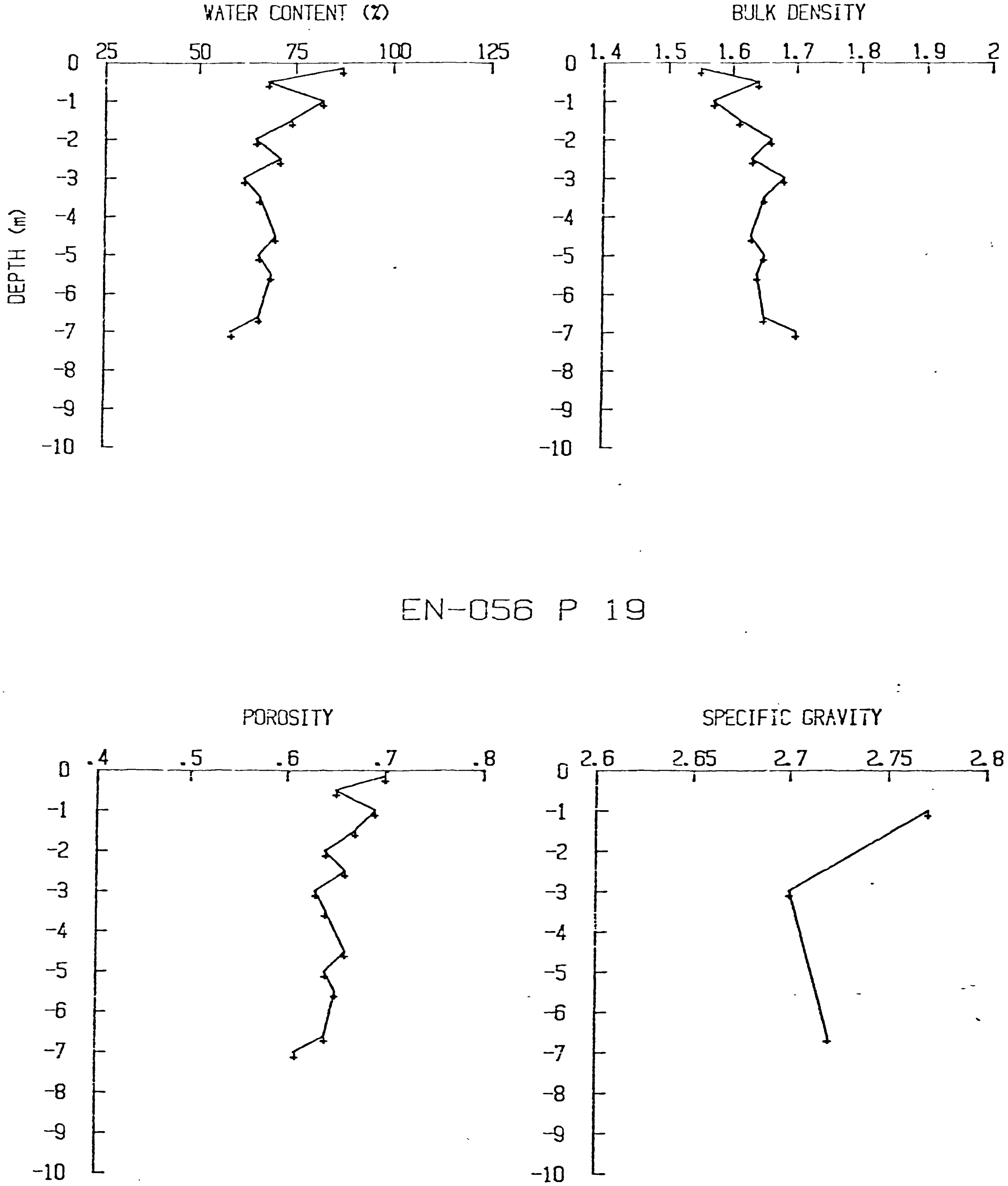

Figure 3s. Water content, bulk density, porosity, and grain-specific gravity vs. depth in core.

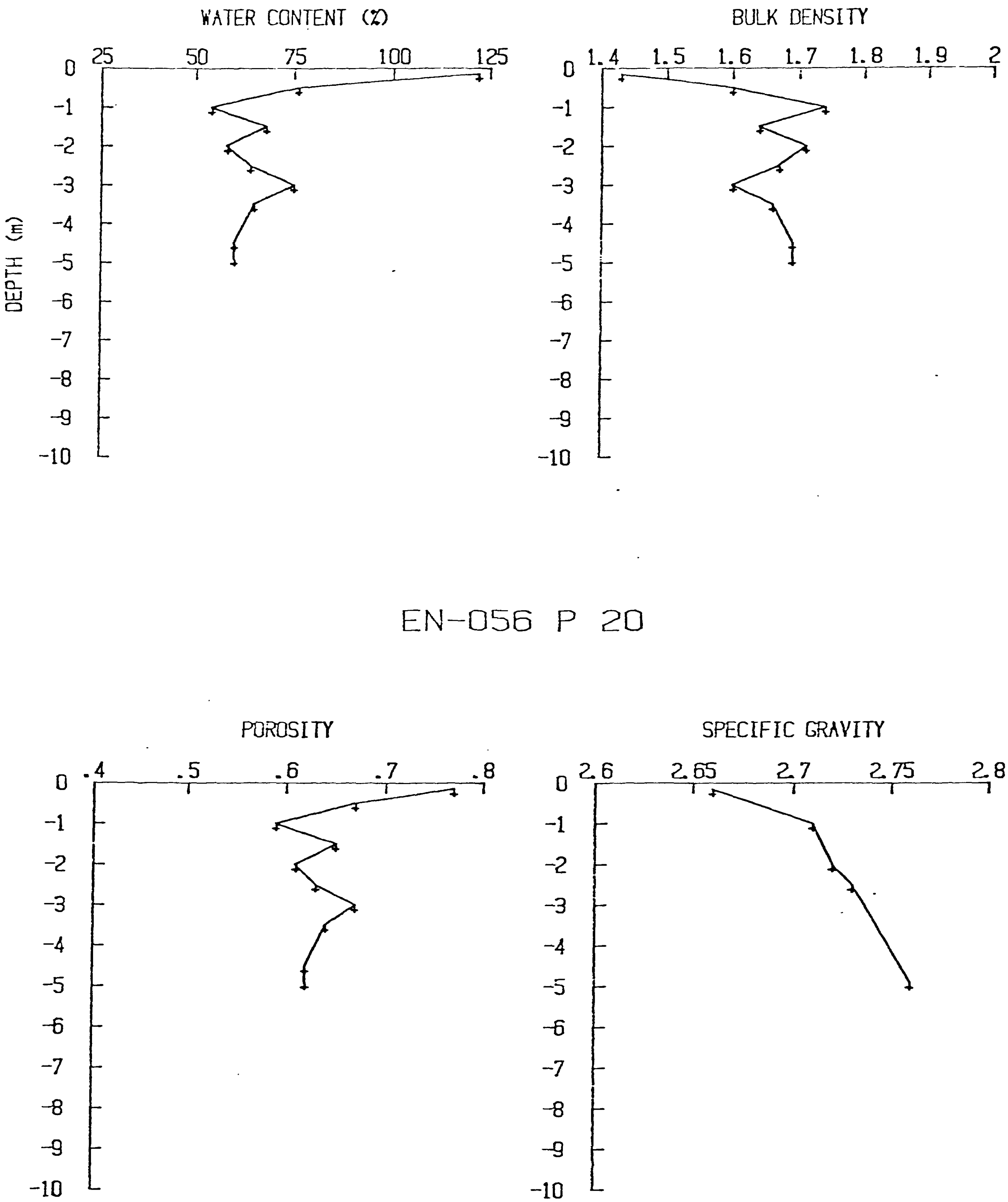

Figure 3t. Water content, bulk density, porosity, and grain-specific gravity vs. depth in core.

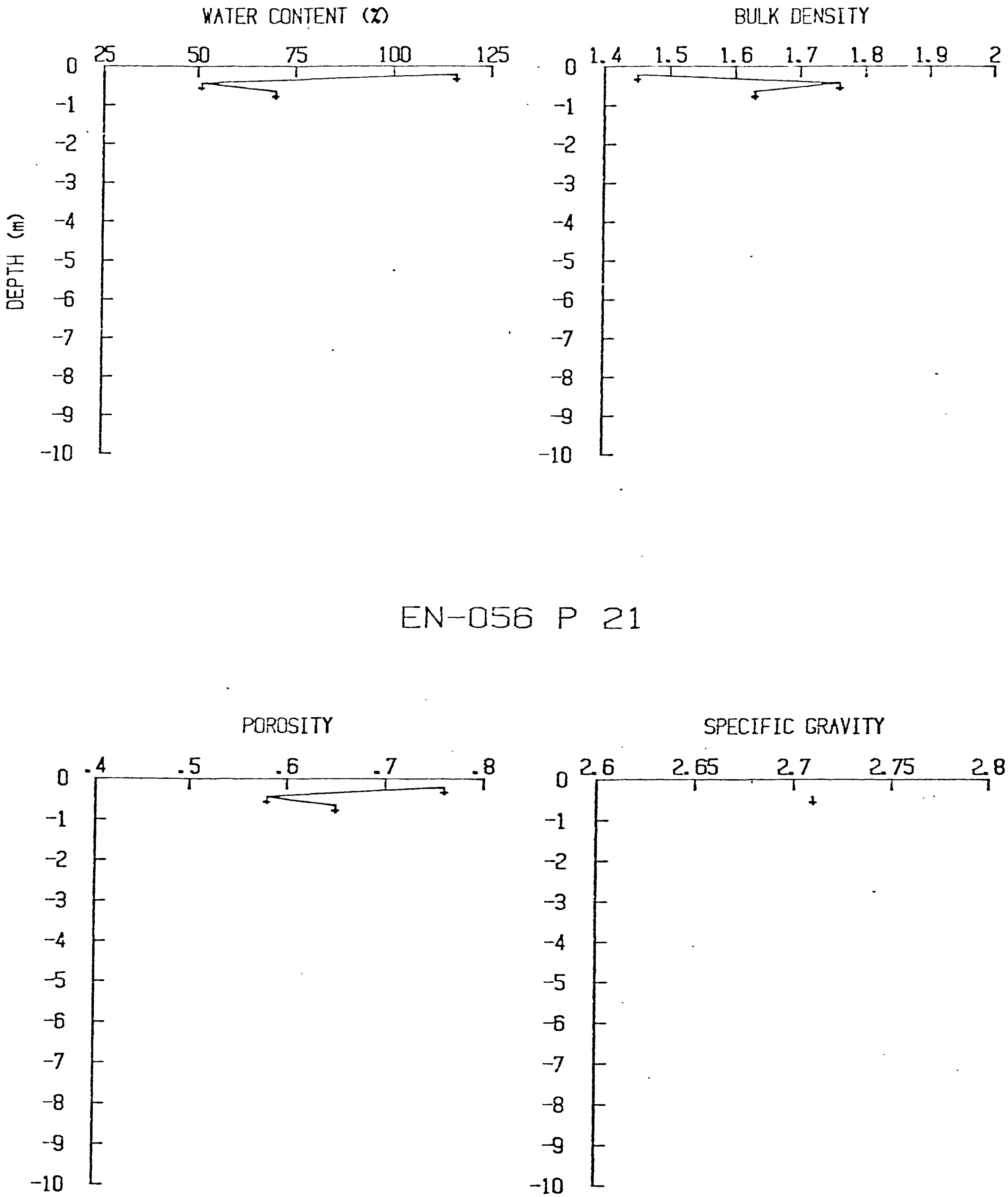

Figure 3u. Water content, bulk density, porosity, and grain-specific gravity vs. depth in core.

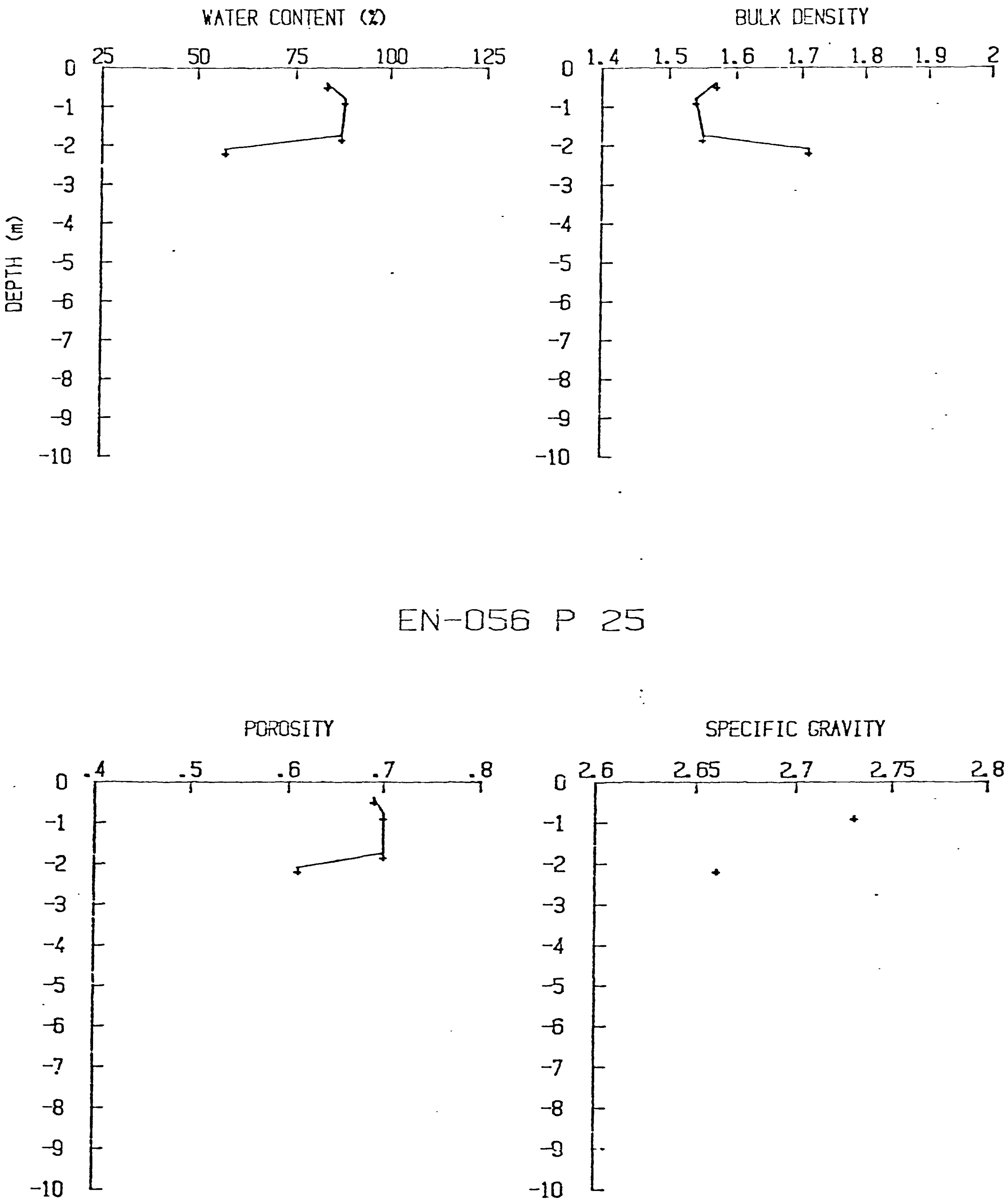

Figure 3v. Water content, bulk density, porosity, and grain-specific gravity vs. depth in core.

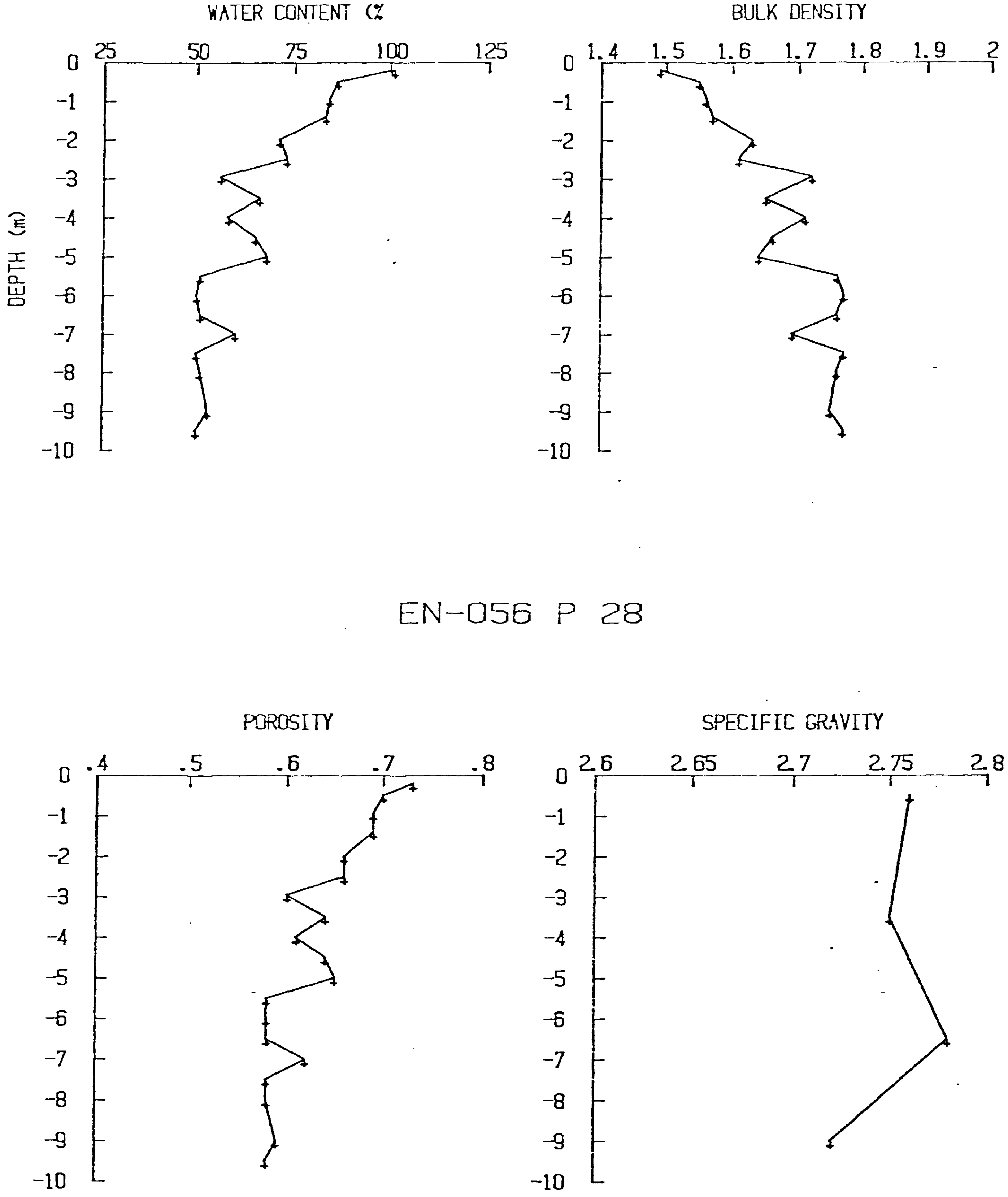

Figure 3w. Water content, bulk density, porosity, and grain-specific gravity vs. depth in core.

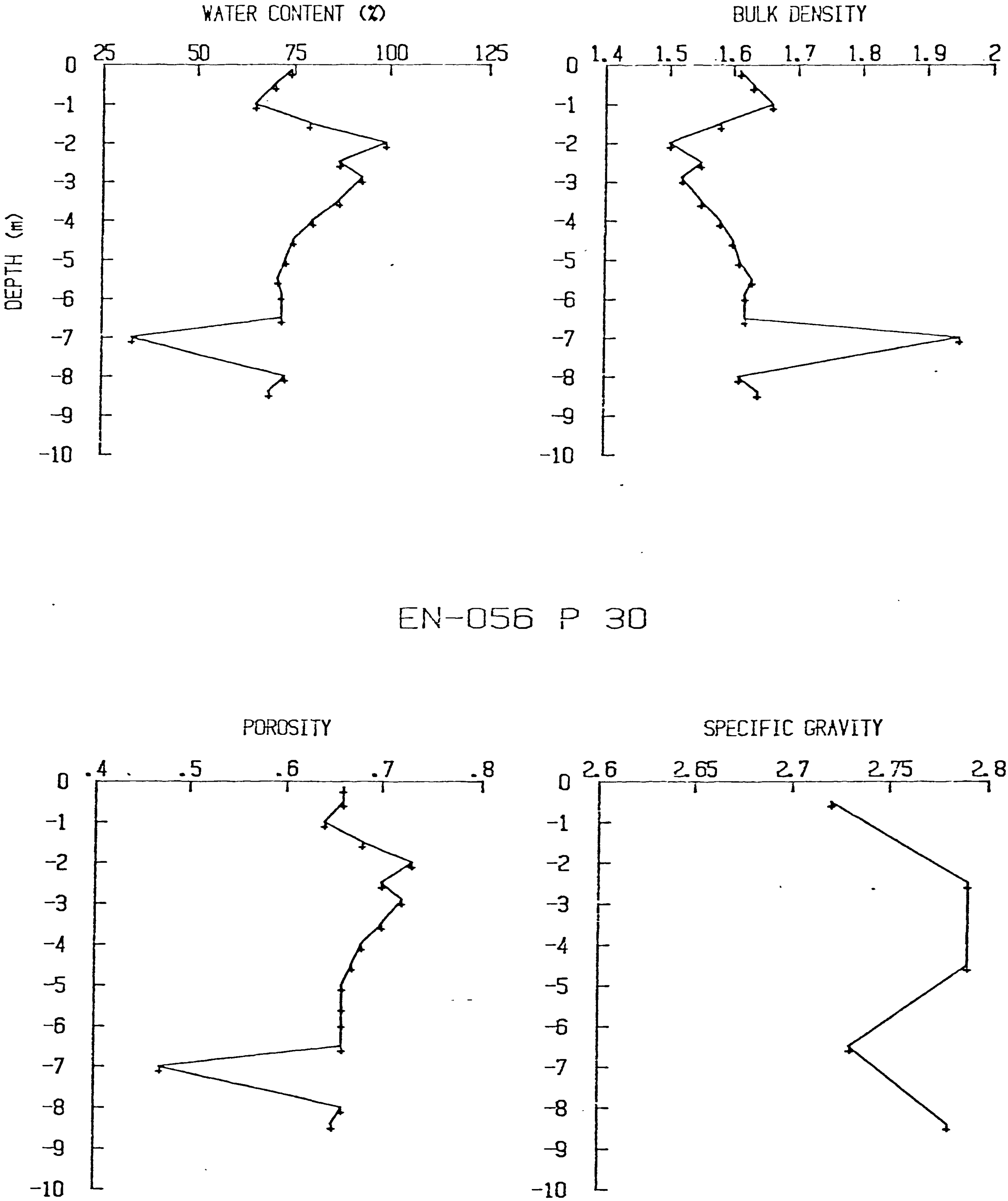

Figure 3x. Water content, bulk density, porosity, and grain-specific gravity vs. depth in core.

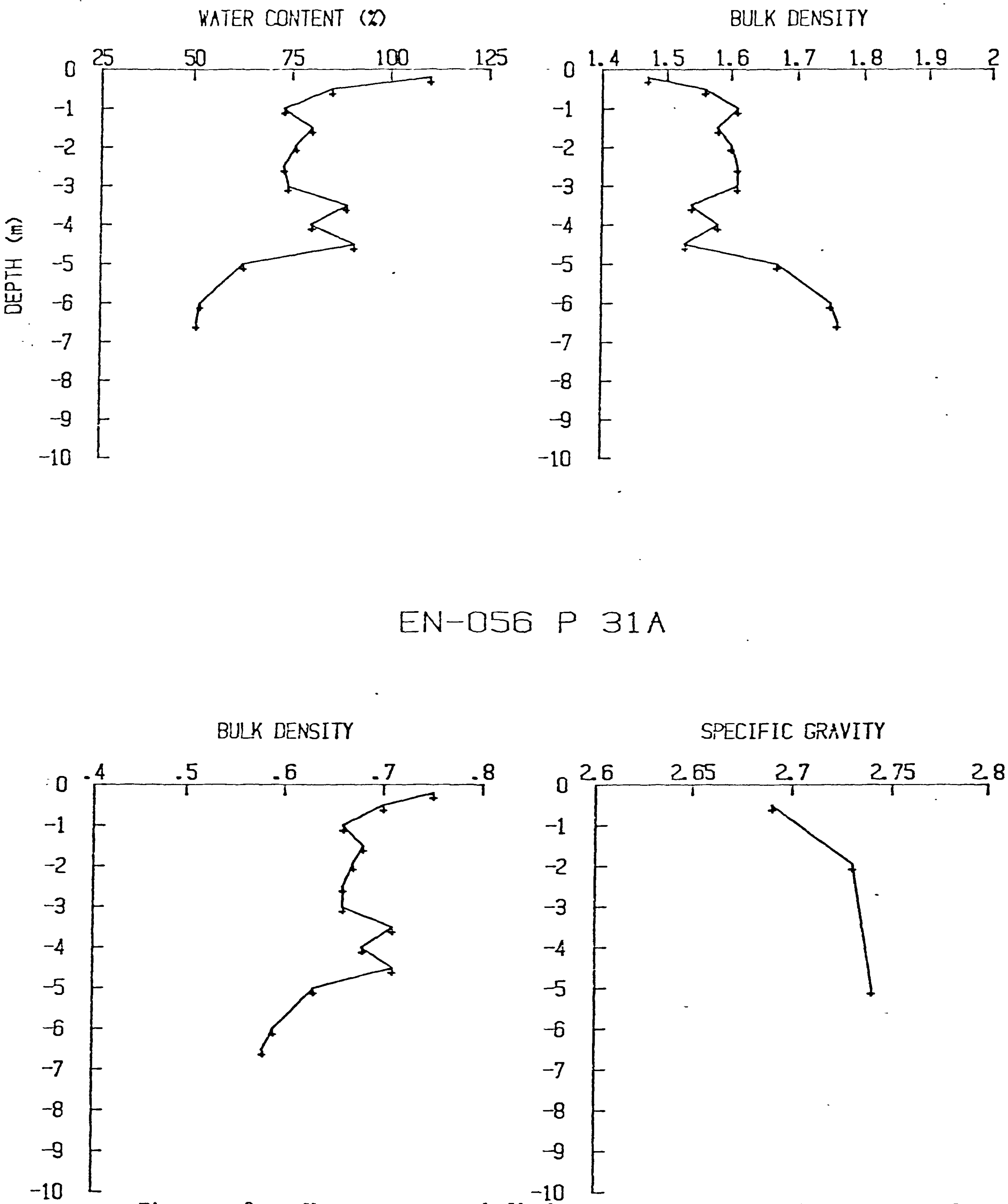

Figure 3y. Water content, bulk density, porosity, and grain-specific gravity vs. depth in core.

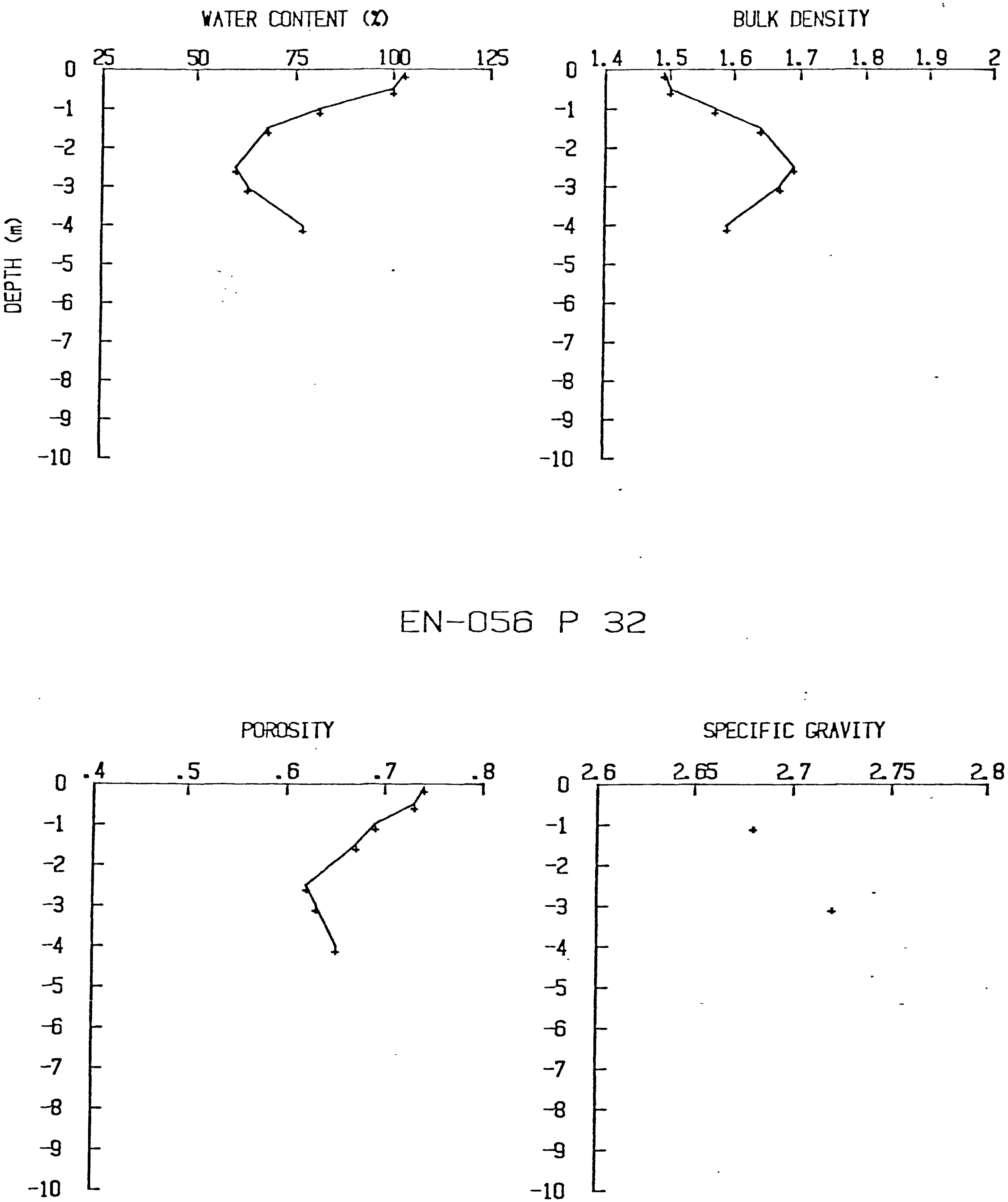

Figure 3z. Water content, bulk density, porosity, and grain-specific gravity vs. depth in core.

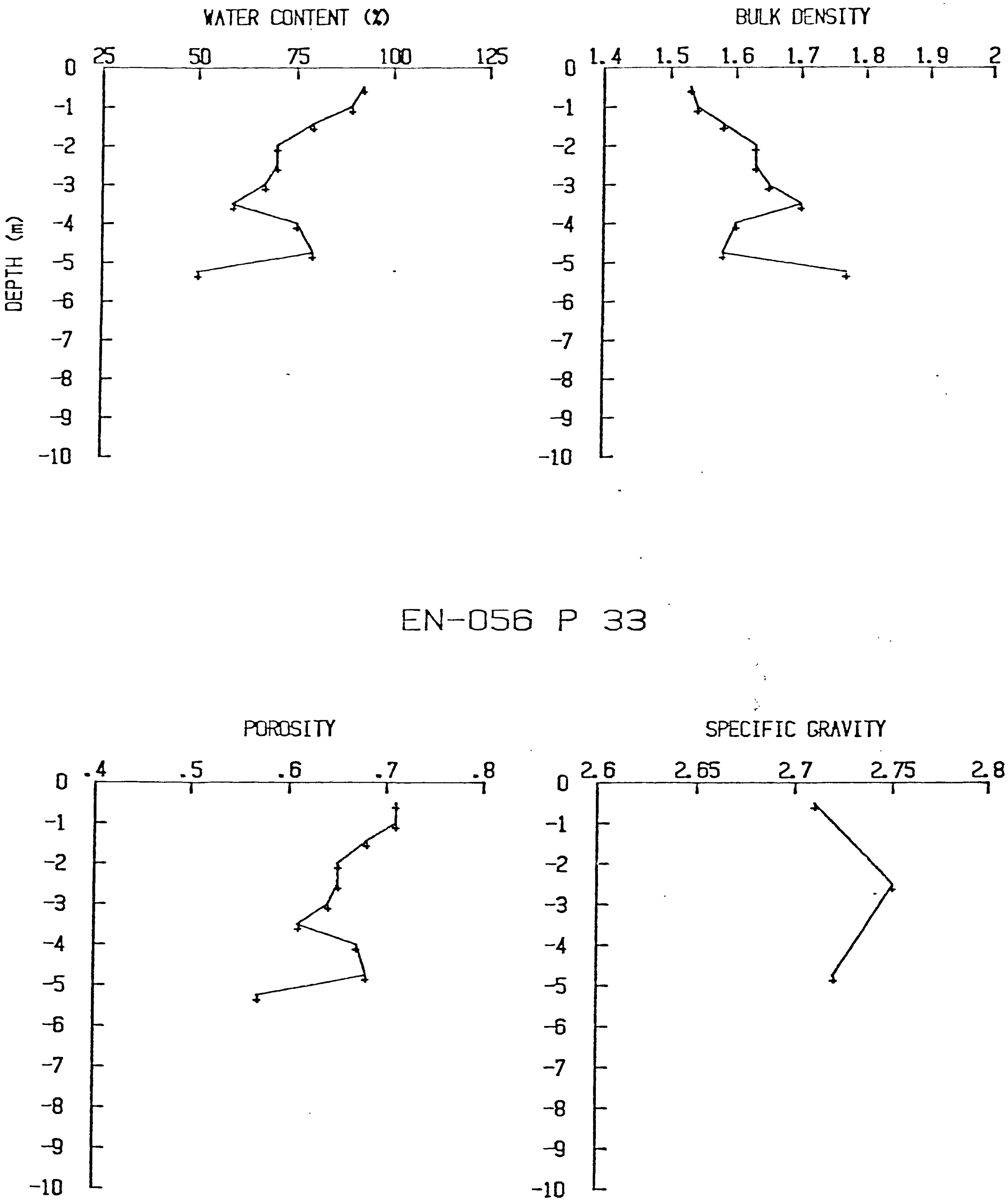

Figure 3aa. Water content, bulk density, porosity, and grain-specific gravity vs. depth in core.

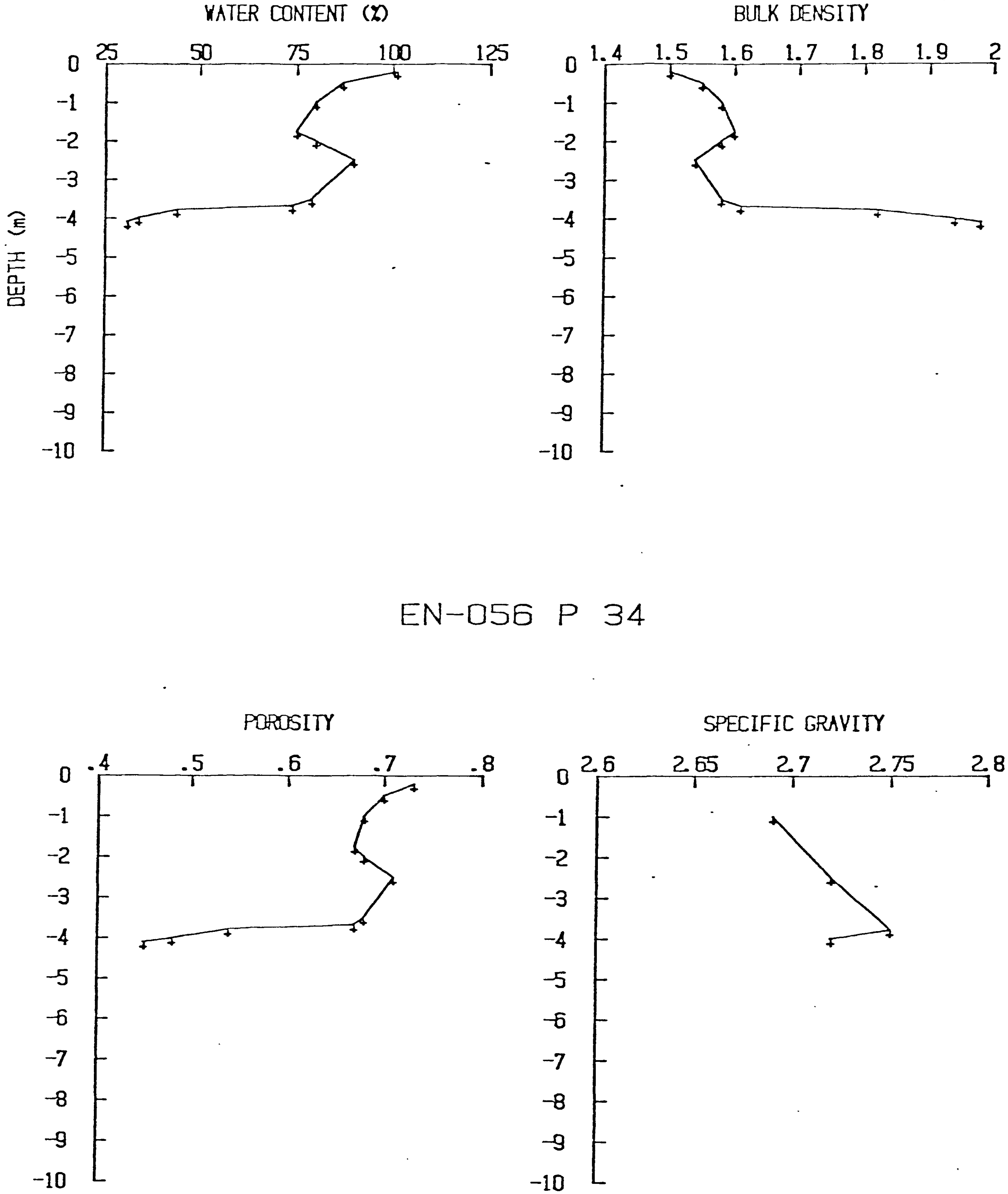

Figure 3bb. Water content, bulk density, porosity, and grain-specific gravity vs. depth in core.

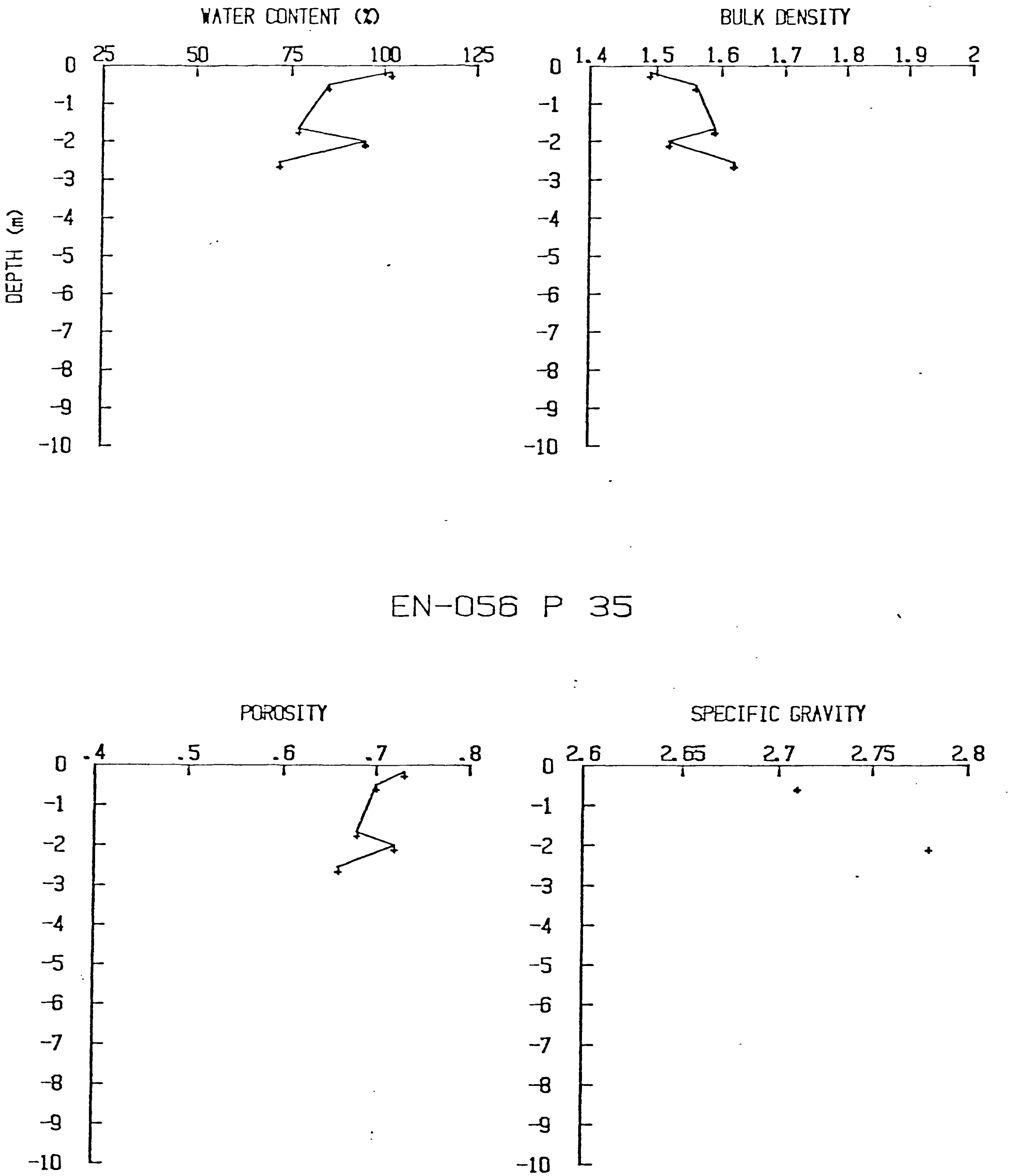

Figure 3cc. Water content, bulk density, porosity, and grain-specific gravity vs. depth in core.

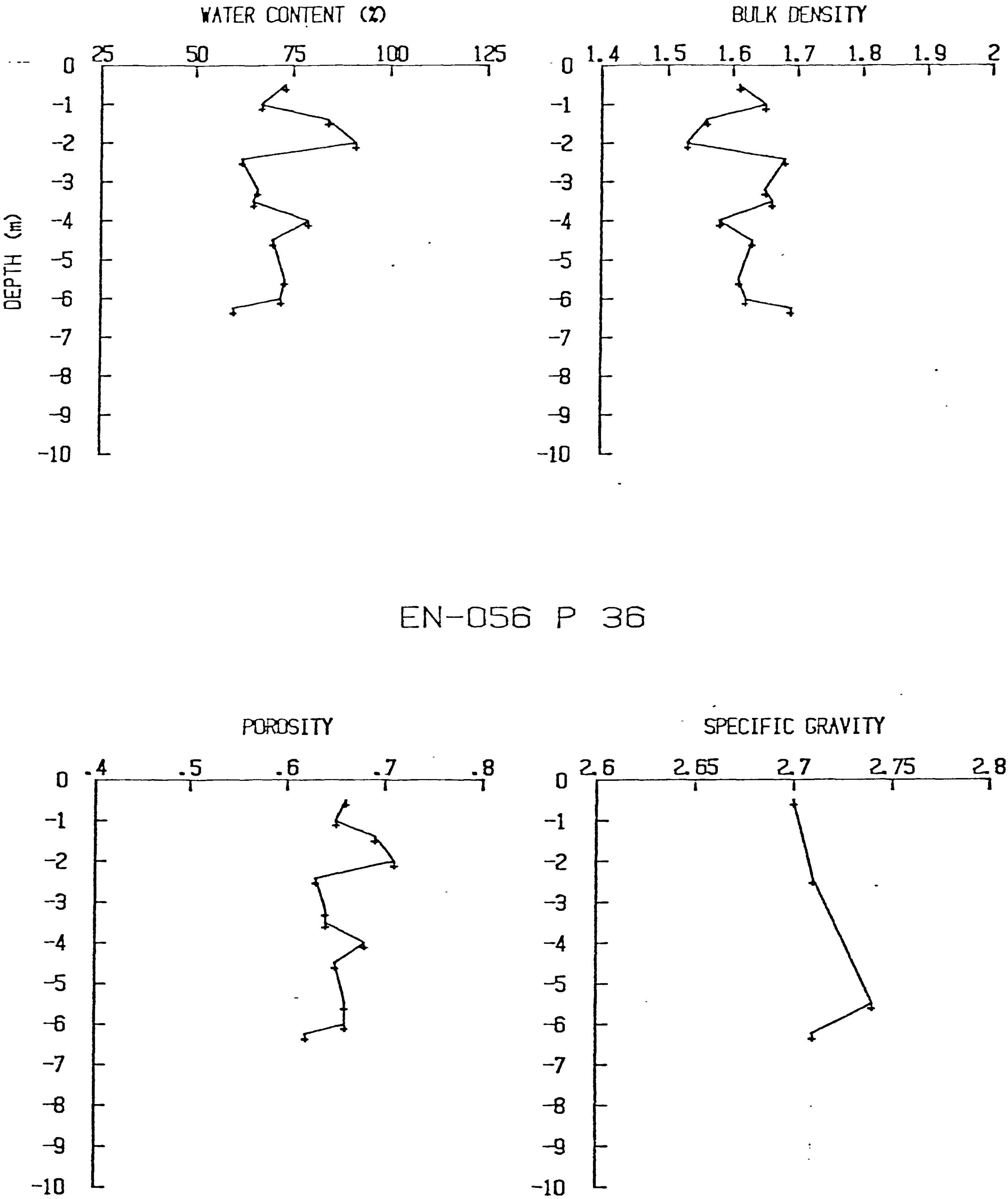

Figure 3dd. Water content, bulk density, porosity, and grain-specific gravity vs. depth in core.

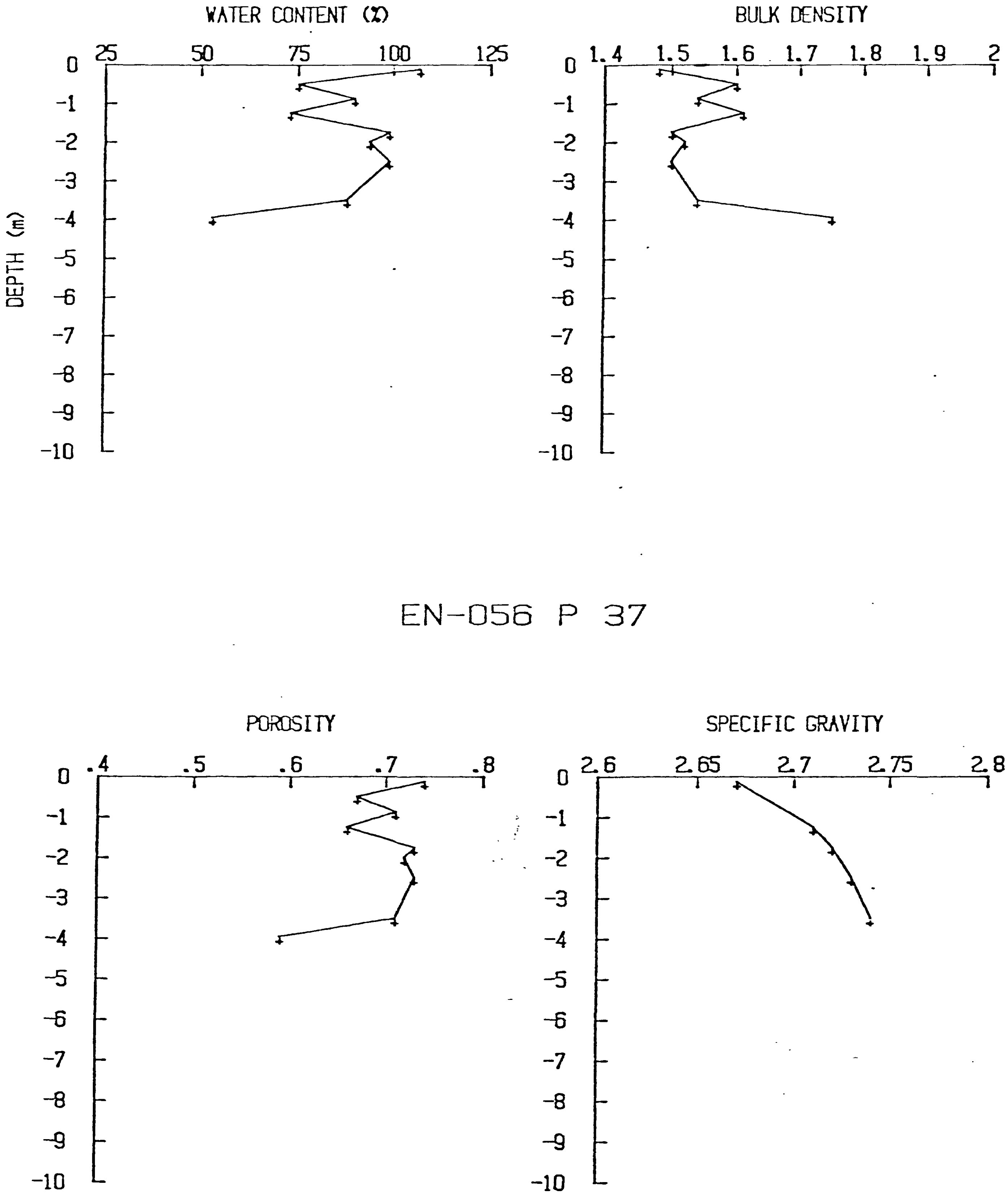

Figure 3ee. Water content, bulk density, porosity, and grain-specific gravity vs. depth in core.

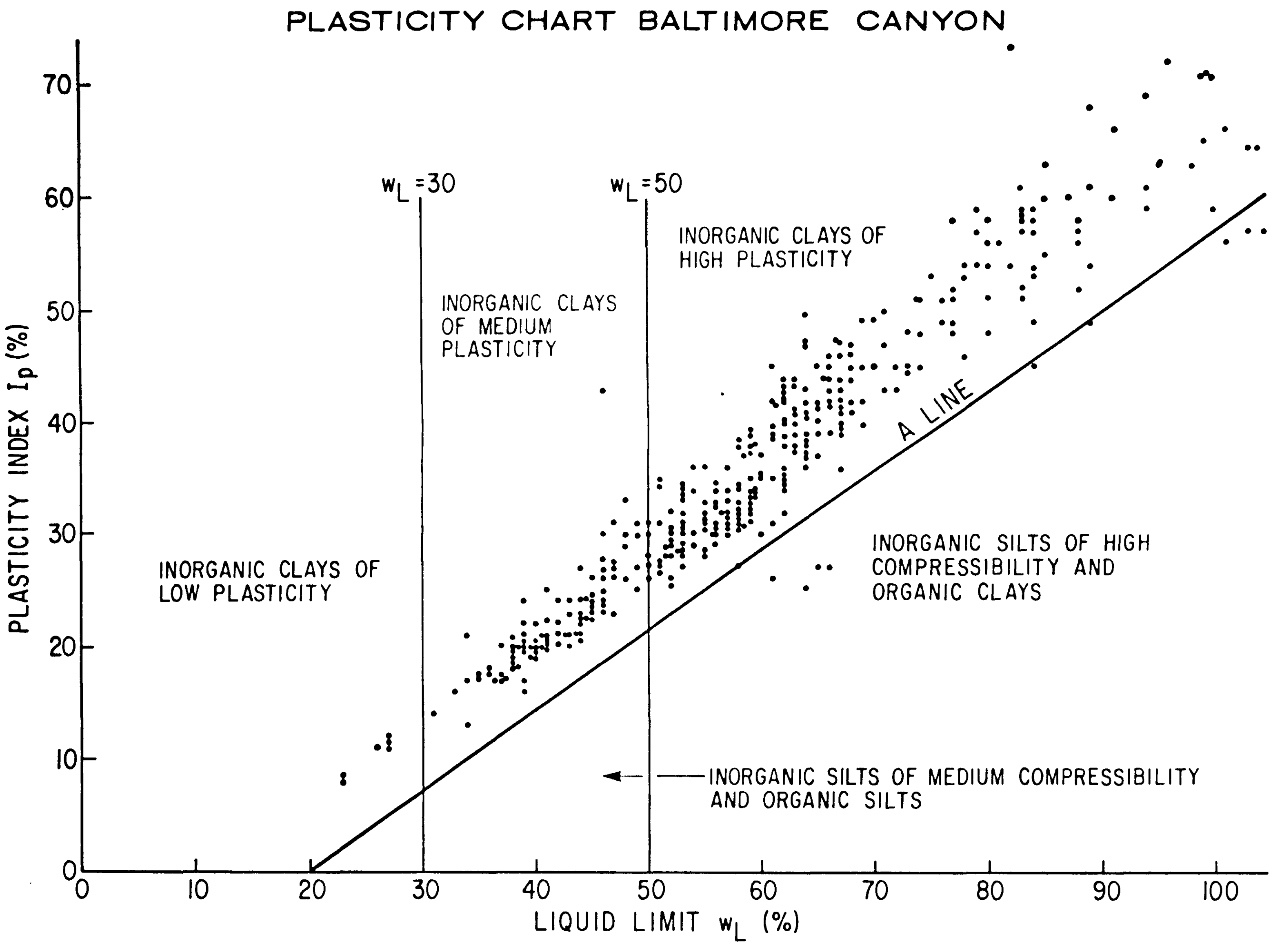

Figure 4. Classification of sediments based on plasticity characteristics.

There are areal trends in the data. Both liquid limit and plastic limit tend to increase in the downslope direction, as does plasticity index. Keller and others (1979) also noted these trends, which apparently are a reflection of a general decrease in grain size in the seaward direction.

The control exerted by grain size over these properties is also reflected in the vertical profiles (fig. 5a-5ee). Downcore fluctuations in values of liquid limit and plastic limit are highly correlated with sediment texture: an increase in these values generally means that finer material is present, and a decrease indicates the presence of coarser material (e.g., PC43, fig. 5f). Mineralogy, which may also have a major effect on these two limits, is fairly constant in these cores (L. J. Poppe, unpub. data, 1982), and, therefore, probably does not represent an important source of variability. The profiles also show that liquid limit is more sensitive than plastic limit (P31A and P36 in figs. 5y and 5dd) and that liquid limit has a slight tendency to decrease downcore. In fact, in almost all cases liquid limit decreases between the core top and the next sampling level (generally at a half meter). This may indicate an influx of finer grain sizes in recent time. The profiles show that, with the exception of a few short cores associated with erosional areas (e.g., P13, fig. 5m), water contents tend to be at or greater than the liquid limit. Underscoring this observation is the average I_L of 1.3 (table II). This phenomena ($w \geq w_L$) is common in the upper few meters of marine fine-grained sediments and implies that upon remolding from dynamic loading or other source of vibration or disturbance these surficial sediments may act more as a viscous fluid than as a plastic material. The fact that some of the short cores have water content values less than the liquid limit indicates that these core sites are erosional. That is, a continued increase in vertical stress from the addition of overburden causes an expulsion of interstitial water, eventually reducing water content to a value less than the liquid limit. Removing the overburden would therefore expose a compacted sediment surface that had a liquidity index of less than one.

Consolidation state and properties

Data on consolidation states are central in an overall geologic analysis. In this study the apparent consolidation states of the slope-rise surface sediment were determined by calculating the overconsolidation ratio (OCR) for several core sites. OCR values are based on the ratio of the preconsolidation stress (the maximum past stress experienced by the sample) to the assumed present overburden stress (the assumption is that pore pressure = hydrostatic pressure). If there is excess overburden relative to the degree of consolidation, OCR value is <1 and the sediment is underconsolidated; if the present overburden represents the greatest stress experienced (i.e., the sediment is fully compacted relative to its present overburden), OCR = 1 and the sediment is normally consolidated; and if there is insufficient overburden to account for the level of compaction, OCR>1 and the sediment is overconsolidated.

The results of the consolidation state analysis are shown in table III. None of the 25 cores tested were underconsolidated. Olsen and others (1982), however, did identify a few underconsolidated sites on the upper slope in this and adjacent areas. Between the two studies (~60 cores analyzed) and based on core-averaged OCR's, approximately 5% of the sites are judged to be underconsolidated. Not only is the distribution of underconsolidated

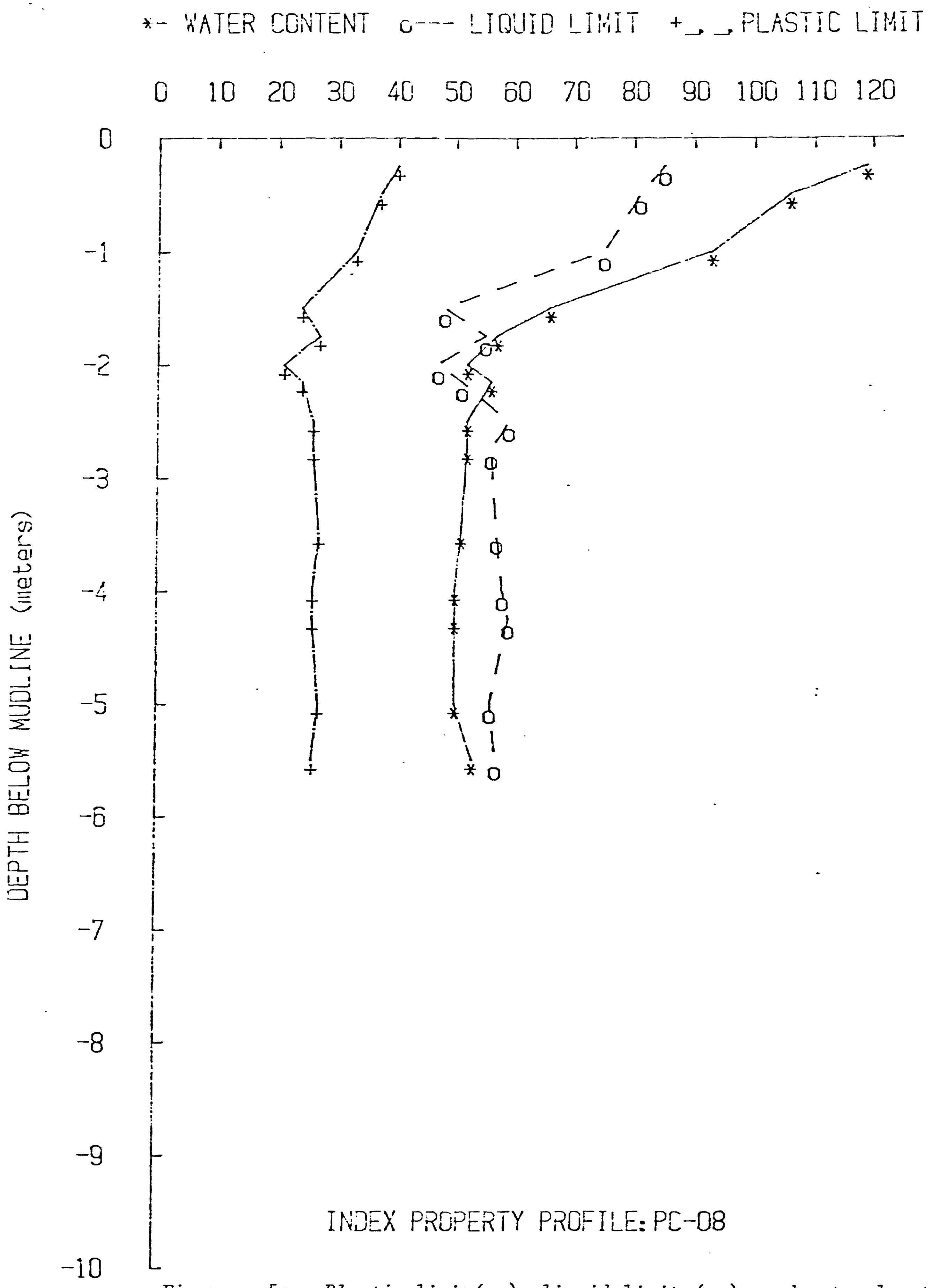

Figure 5a. Plastic limit(w_p), liquid limit (w_L), and natural water content (w) vs. depth in core.

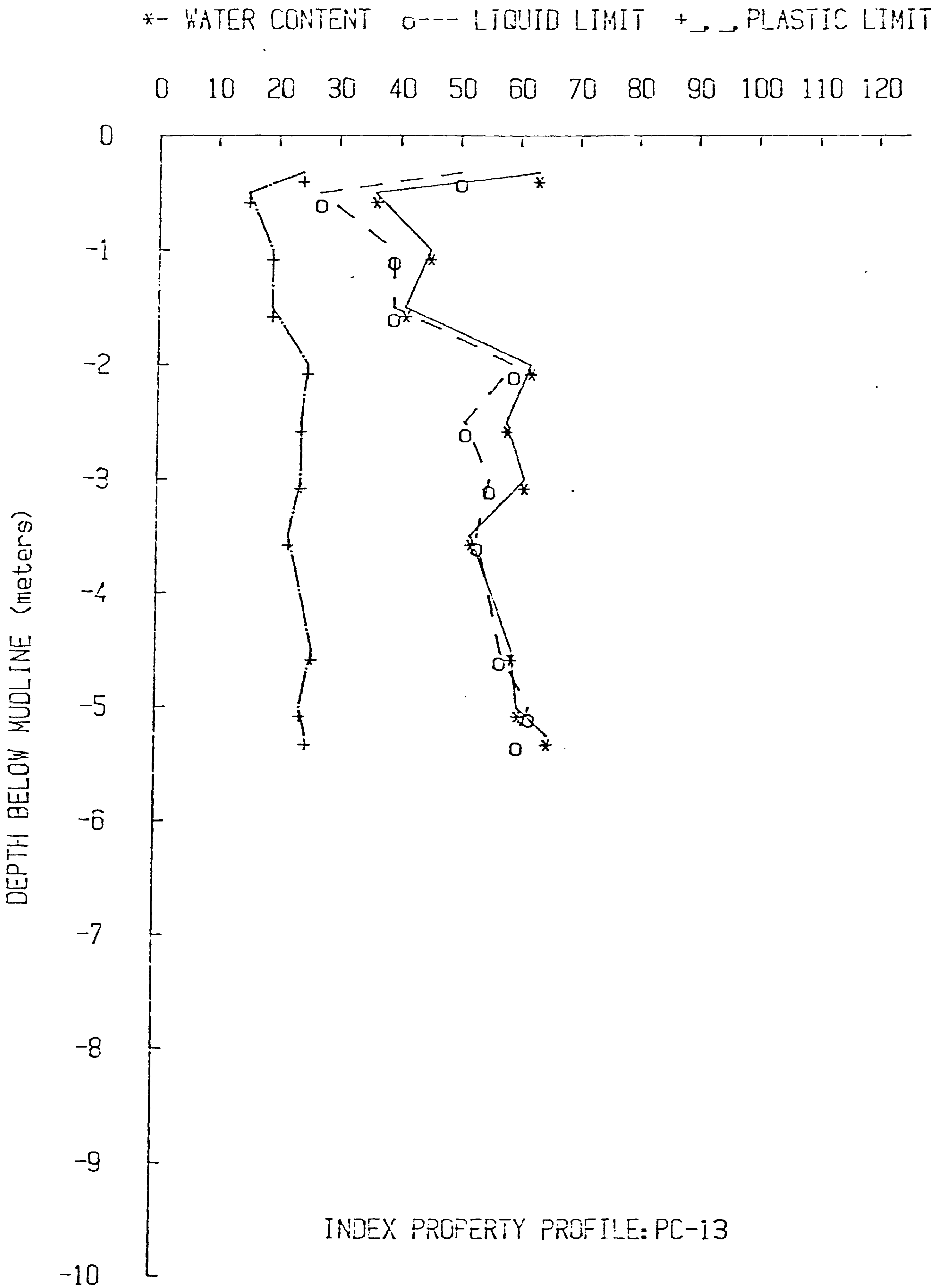

Figure 5b. Plastic limit (w_p), liquid limit (w_L), and natural water content (w) vs. depth in core.

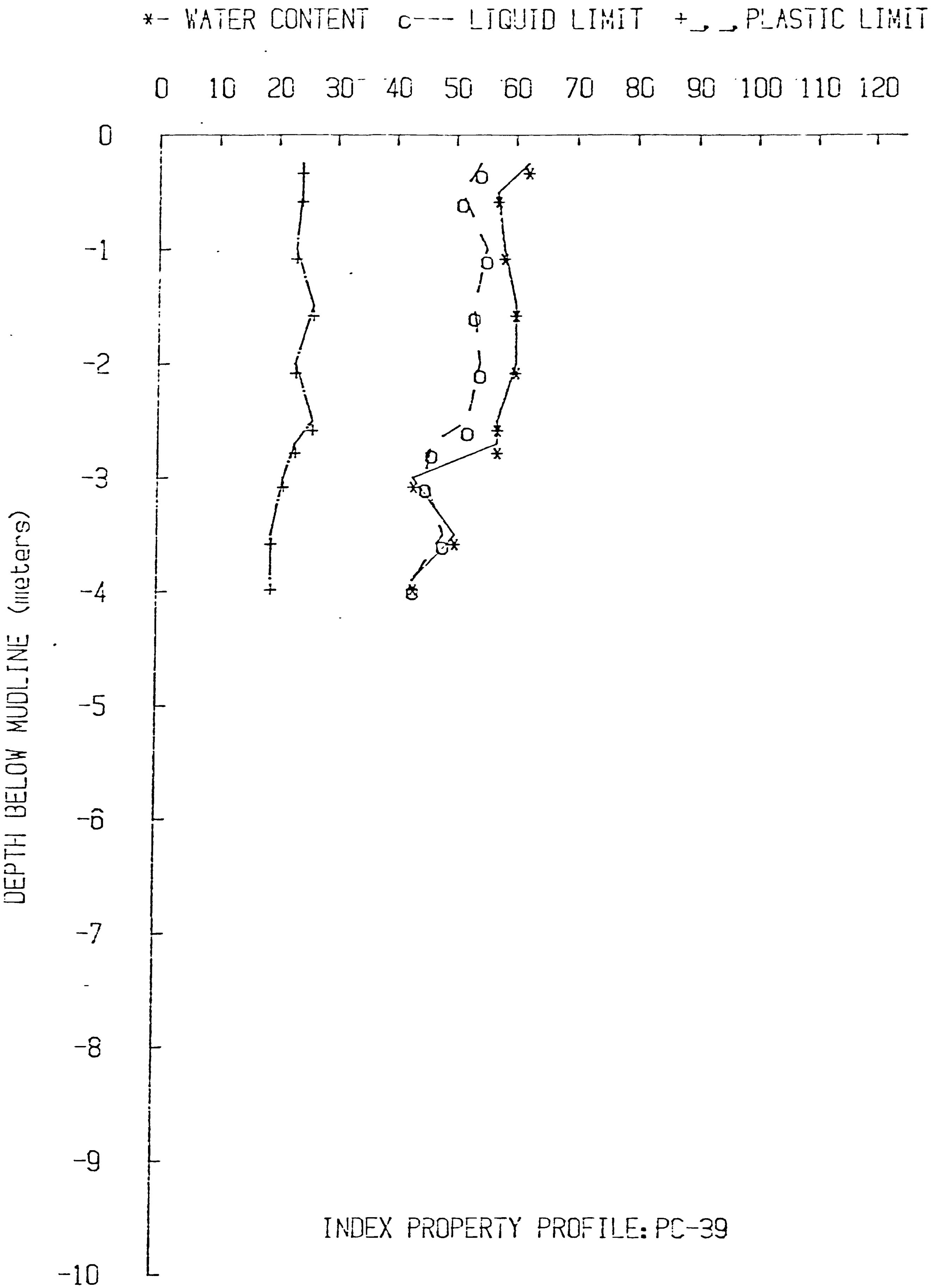

Figure 5c. Plastic limit (w_p), liquid limit (w_L), and natural water content (w) vs. depth in core.

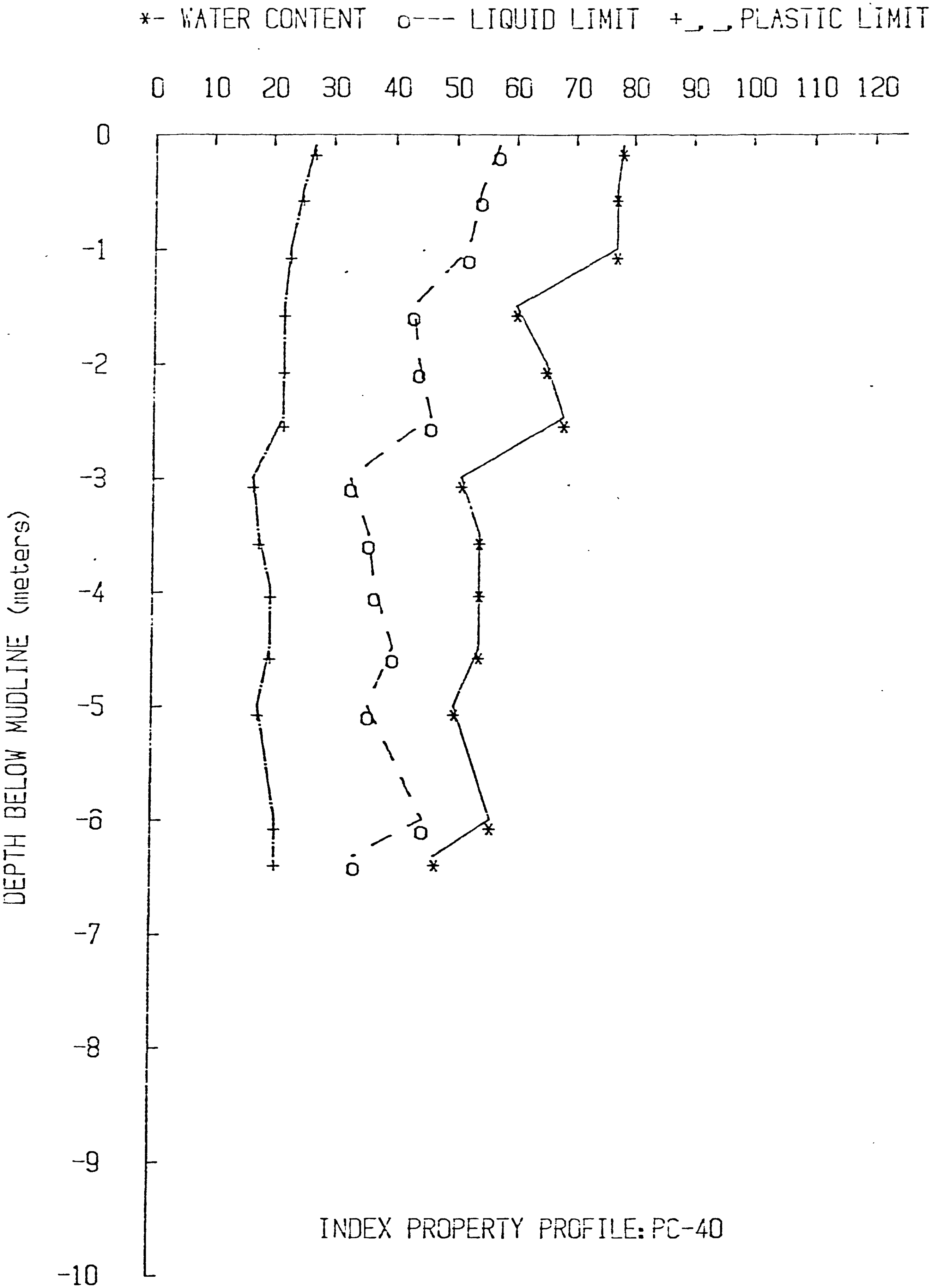

Figure 5d. Plastic limit (w_p), liquid limit (w_L), and natural water content (w) vs. depth in core.

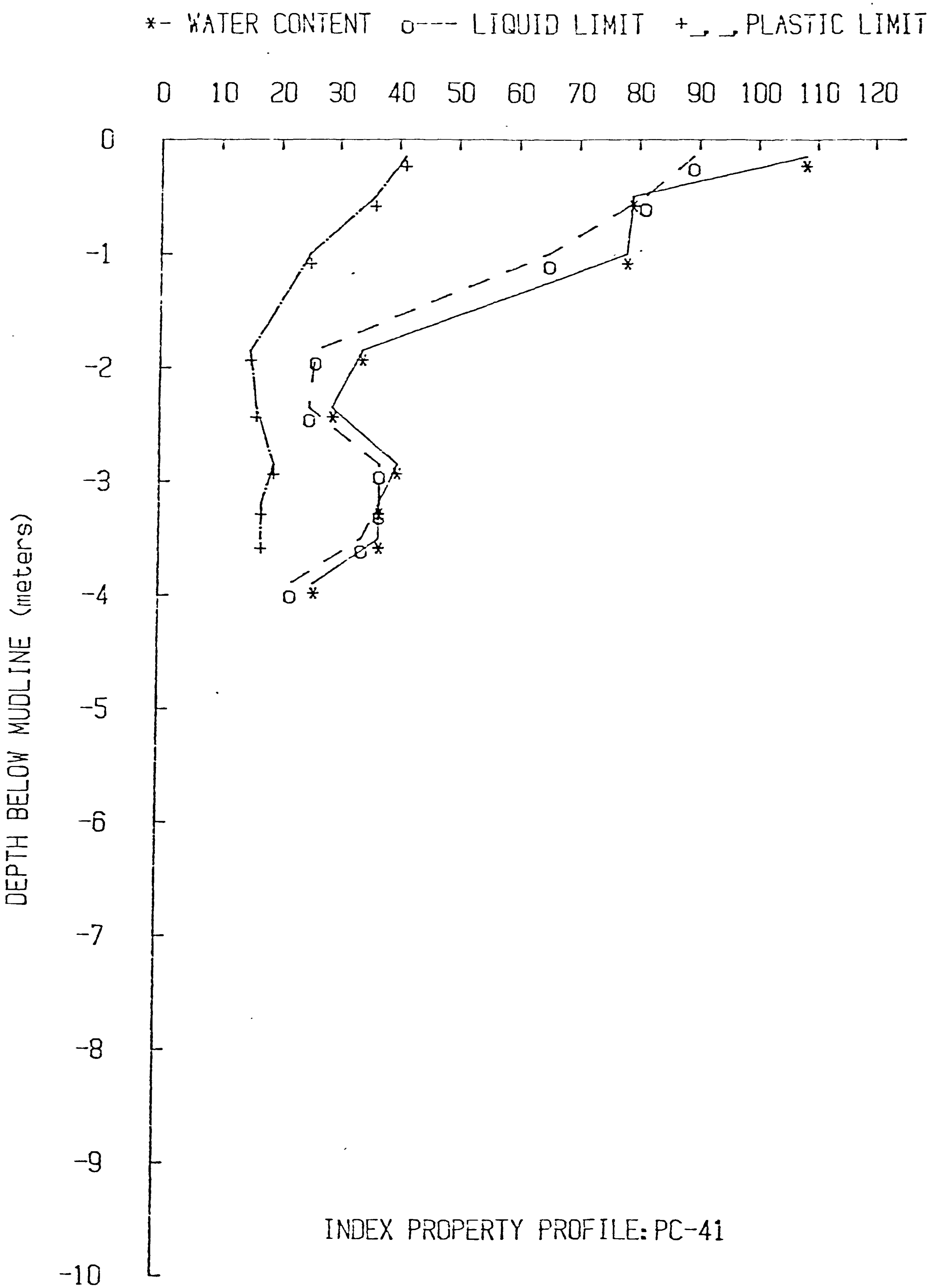

Figure 5e. Plastic limit (w_p), liquid limit (w_L), and natural water content (w) vs. depth in core.

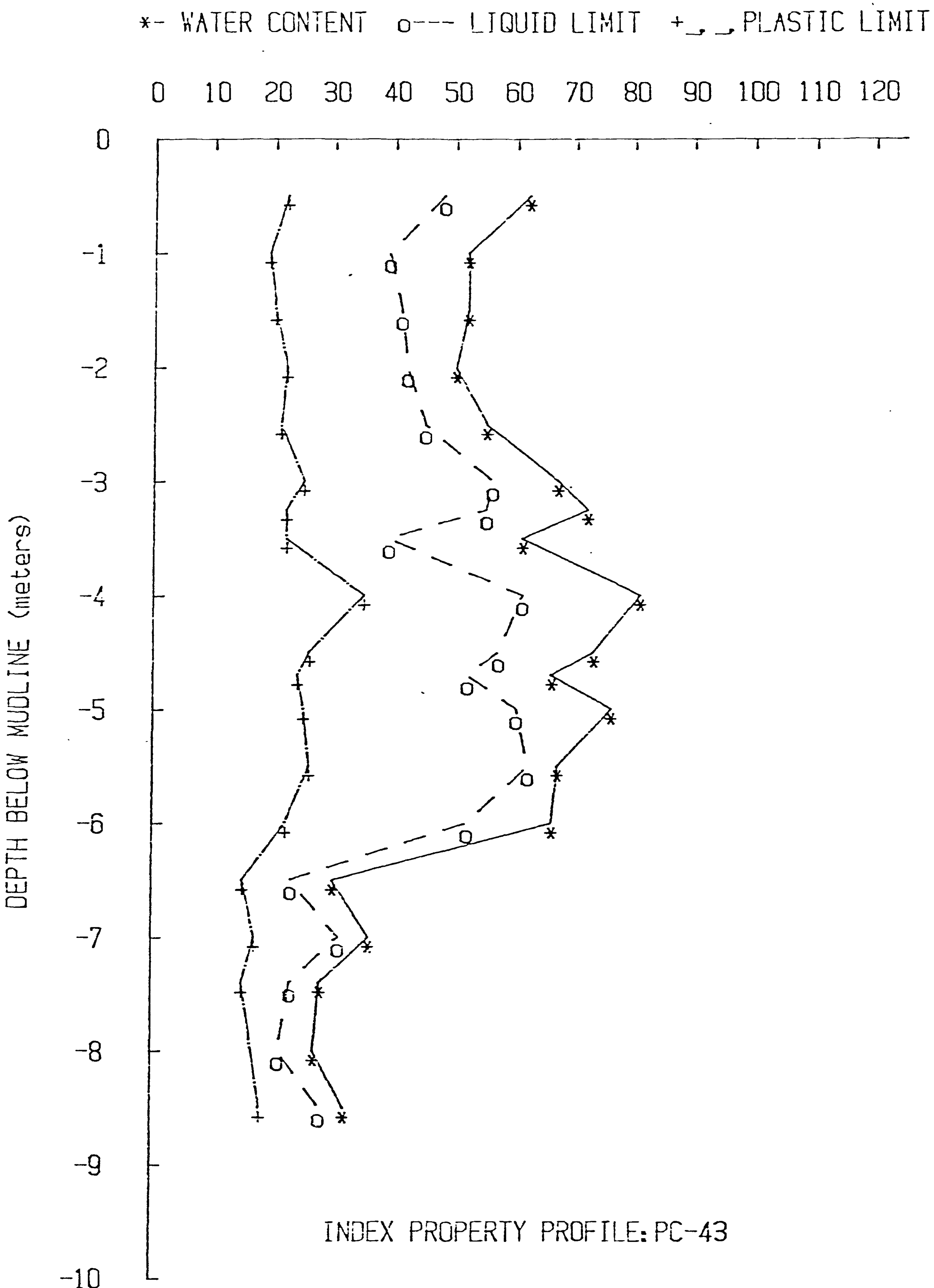

Figure 5f. Plastic limit (w_p), liquid limit (w_L), and natural water content (w) vs. depth in core.

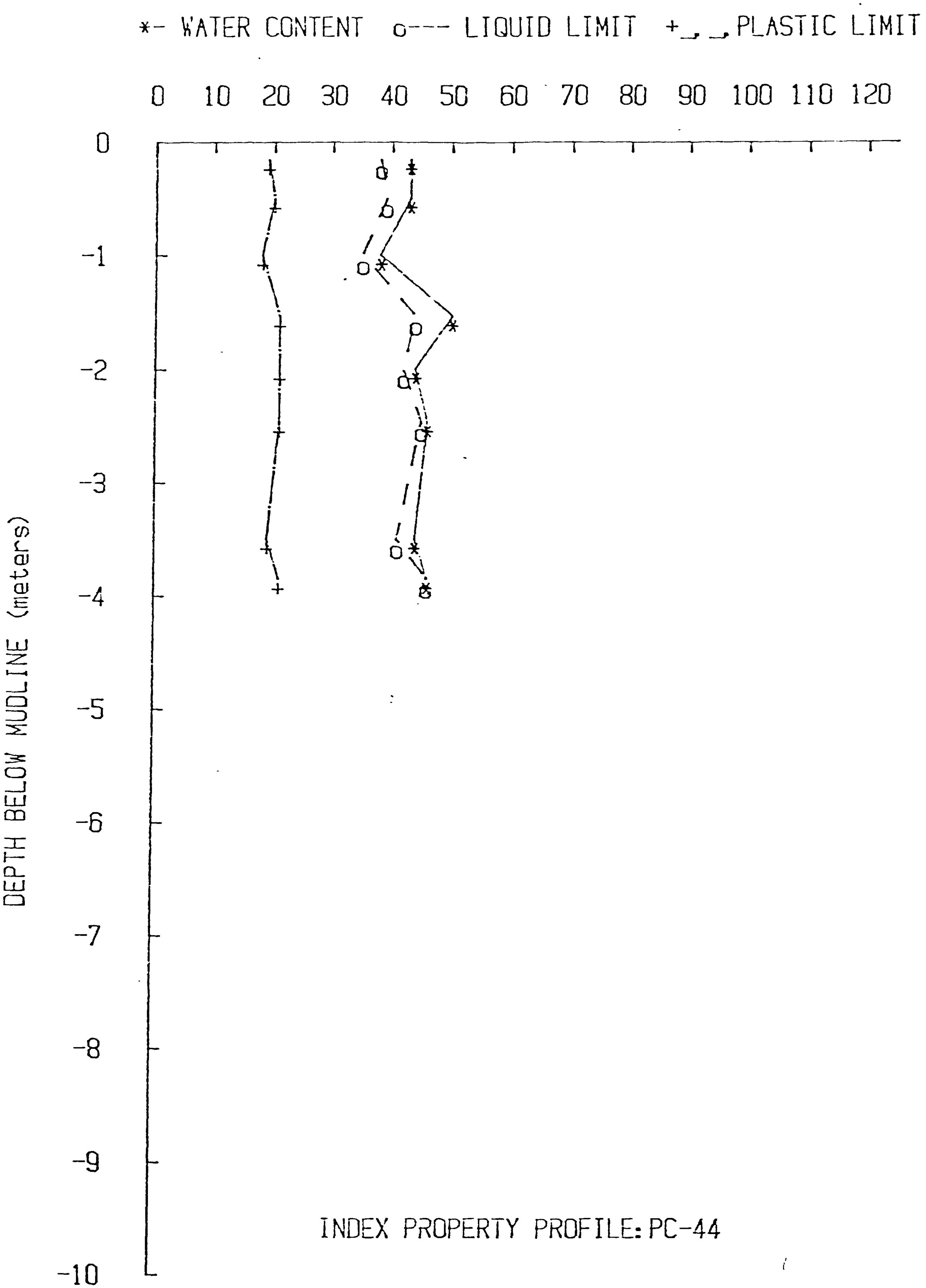

Figure 5g. Plastic limit (w_p), liquid limit (w_L), and natural water content (w) vs. depth in core.

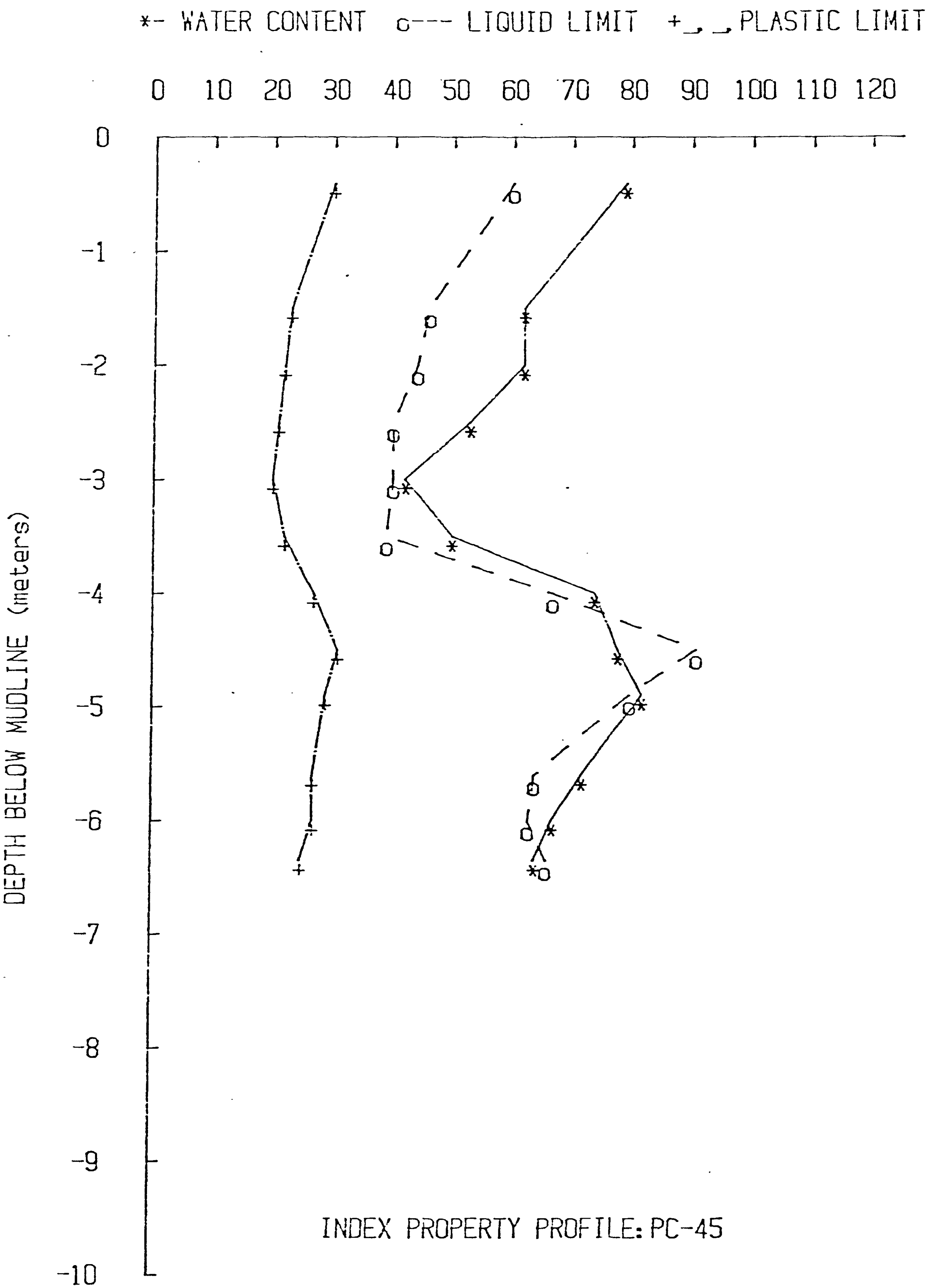

Figure 5h. Plastic limit (w_p), liquid limit (w_L), and natural water content (w) vs. depth in core.

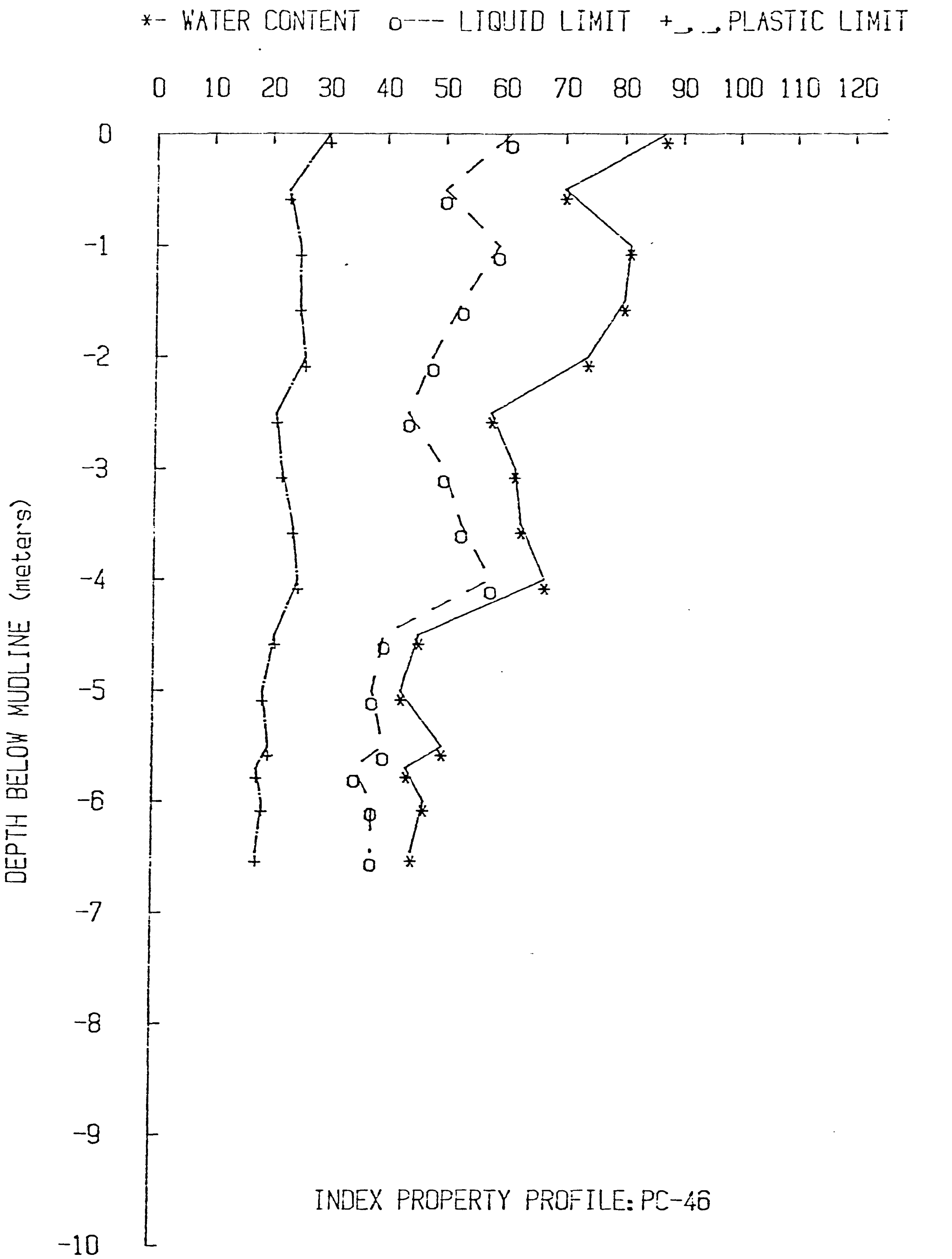

Figure 5i. Plastic limit (w_p), liquid limit (w_L), and natural water content (w) vs. depth in core.

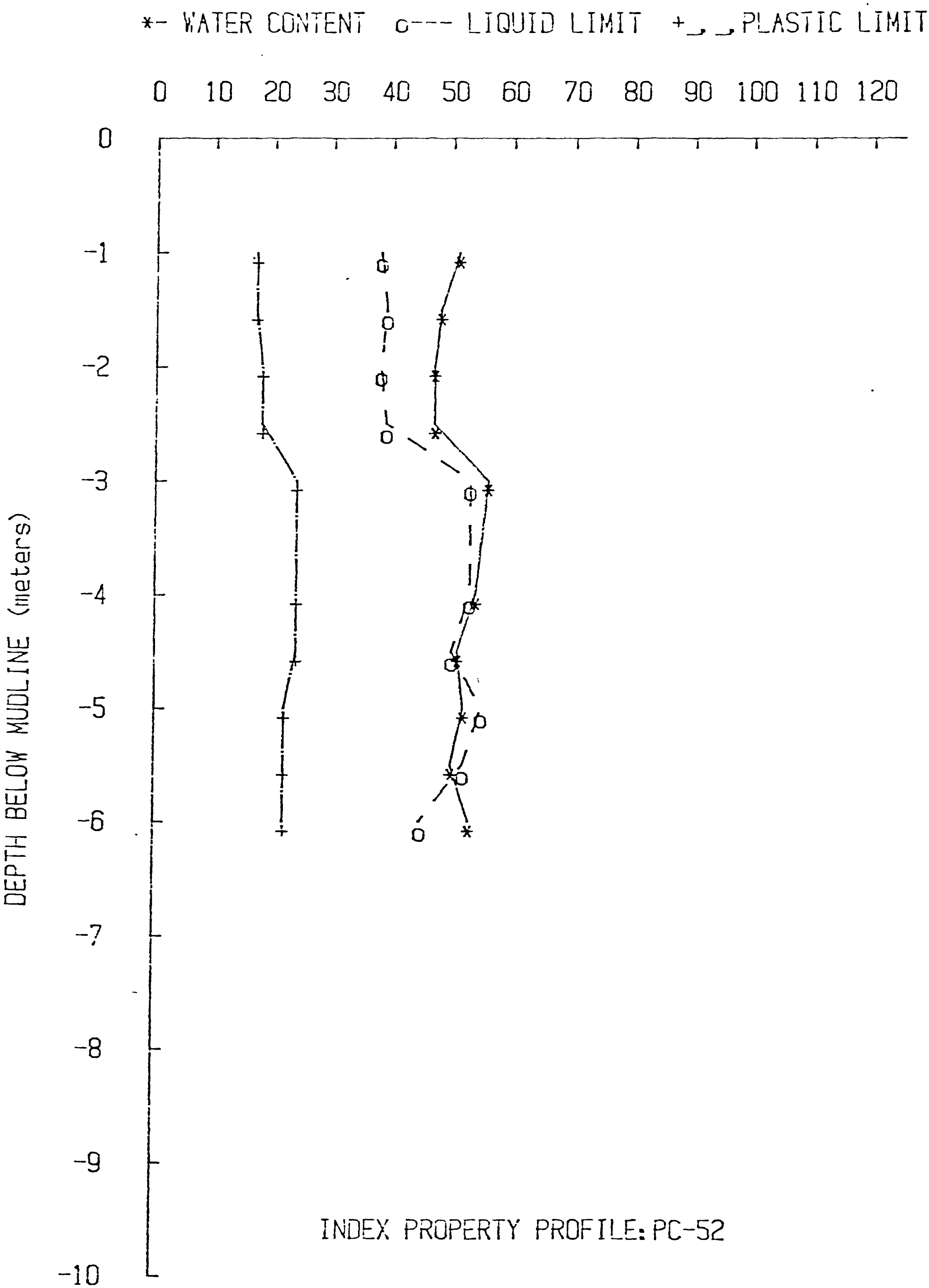

Figure 5j. Plastic limit (w_p), liquid limit (w_L), and natural water content (w) vs. depth in core.

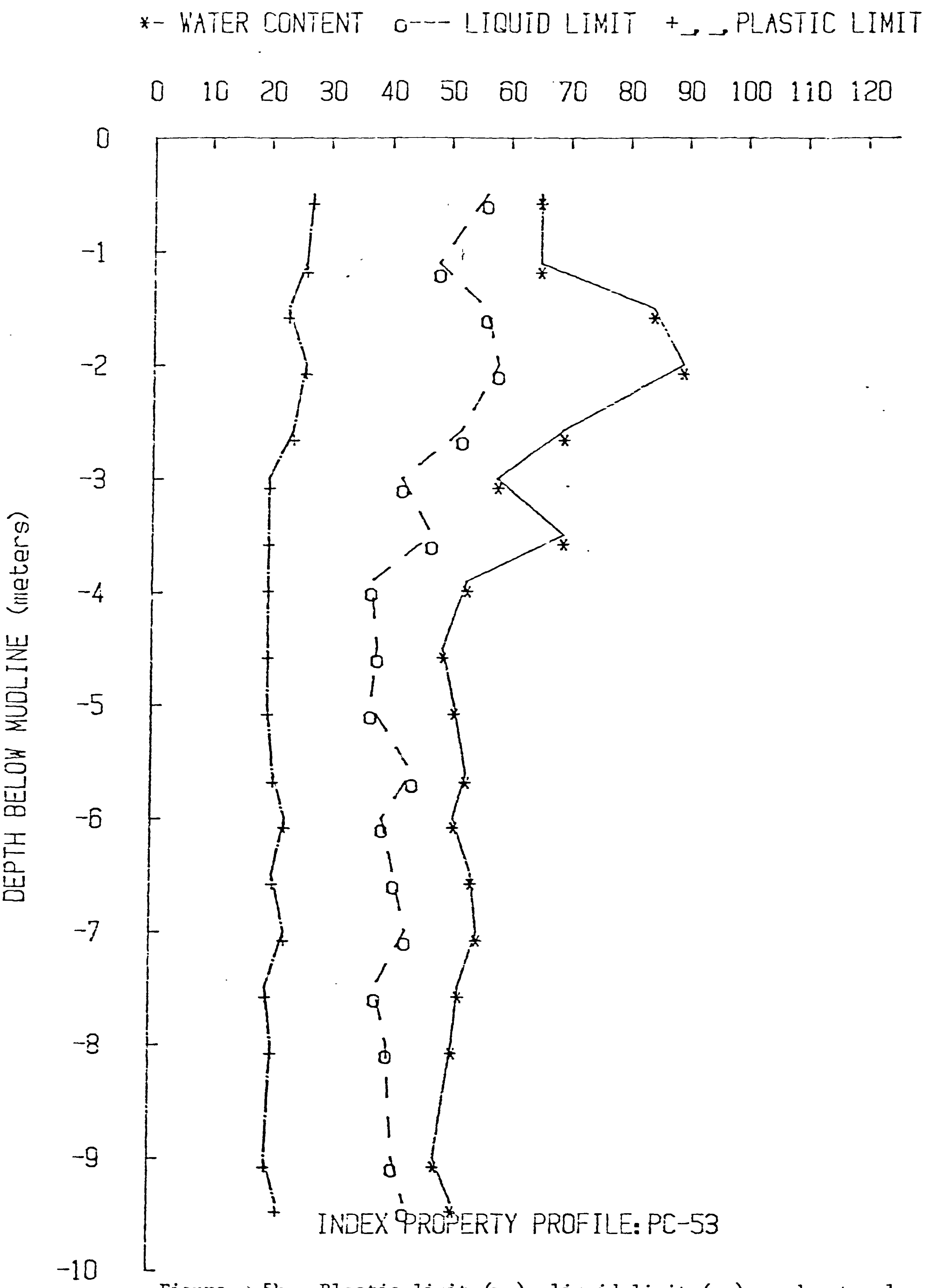

Figure 5k. Plastic limit (w_p), liquid limit (w_L), and natural water content (w) vs. depth in core.

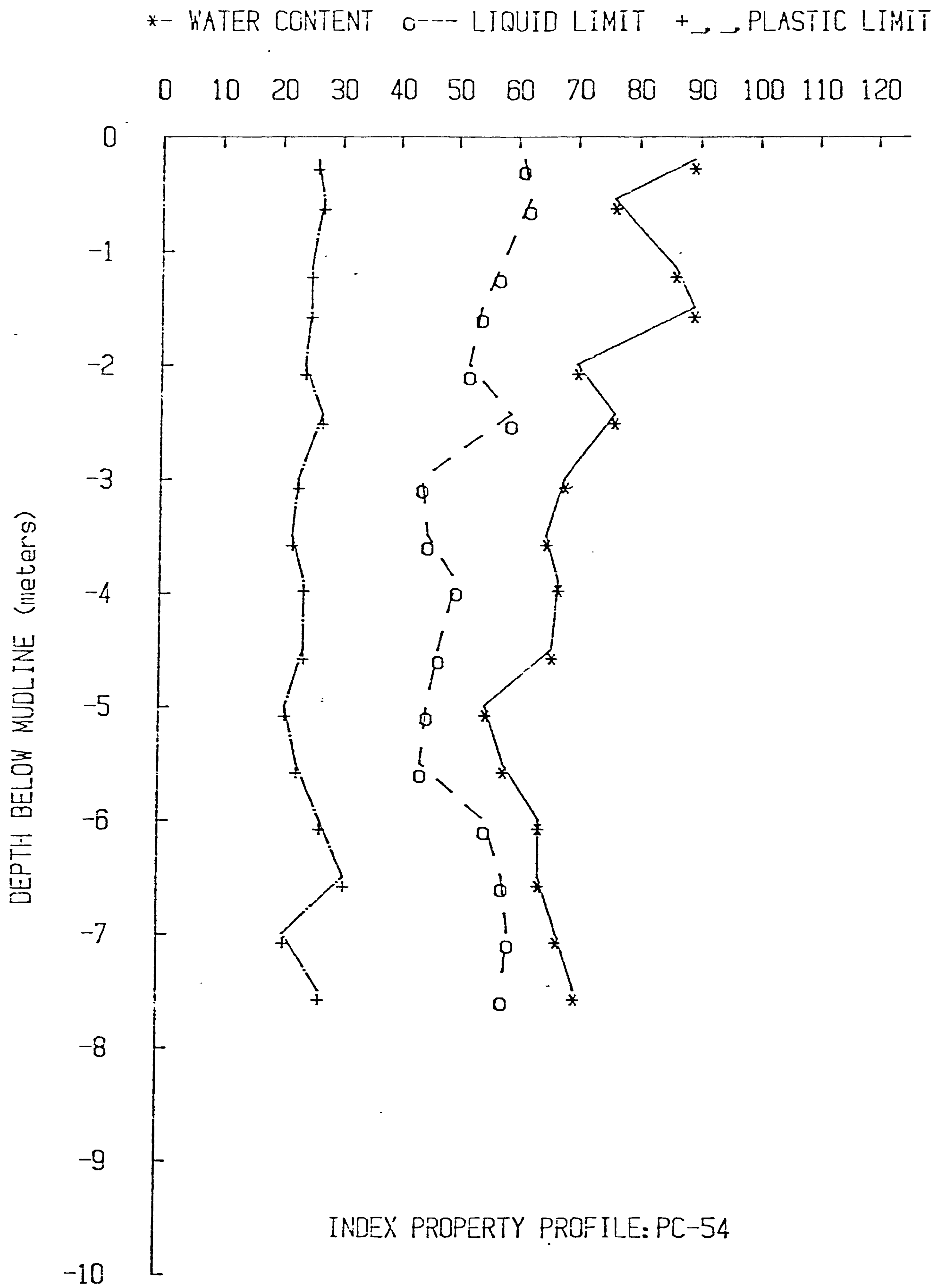

Figure 51. Plastic limit (w_p), liquid limit (w_L), and natural water content (w) vs. depth in core.

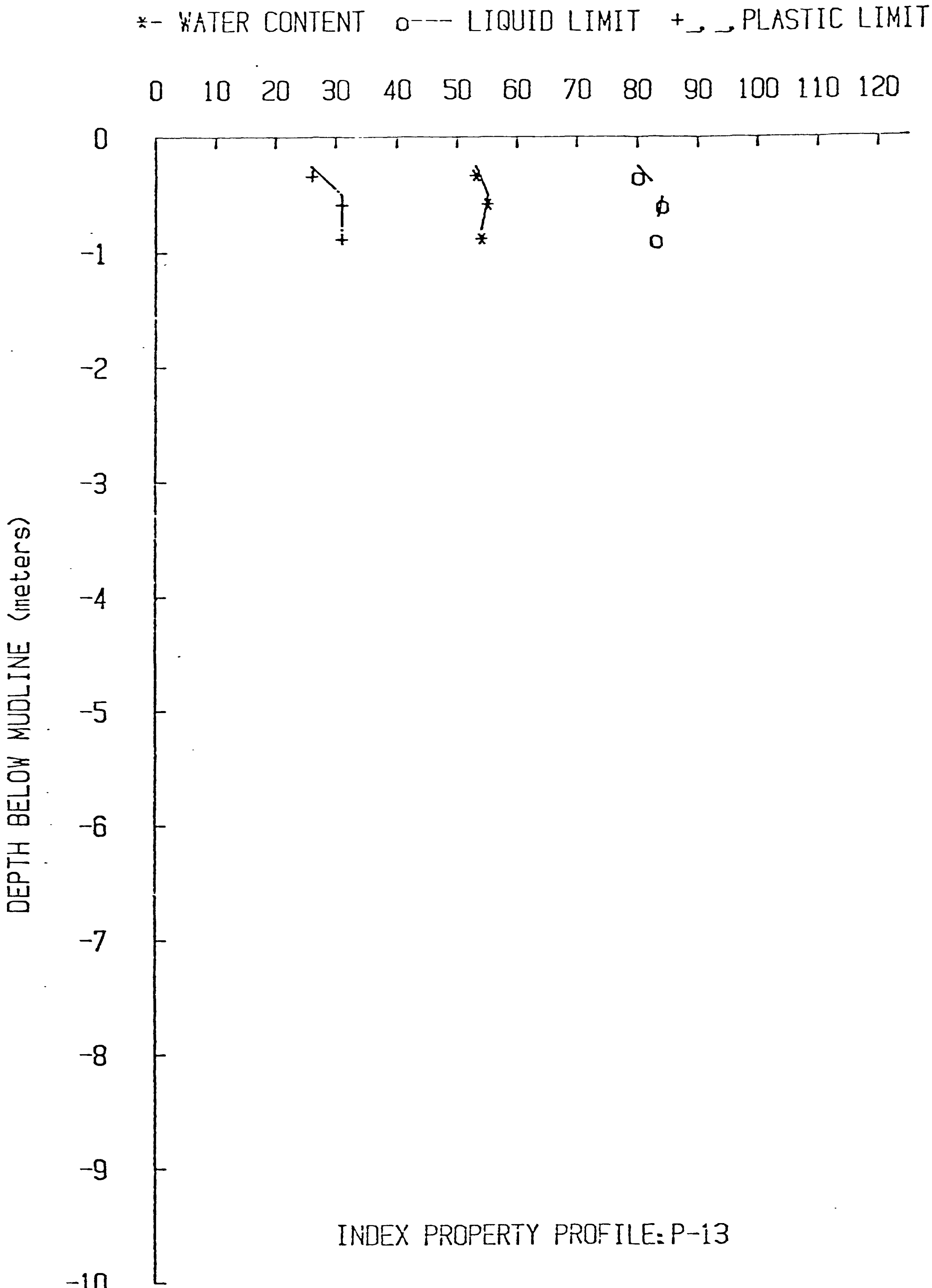

Figure 5m. Plastic limit (w_p), liquid limit (w_L), and natural water content (w) vs. depth in core.

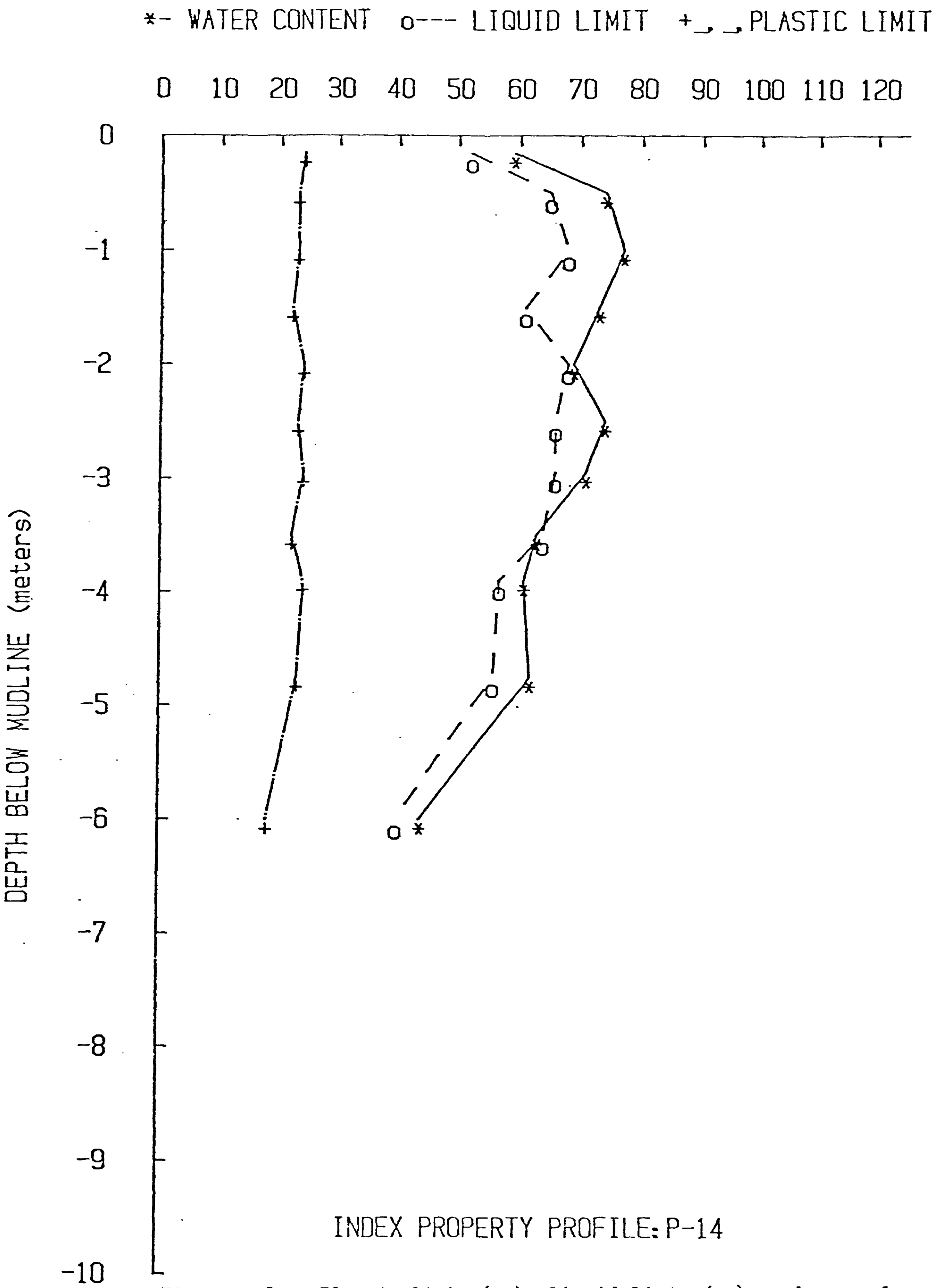

Figure 5n. Plastic limit (w_p), liquid limit (w_L), and natural water content (w) vs. depth in core.

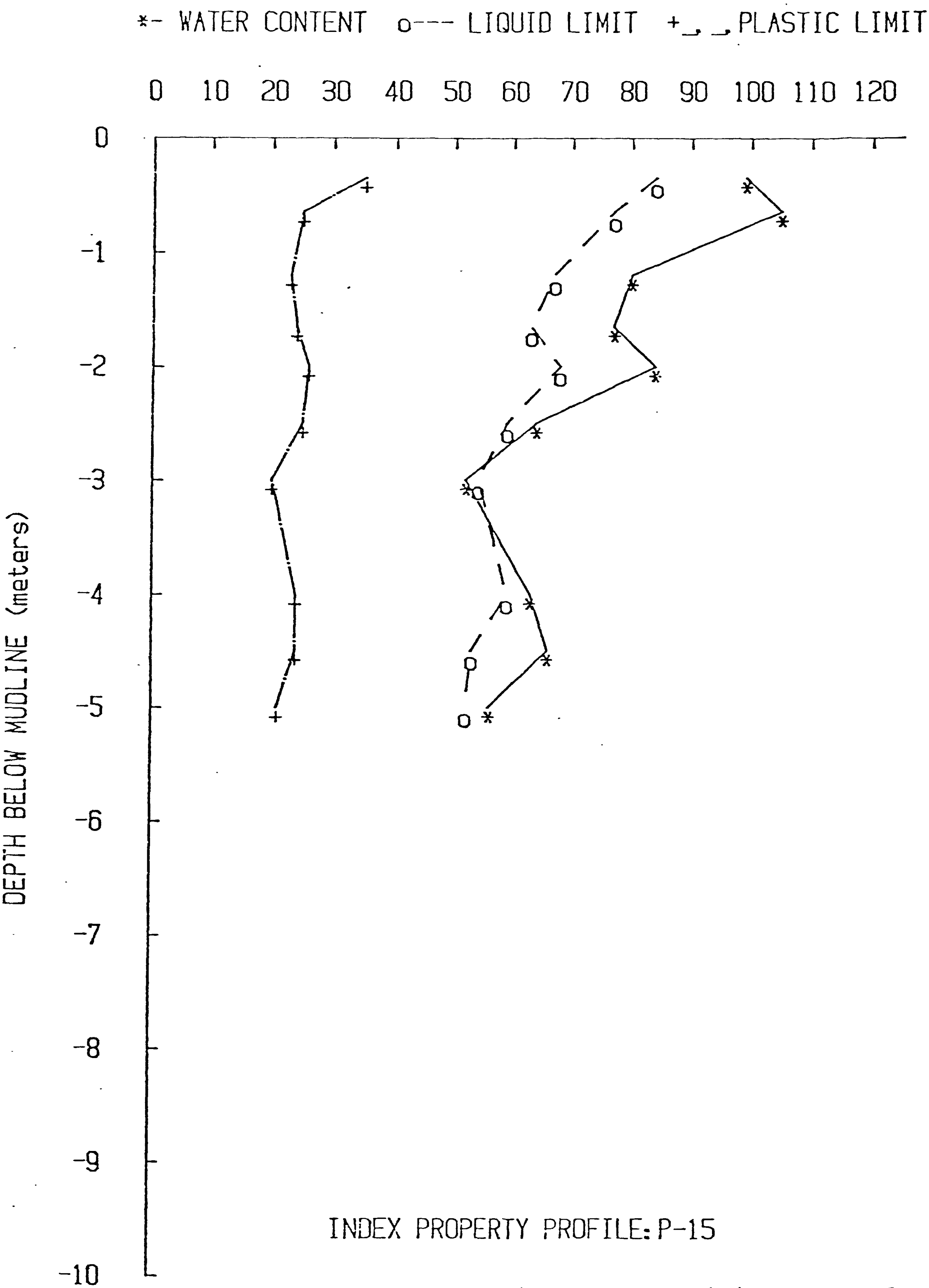

Figure 5o. Plastic limit (w_p), liquid limit (w_L), and natural water content (w) vs. depth in core.

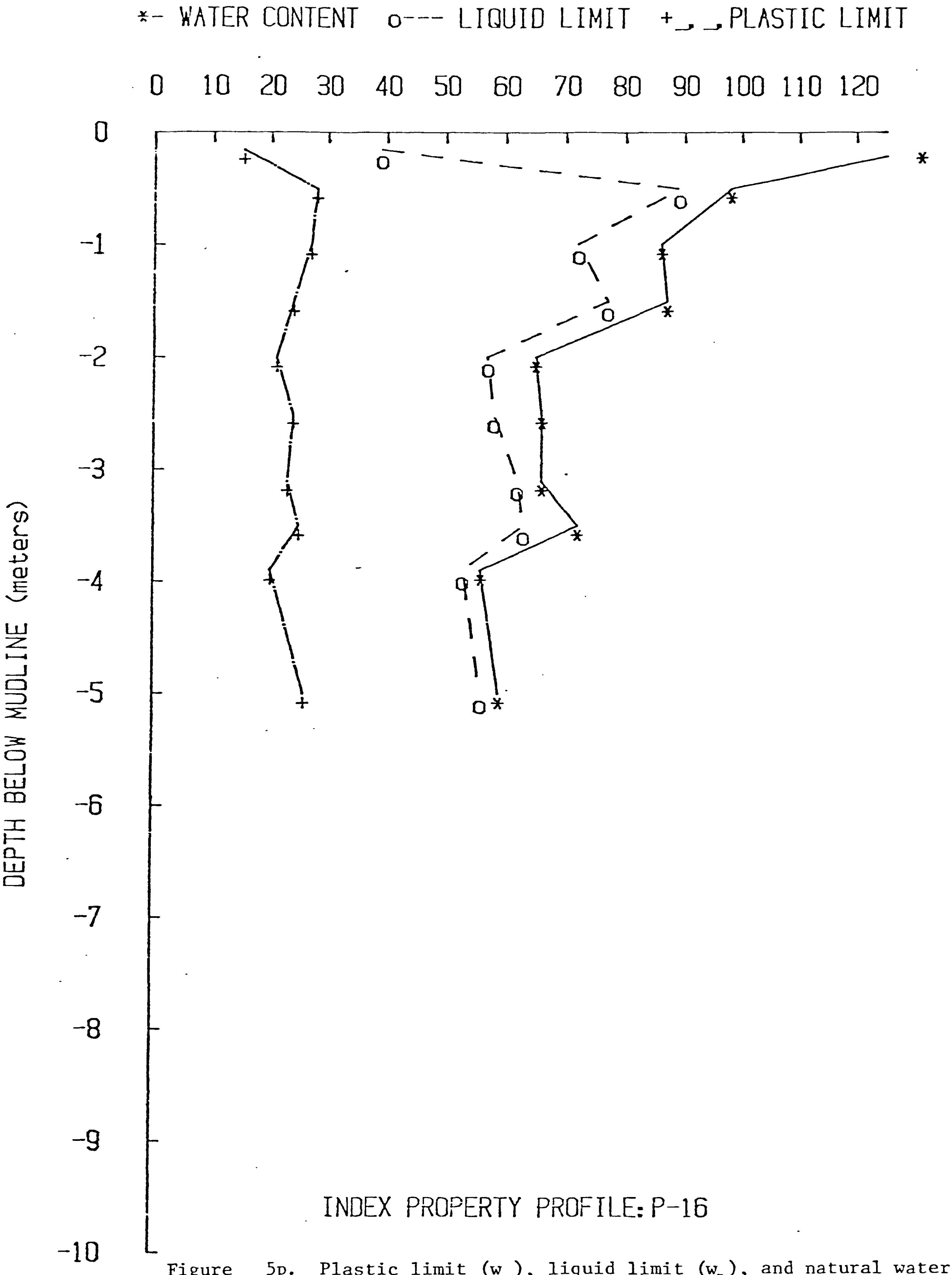

Figure 5p. Plastic limit (w_p), liquid limit (w_L), and natural water content (w) vs. depth in core.

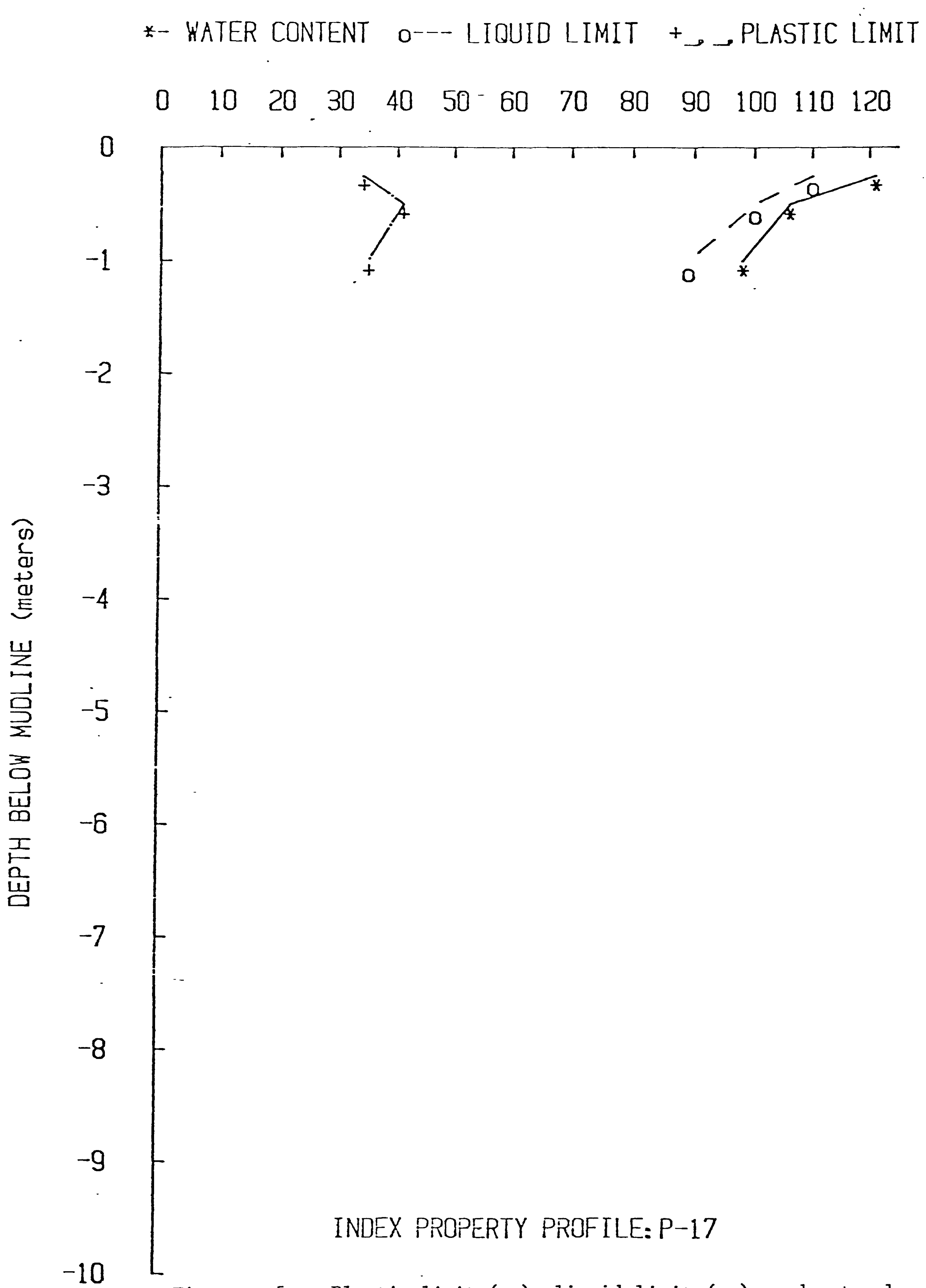

Figure 5q. Plastic limit (w_p), liquid limit (w_L), and natural water content (w) vs. depth in core.

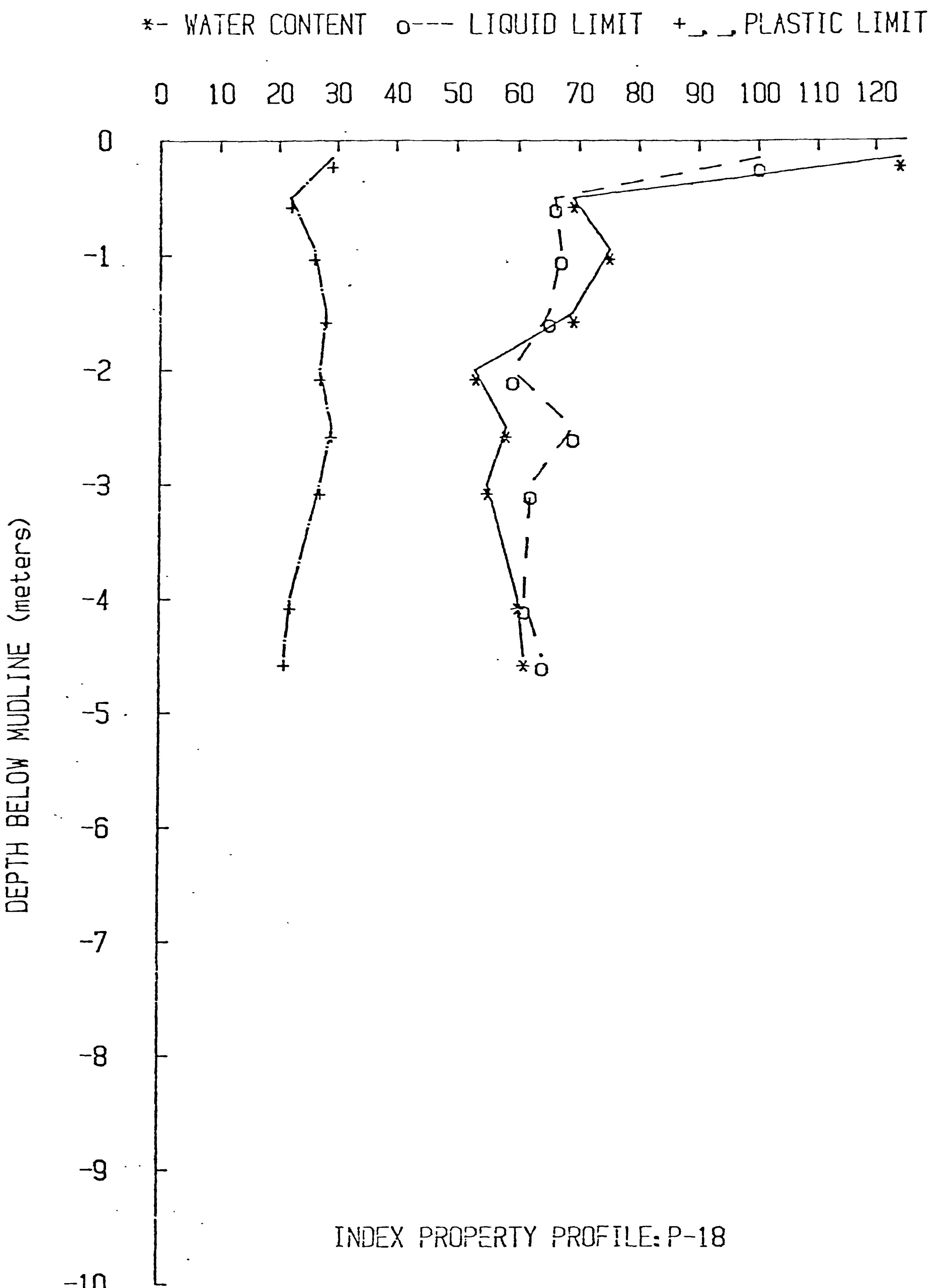

Figure 5r. Plastic limit (w_p), liquid limit (w_L), and natural water content (w) vs. depth in core.

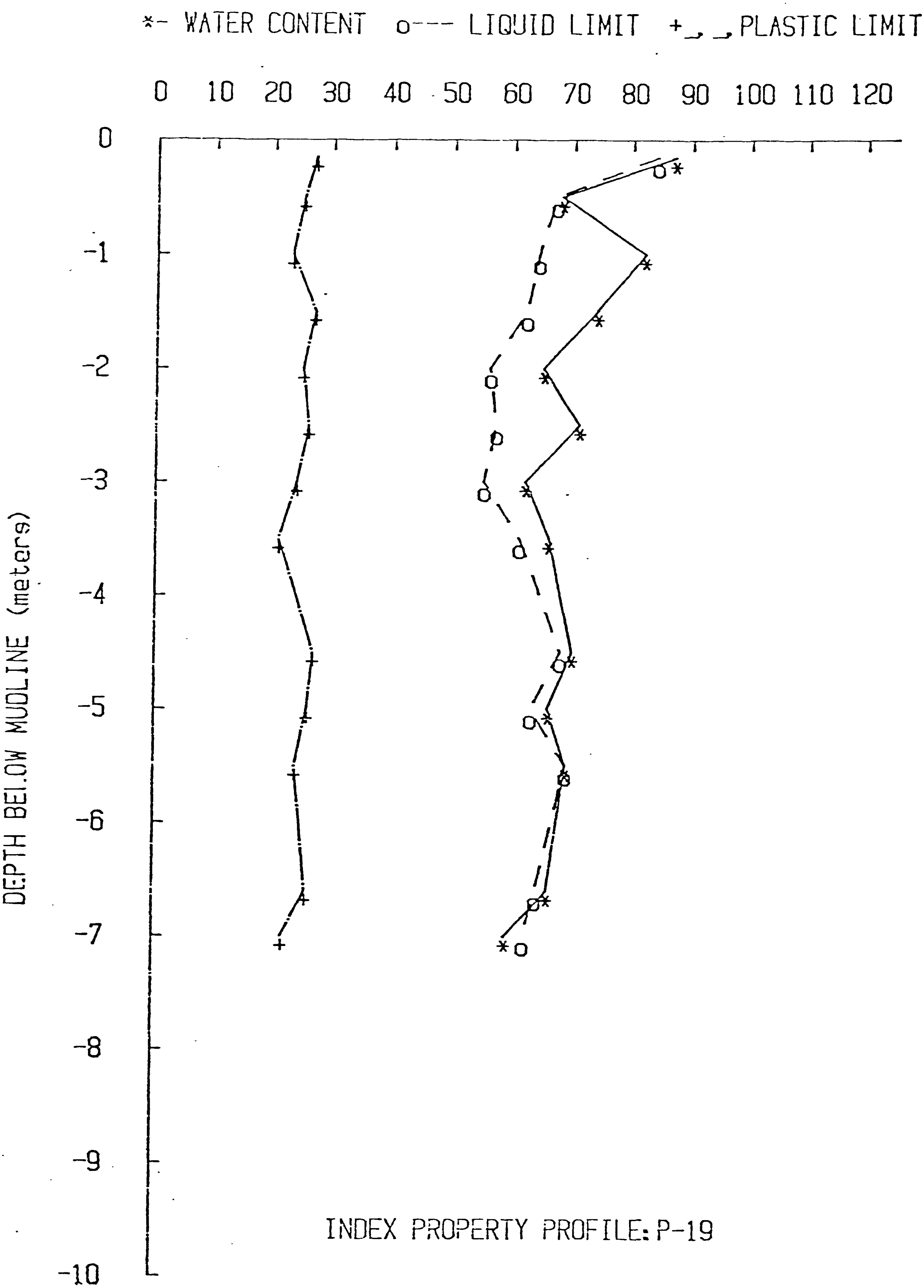

Figure 5s. Plastic limit (w_p), liquid limit (w_L), and natural water content (w) vs. depth in core.

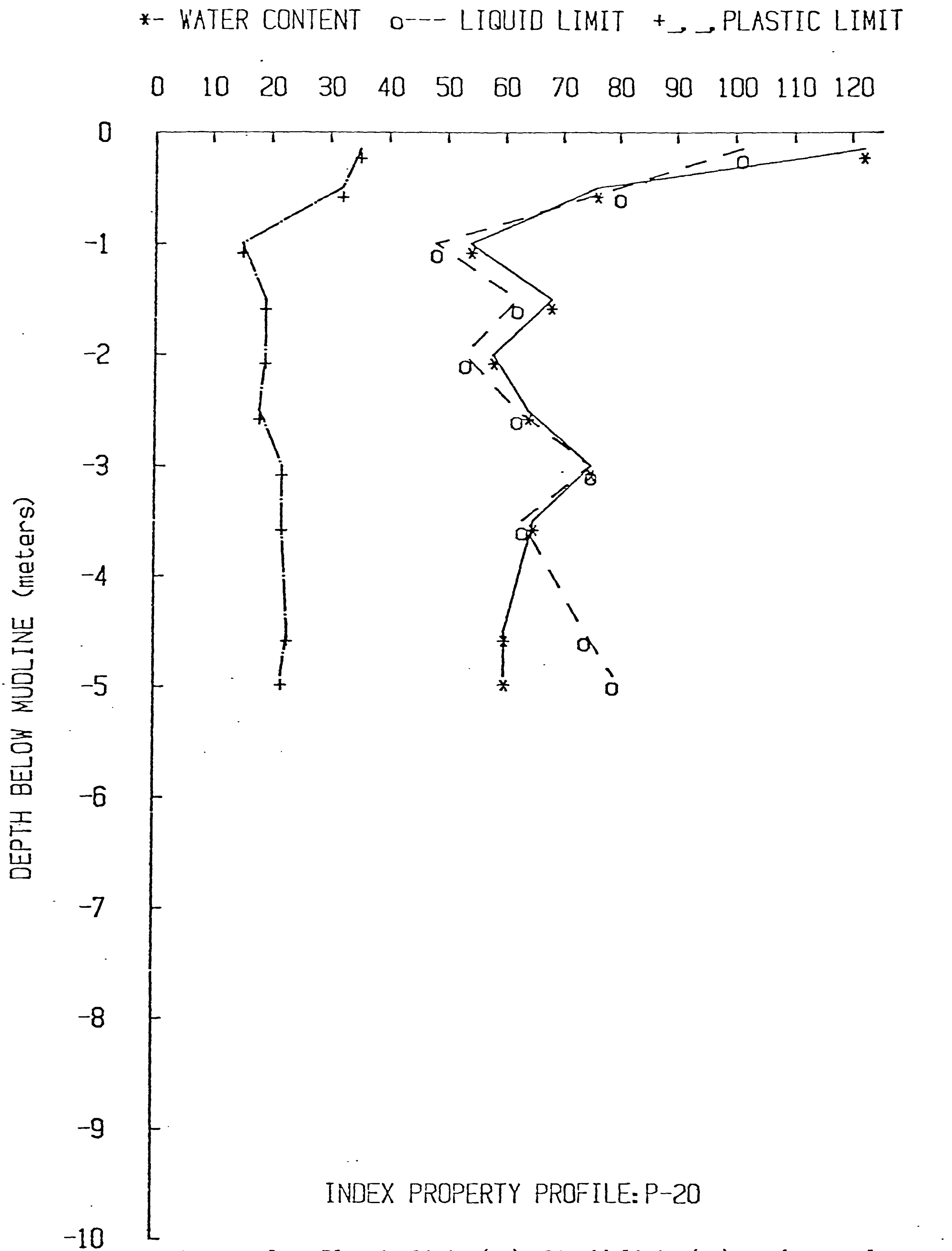

Figure 5t. Plastic limit (w_p), liquid limit (w_L), and natural water content (w) vs. depth in core.

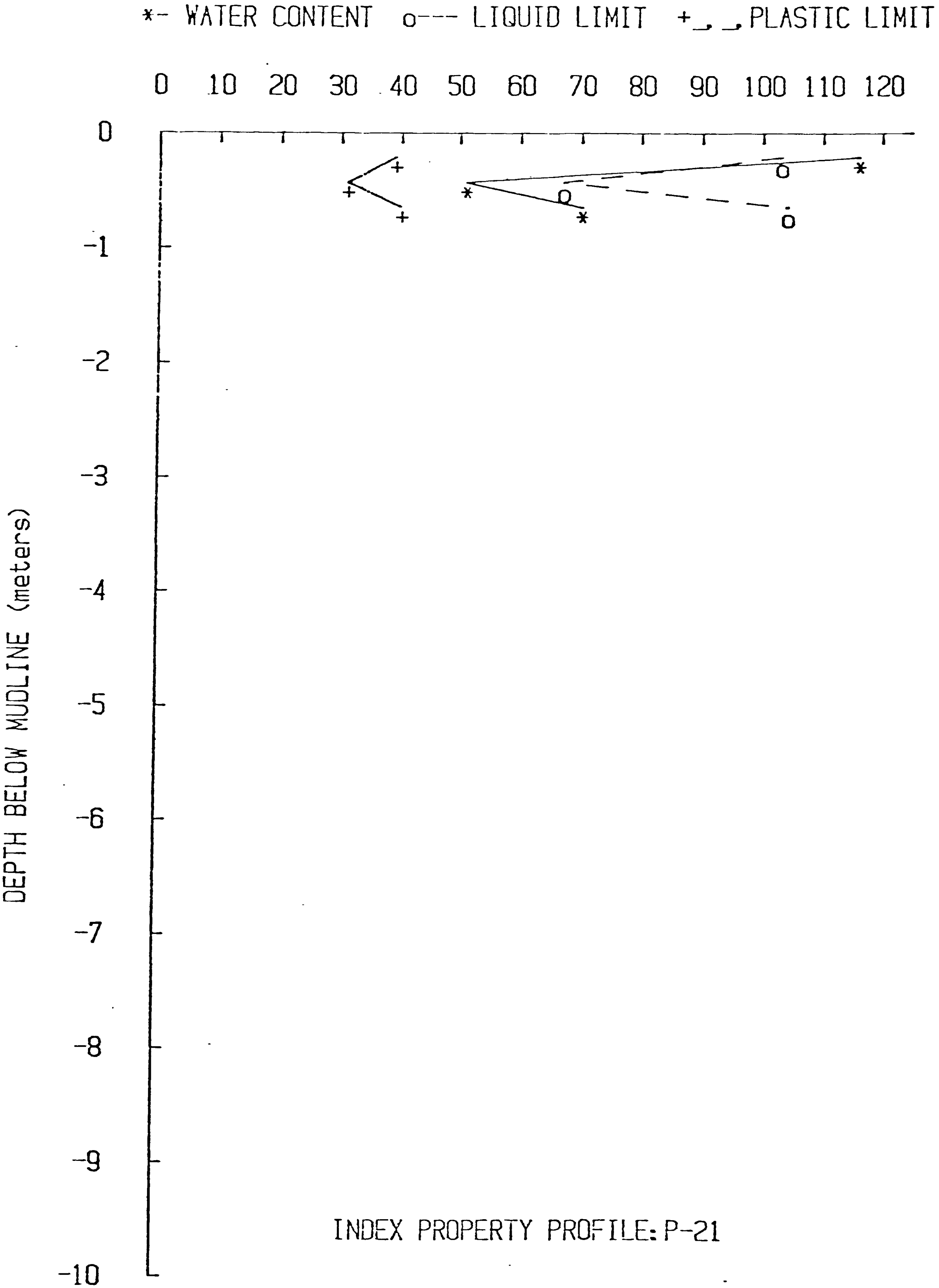

Figure 5u. Plastic limit (w_p), liquid limit (w_L), and natural water content (w) vs. depth in core.

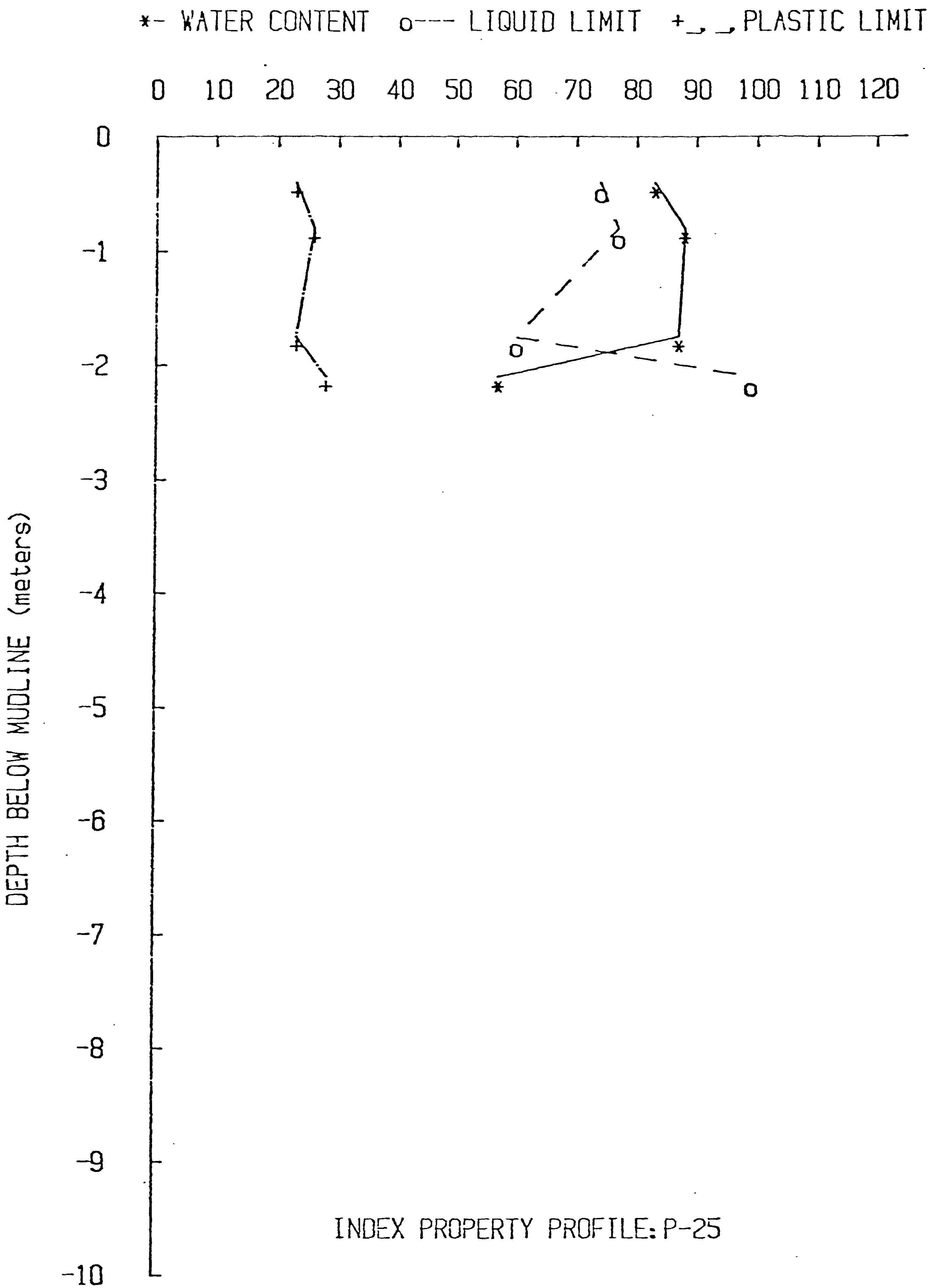

Figure 5v. Plastic limit (w_p), liquid limit (w_L), and natural water content (w) vs. depth in core.

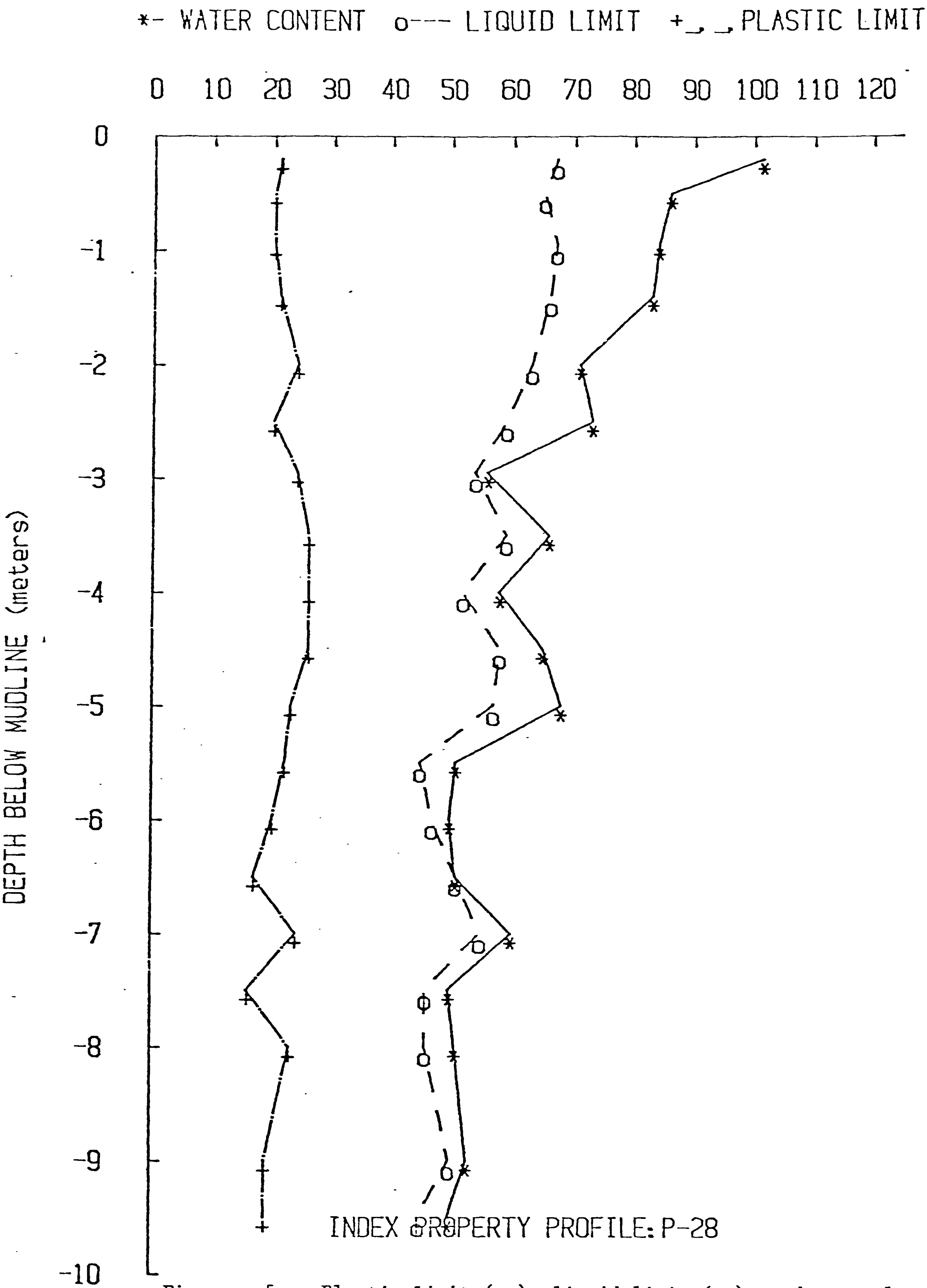

Figure 5w. Plastic limit (w_p), liquid limit (w_L), and natural water content (w) vs. depth in core.

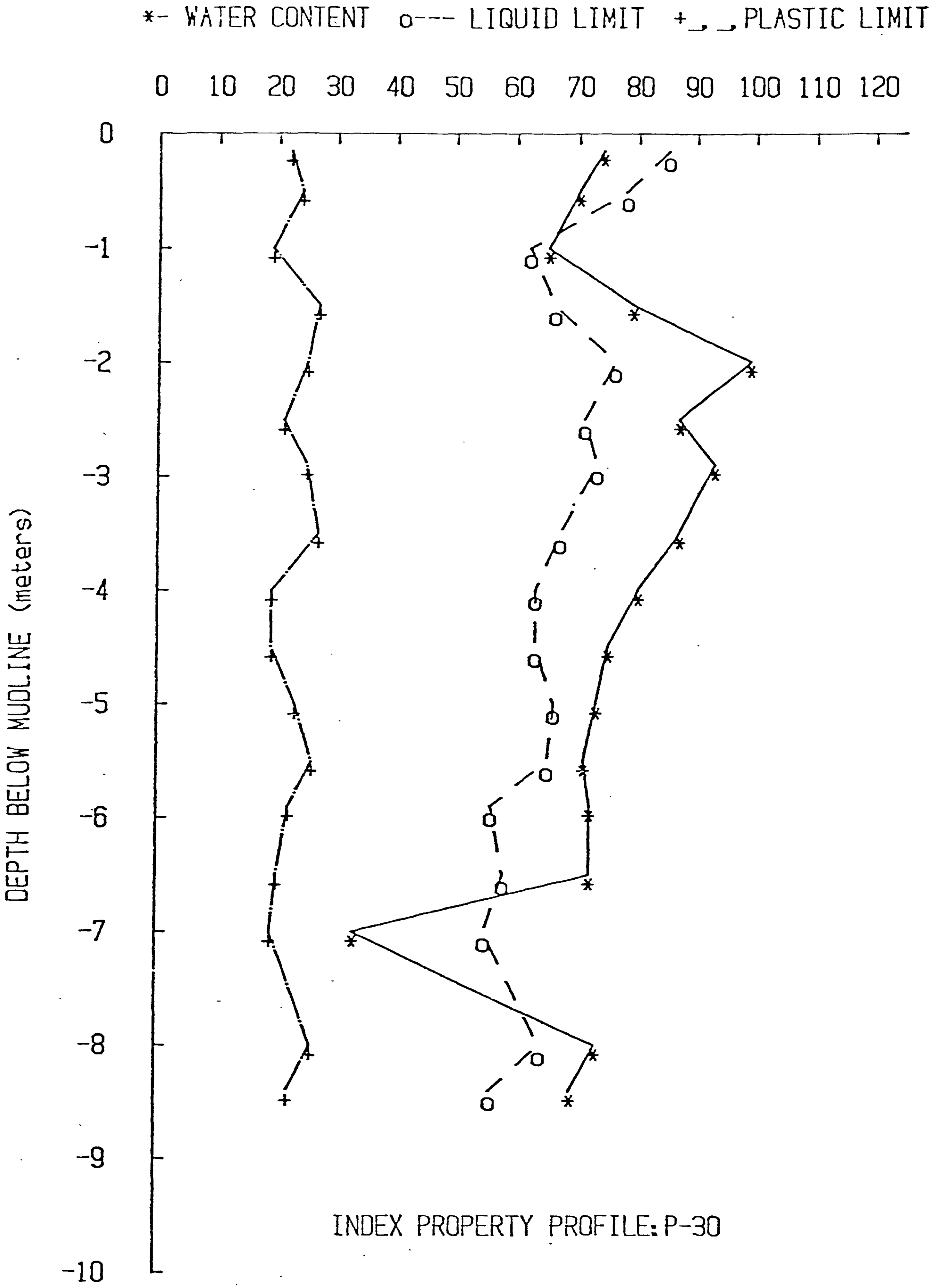

Figure 5x. Plastic limit (w_p), liquid limit (w_L), and natural water content (w) vs. depth in core.

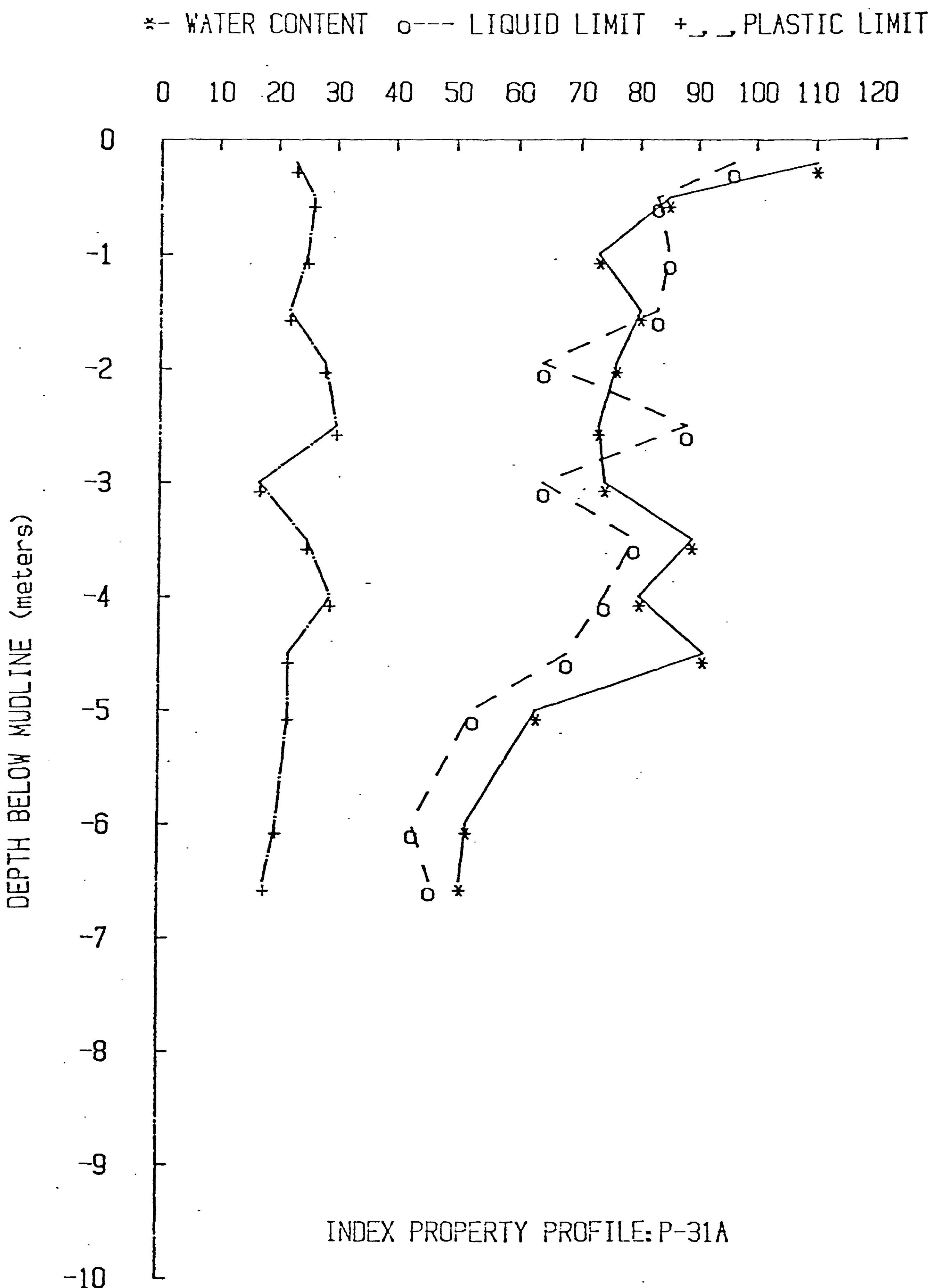

Figure 5y. Plastic limit (w_p), liquid limit (w_L), and natural water content (w) vs. depth in core.

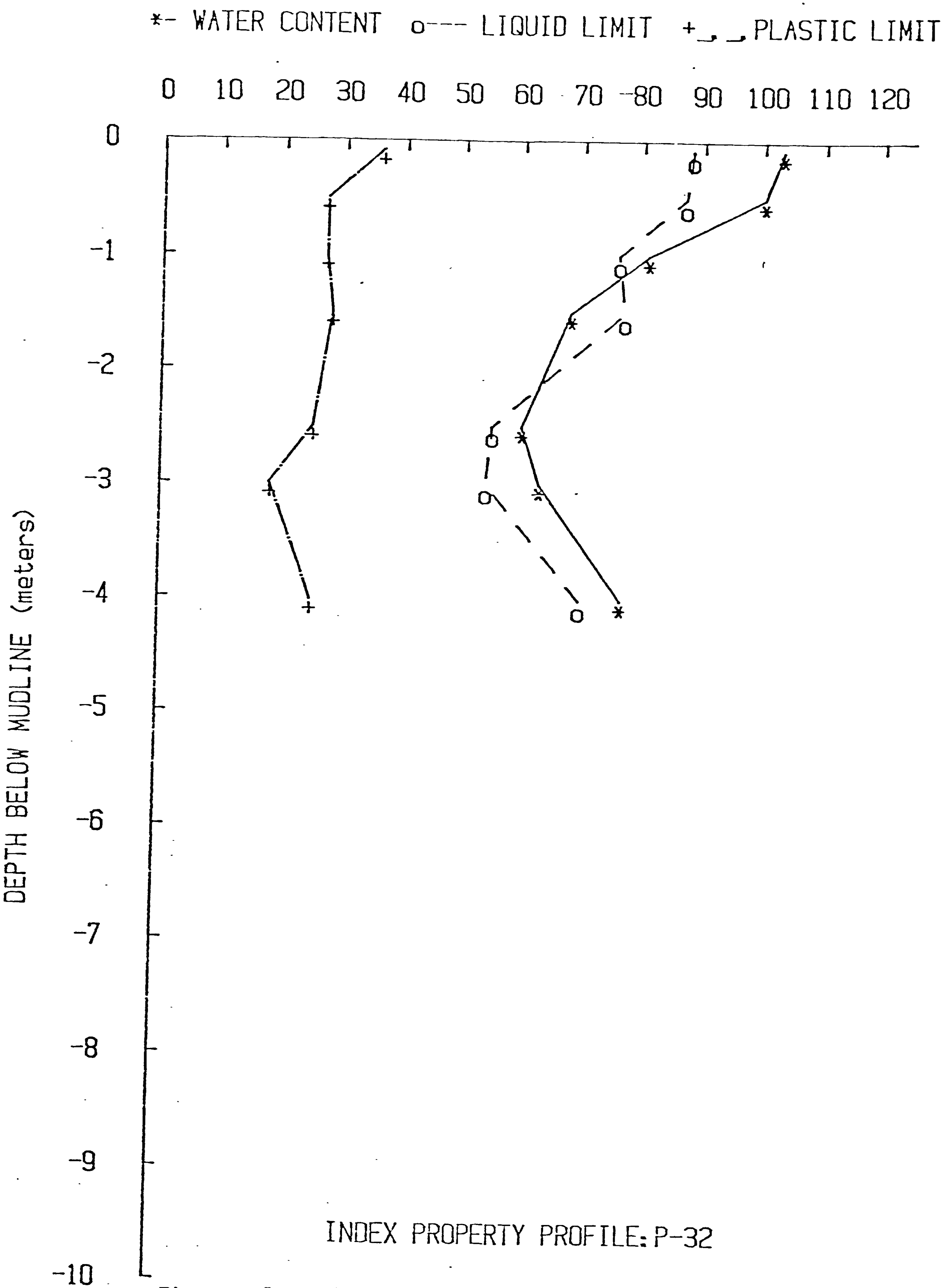

Figure 5z. Plastic limit (w_p), liquid limit (w_L), and natural water content (w) vs. depth in core.

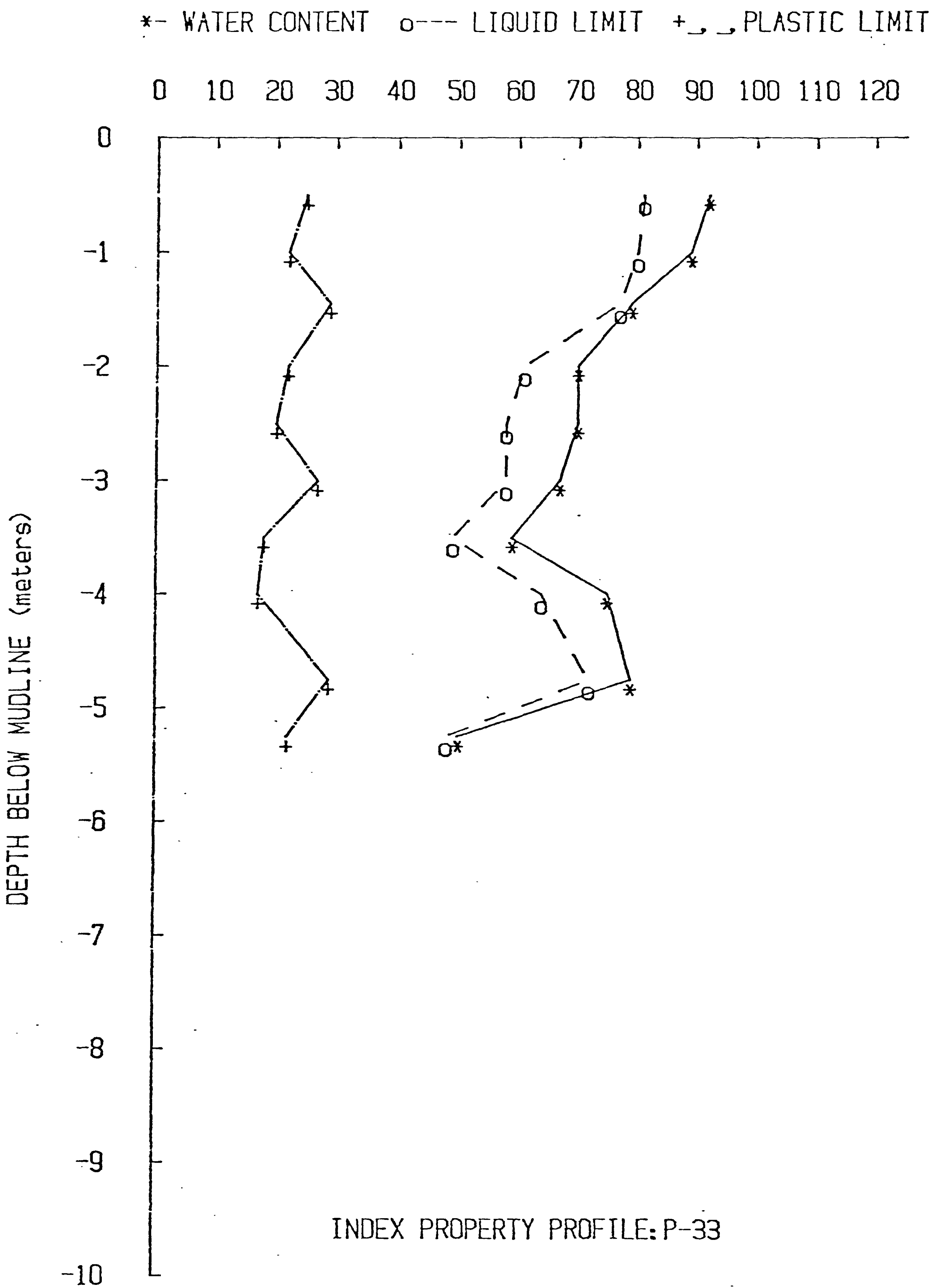

Figure 5aa. Plastic limit (w_p), liquid limit (w_L), and natural water content (w) vs. depth in core.

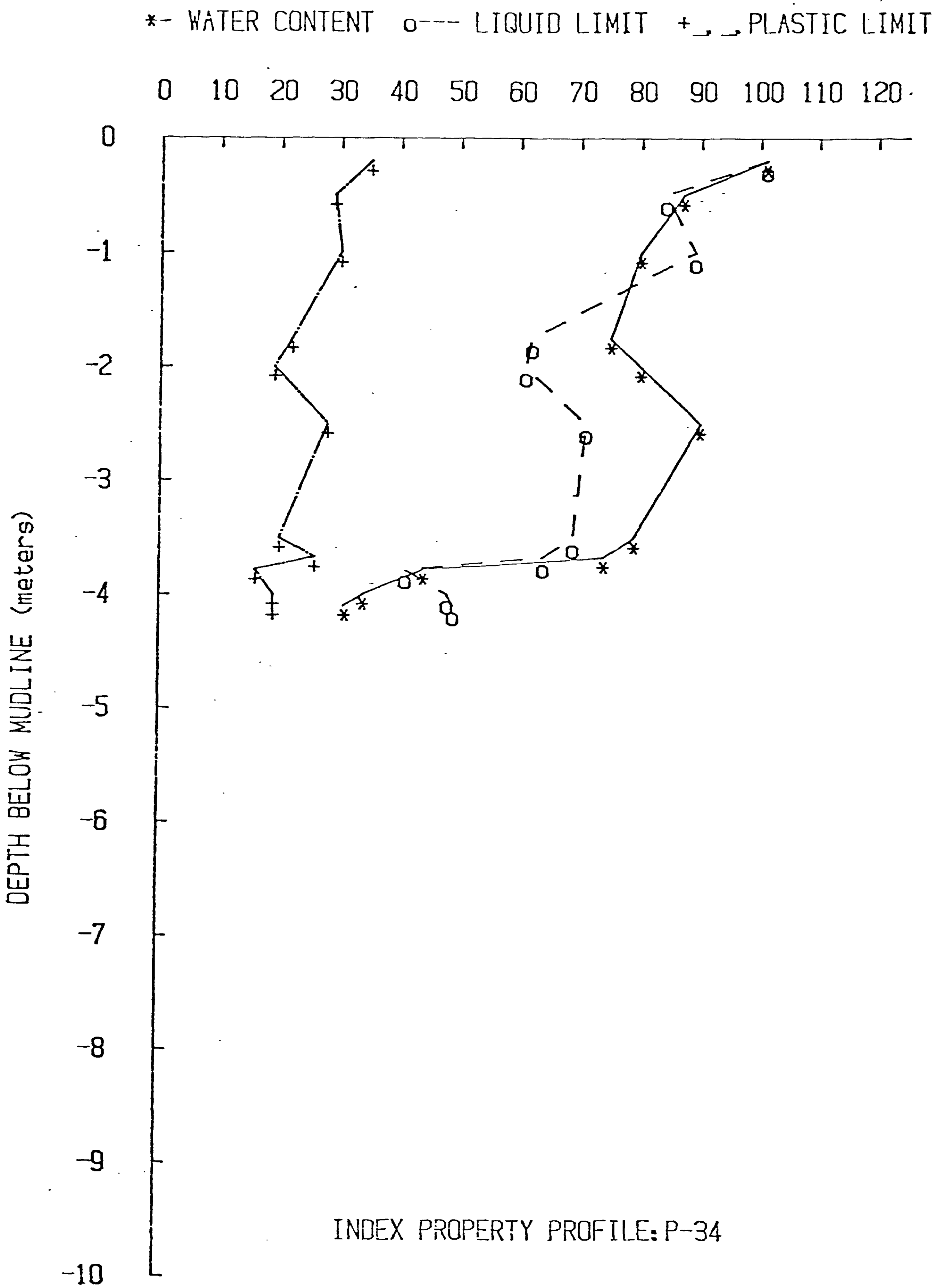

Figure 5bb. Plastic limit (w_p), liquid limit (w_L), and natural water content (w) vs. depth in core.

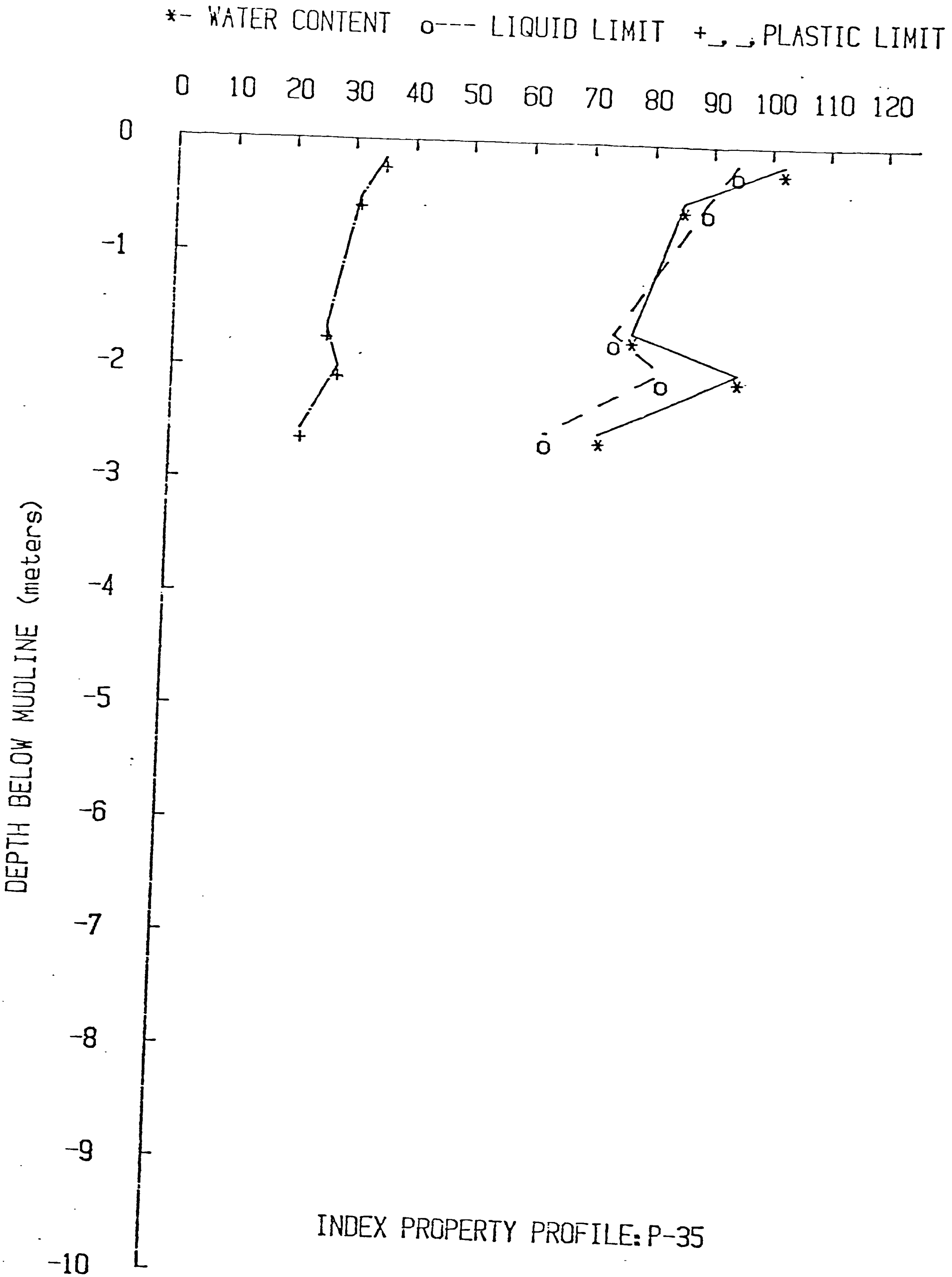

Figure 5cc. Plastic limit (w_p), liquid limit (w_L), and natural water content (w) vs. depth in core.

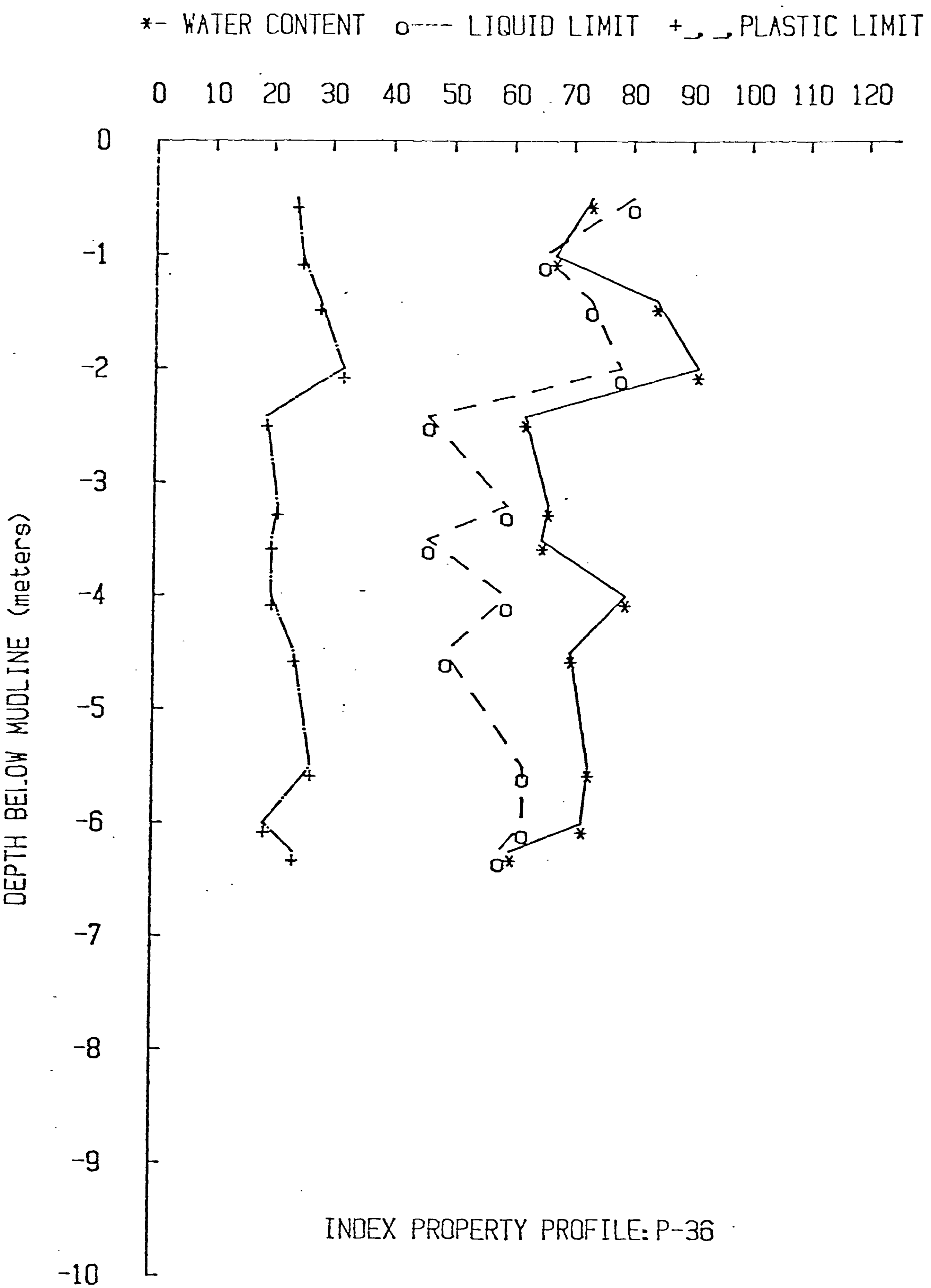

Figure 5dd. Plastic limit (w_p), liquid limit (w_L), and natural water content (w) vs. depth in core.

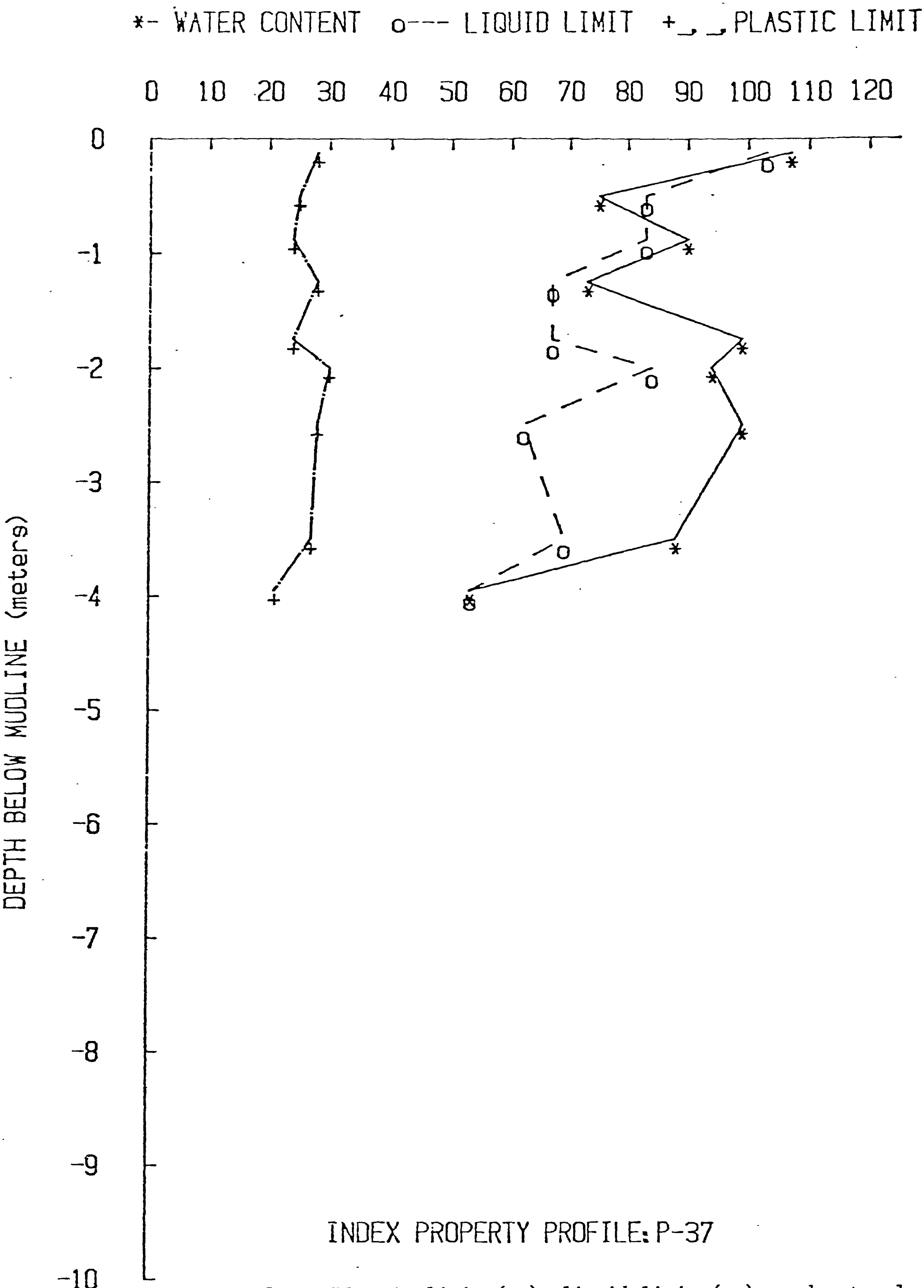

Figure 5ee. Plastic limit (w_p), liquid limit (w_L), and natural water content (w) vs. depth in core.

Table III.

Mid-Atlantic results of consolidation tests

Core ID	Depth in core (m)	σ'_{vo} (kPa)	σ'_{vm} (kPa)	$\sigma'_{vm}-\sigma'_{vo}$ (kPa)	OCR	C_c	$c_v(\sigma'_{vo})$ (cm^2/s)	$c_v(\sigma_{vm}')$ (cm^2/s)	$k(\sigma_{vo}')$ (cm/s)	$k(\sigma_{vm}')$ (cm/s)	I_D*	Degree of disturbance
PC39	4.54	32	92	60	2.9	0.28	$5.7x10^{-4}$	$6.8x10^{-4}$	$1.7x10^{-7}$	$1.9x10^{-7}$	0.30	small
PC40	5.58	37	83	46	2.2	.20	$2.1x10^{-3}$	$1.5x10^{-3}$	$4.0x10^{-7}$	$4.7x10^{-7}$	.41	moderate
PC43	8.83	65	447	382	6.9	.22	$1.5x10^{-3}$	$2.5x10^{-3}$	$2.4x10^{-7}$	$6.2x10^{-7}$	.63	much
PC44	3.02	25	204	179	8.2	.34	$\sim 1.0x10^{-1}$	$4.2x10^{-2}$	$\sim 6.6x10^{-6}$	$1.3x10^{-6}$	.30	small
PC45	4.31	28	87	59	3.1	.33	$4.7x10^{-3}$	$7.7x10^{-4}$	$5.9x10^{-7}$	$3.1x10^{-7}$	.25	small
PC46	5.55	36	135	99	3.8	.14	$1.9x10^{-3}$	$1.6x10^{-3}$	$2.9x10^{-7}$	$4.4x10^{-7}$	.28	small
PC53	8.54	54	83	29	1.5	.36	$6.9X10^{-4}$	$5.3x10^{-4}$	$1.4x10^{-7}$	$1.4x10^{-7}$	.29	small
PC54	7.17	44	110	66	2.5	.37	$2.8x10^{-3}$	$1.2x10^{-3}$	$4.5X10^{-7}$	$4.1X10^{-7}$	.40	moderate
P13	2.11	15	1148	1133	76	.69		$3.2X10^{-3}$		$1.8x10^{-6}$	.30	moderate
P14	4.96	30	81	51	2.7	.31	$2.0x10^{-3}$	$1.1x10^{-3}$	$8.0x10^{-7}$	$1.0x10^{-6}$	.15	very little
P15	5.52	34	105	71	3.1	.32	$1.6x10^{-3}$	$6.7x10^{-4}$	$2.6x10^{-7}$	$2.6x10^{-7}$	.25	small
P16	5.27	31	100	69	3.2	.39	$9.0x10^{-4}$	$6.4x10^{-4}$	$2.4x10^{-7}$	$2.5x10^{-7}$	.46	moderate
P17	1.92	8.9	1660	1651	187	.48		$2.0x10^{-2}$		$8.5x10^{-6}$	.31	moderate
P18	4.89	31	166	135	5.4	.36	$5.2x10^{-4}$	$3.9x10^{-4}$	$8.8x10^{-8}$	$1.3x10^{-7}$	.29	small
P19	5.80	35	115	80	3.3	.35	$4.3x10^{-4}$	$8.2x10^{-4}$	$1.1x10^{-7}$	$4.0x10^{-7}$	.22	small
P20	5.02	31	447	416	14	.77	$\sim 2.5x10^{-3}$	$1.6x10^{-3}$	$\sim 1.0x10^{-6}$	$9.5x10^{-7}$	.14	very little
P21	.86	5.0	1862	1857	372	1.02	$\sim 1.6x10^{-3}$	$1.3x10^{-3}$	$\sim 7.3x10^{-8}$	$9.2x10^{-7}$	.18	small
P24	1.08	11	1047	1036	95	.69		$9.7x10^{-3}$		$4.7x10^{-6}$	.36	moderate
P28	9.87	65	148	83	2.3	.37	$1.9x10^{-3}$	$1.1x10^{-3}$	$6.6x10^{-7}$	$5.9x10^{-7}$	.23	small
P30	8.60	50	63	13	1.3	.39	$5.4x10^{-4}$	$4.3x10^{-4}$	$9.8x10^{-7}$	$8.1x10^{-7}$	.20	small
P31A	6.69	40	51	11	1.3	.33	$6.7x10^{-4}$	$5.9x10^{-4}$	$2.1x10^{-7}$	$2.3x10^{-7}$	.17	small
P32	3.29	19	71	52	3.7	.48	$9.2x10^{-4}$	$5.8x10^{-4}$	$5.6x10^{-7}$	$3.4x10^{-7}$	.22	small
P33	5.50	33	40	7	1.2	.32	$1.2x10^{-3}$	$5.7x10^{-4}$	$2.4x10^{-6}$	$1.5x10^{-6}$	.11	very little
P34	2.78	15	20	5	1.3	.38	$4.3x10^{-4}$	$2.8x10^{-4}$	$1.1x10^{-7}$	$1.0x10^{-7}$	.22	small
P37	4.89	28	813	785	29	.42	$9.2x10^{-4}$	$9.7x10^{-4}$	$4.4x10^{-7}$	$3.3x10^{-7}$	.25	small

where:

σ'_{vo} = Assumed in situ effective overburden stress
σ'_{vm} = Maximum past overburden stress (determined by Casagrande method)
OCR = Overconsolidation ratio
I_D = Disturbance index
C_c = Compression index
c_v = Coefficient of consolidation
k = Coefficient of permeability
* = I_D computed from methods suggested by Silva (1974)

sediments confined spatially (upper slope) as reported by Olsen and others (1982), but normally consolidated sediments appear to be as well. They are most often found on the mid to upper slope. All five of the cores which have OCR values less than 1.5 (table III) are so positioned. In the study by Olsen and others (1982), which was restricted to the upper slope, a similar, perhaps slightly higher, percentage of normally consolidated sediment was reported. In both studies most cores (70%-80%) were lightly to heavily overconsolidated. As partial explanation for this dominance of overconsolidated sediments, all of the cores with extreme OCR values (>15) were recovered from within submarine canyons (e.g., P13 and P17) or from areas where Tertiary sediments are exposed (e.g., P21 and P24). However, most of the other overconsolidated sites were not.

This widespread apparent overconsolidation in the upper few meters has been observed in many other marine sediments. In this case, overconsolidation that resulted from mechanical compaction and subsequent erosion or mass wasting (true overconsolidation) accounts for only a minor portion of the anomalous values. Yet, what evidence is there that the other sites are not erosional as well? Although a complete discussion of this is beyond the scope of this report, we feel that correlation between OCR and the depth in the core from which the sample was taken is especially pertinent. Briefly, the OCR value tends to decrease downcore. This implies that a state of true overconsolidation probably does not exist in most of these sediments and that other explanations, such as the presence of cements, changes in redox potential, alteration in fabric, or origin cohesion, should be investigated.

The compression index (C_c) is a measure of the decrease in porosity or void ratio with increase in overburden. It is largely a function of composition - especially mineralogy, but "environmental" factors may also play a role (see Mitchell, 1976). Table III shows the compression indices for these cores. The rather large range is due mainly to the high values associated with the cores recovered from the heavily overconsolidated sediments. We are not certain why this association exists, although some of the cores were identified as Tertiary chalky silts and are rich in calcareous nannofossils (e.g., P21) (P. C. Valentine, written commun., 1983). Thus, grain crushing (of faunal and floral remains) may be involved. The remainder of the cores have an average C_c of 0.36. According to Mitchell (1976), values less than 0.5 are normal for most soils. In fact, the empirical equation based on liquid limit suggested by Terzaghi and Peck (1967) accurately predicts the range and mean C_c value for most of the sediments in this study. Other investigations in marine sediment, however, have noted significant discrepancies between measured values and those predicted by the empirical equation (e.g., McClelland, 1967; Silva and Hollister, 1979) and the aforementioned high values in this study likewise do not fit it. The fact that some of these marine sediments are more compressive than would be predicted may reflect the presence of organic matter, fragile (crushable) biota remains, or mica, for example.

Coefficient of consolidation (C_v) relates permeability and compression; it also is largely a function of composition and, by association, texture. Table III shows C_v values for both the assumed in situ effective overburden (σ'_{vo}) and the maximum past overburden stress (σ'_{vm}). The range of 10^{-3}-10^{-4} cm^2/s is typical for fine-grained sediments (Morgenstern, 1967). The sole exception was in PC44. At $C_v = 10^{-1}$ cm^2/s it is much higher than normal for this type of sediment.

Permeability

Permeability varies in a narrow range for the samples tested. Values, expressed in terms of the coefficient of permeability (k), lie between 10^{-6} cm/s and 10^{-8} cm/s (table III). These sediments are therefore classified as having "very low" permeability to being "practically impermeable" (Lambe and Whitman, 1969). The values found in this study are in accord with those normally reported for soils of this texture and composition.

Strength parameters

The fundamental strength parameters of the sediment, as determined from triaxial tests, are shown in table IV. No attempts were made to normalize or apply correction factors to these data.

The strength to overburden ratio (S_u/σ'_{vo}) for these sediments is generally higher than the values predicted or assumed for normally consolidated sediment. Specifically, according to the empirical equations developed by Skempton (1954), Hansbo (1957), and others (e.g., Ladd and others, 1977) values for normally consolidated sediment of the type in the study area typically fall between 0.2 and 0.3. Less than 30% of the test results fell into this range. The remainder of the test results indicate that most core sites have a higher strength-to-overburden ratio than would be predicted. Overconsolidation is implied. Thus, the S_u/σ'_{vo} data tend to support the evidence from the consolidation tests. The relationship is evident when the OCR values of table III are compared to S_u/σ'_{vo} values shown in table IV. Perfect agreement is not observed, but general agreement is obvious: the correlation coefficient (r) is 0.87 (n=18). The S_u/σ'_{vo} values may also be used in conjunction with slope angle to calculate slope stability (i.e., in total stress cases). This subject is treated in the next section.

Also a descriptor of the sediments is the amount of strain that can be accumulated before failure occurs. Table IV shows a spread of 2% to 20% in the cores tested (the strain limit in the analytical procedure was 20%). Failure at 5%-15% strain is the norm for sediments of this general type. However, large strains without finite failure (e.g., PC52 in table IV) are not uncommon. P19 and P31A failed at 2% strain. These, along with the other cores that failed in the 2%-4% strain range, are less plastic than expected. The low values may imply that cements are present in some of these sediments. However, none of the other geotechnical criteria suggested by Nacci and others (1974) is satisfactorily met. All failures observed in the triaxial tests were plastic; no discrete failure planes were observed.

Cohesion, or the strength of a soil at zero effective stress, is due to interparticle attraction, cements, or other agents or phenomena that are independent of overburden and associated frictional effects (for discussion, see Mitchell, 1976). The range of 0 to 9 kPa shown in table IV for c' is characteristic of fine-grained marine sediments.

Central to slope-stability calculations as well as being a basic strength parameter is the angle of internal friction (here, with respect to effective stress (ϕ')). In these Continental Slope sediments the mean ϕ' value is about 25°, which is in accord with established relationships between plasticity and ϕ' for normally consolidated clays (Kenney, 1959) or for clays that are

Table IV.

Results of Mid-Atlantic triaxial tests

Core	Depth in core (m)	S_u/σ'_{vo}	Strain at failure (%)	c' (kPa)	ϕ' (^{o})
PC39	4.79	.65	5	8	25
PC40	6.56	.25	3	4	24
PC41	4.22	.70	10	0	26
PC43	9.07	.53	16	9	30
PC44	4.18	.73	16	7	28
PC45	6.60	.44	16	3	29
PC46	4.19	.45	4	2	24
PC52	6.37	.46	>20	5	28
PC53	9.66	.23	15	2	22
PC54	8.28	.38	3	6	22
P14	5.35	.30	12	2	23
P15	5.95	.43	3	8	22
P16	5.70	.33	3	5	21
P17	1.45		7	0	31
P18	3.23	.43	5	3	26
P19	3.96	.55	2	5	16
P20	5.37	1.00	6	2	33
P28	8.65	.42	4	2	29
P31A	5.52	.30	2	8	12
P33	4.38	.40	5	0	28
P34	1.54	.30	7	0	14
P35	1.27	.20	8	1	20
P36	2.79	.35	6	0	31

S_u/σ'_{vo} = ratio of undrained shear strength to effective overburden pressure.
c' = Cohesion (effective stress).
ϕ' = Angle of internal friction (effective stress).

lightly overconsolidated and thus may have slightly depressed ϕ' values (Lambe and Whitman, 1969). The values (table IV) are also similar to those published by Olsen and others (1982) for the upper slope sediments within and proximal to this study area. The anomalously low ϕ' values of 12^{o}- 16^{o} (P19, P31A, P34) suggest that the basic sediment structure may have been altered. The values are, in fact, close to the residual ϕ' values which would be predicted on the basis of plasticity (Mitchell, 1976), and are in the range reported by Olsen and others (1981). Deformation of the sediment is possible, through natural processes or disturbance, and would work to decrease the friction angle, but other possibilities may also cause a reduction in or an anomalously low value of ϕ'. It is also possible that some of the values are a result of applying insufficient stress levels relative to σ'_{vm} during testing. Spatial trends were not evident in the strength parameter data.

MASS MOVEMENT

The inconsistent areal distribution of mass-movement evidence on the Mid-Atlantic Continental Slope and Rise and, in particular, the general absence of such evidence within the area investigated, has led to considerable uncertainty regarding the geologic conditions and processes which have promoted slope failures in the past. Further uncertainty exists concerning slope failure potential - both in areas that have shown evidence of past events (such as the location of core P24, which shows evidence of a possible debris flow) and those which have not. Inasmuch as documentation of past slope failures has come largely from high-resolution seismic-reflection profiles and sidescan-sonar images, a quantitative basis for addressing these uncertainties is lacking. That is, while pertinent for identifying features, establishing geometry, and classifying failure types, these data alone do not provide the means for evaluating mass-movement potential or answering other geologic questions.

Slope-stability analysis, especially when combined with the acoustic data, does lend itself to these questions by providing information on the potential for mass movement, and by permiting evaluation of several geologic factors which control slope stability. Thus, it bears on establishing the level of activity of geologic processes in the area. In addition, slope-stability analysis represents an approach capable of providing quantitative information pertinent to commercial development of the region.

There are numerous methods (covering a variety of conditions) available for analyzing slope stability. Selection of a basic method along with its variations depends largely on the geology, the environment, the stress history, a postulated failure surface, general geometry, and a postulated failure type--as well as on available data and the level of accuracy required. Figure 6 gives an idea of the selection process and some of the decisions which must be made. Inasmuch as our study was concentrated on regional slopes (i.e., noncanyon areas), local-slope methods, such as Bishop's Simplified Method of Slices and Wedge Analysis, were not considered. We assume for simplicity that the potential failure surface would be planar and oriented parallel to the plane of the Continental Slope surface and that a slide derived from this geometry would therefore be translational. Finally, the method chosen should be versatile and uncomplicated. The basic infinite-slope method meets each of these requirements and thus was chosen for use in this study.

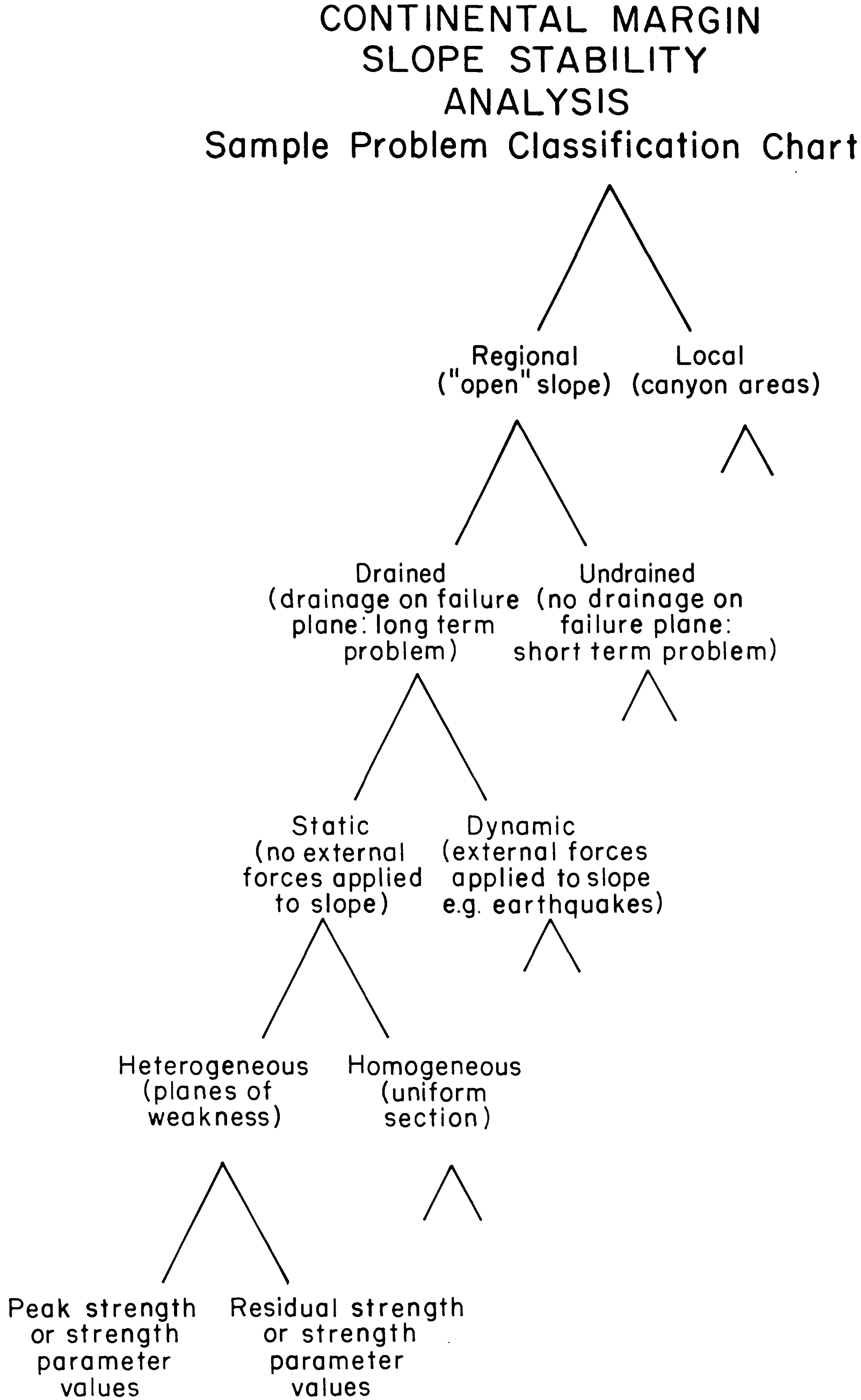

Figure 6. Example of analysis options attendant to slope-stability problems.

The infinite-slope model is shown in figure 7. As implied by the force polygon, it is an expression of balance between resisting forces and shearing forces. The ratio between the two forces is the factor of safety (F) against slope failure: F=resisting forces/shearing forces, where F>1 indicates stability, F<1 indicates instability, and F=1 indicates limit equilibrium. Two equations may be used to analyze static conditions (dynamic conditions will be discussed subsequently):

$$\text{Drained case:} \quad F_d=(1-u_e/\gamma' z \cos^2\alpha) \tan \phi'/\tan \alpha \tag{1}$$

$$\text{Undrained case:} \quad F_u=[S_u/\sigma'_v(1-u_e/\gamma' z)]/\sin \alpha \cos \alpha \tag{2}$$

In the equations u_e is excess pore pressure (i.e., pore pressure in excess of hydrostatic pressure), γ' is the buoyant (submerged) unit weight of the sediment, z is the sediment thickness under consideration, α is the slope angle, ϕ' is the angle of internal friction with respect to effective stress, S_u is the undrained shear strength, and σ'_{vo} is the effective overburden stress. The derivation of these equations may be found in many soil mechanics publications (e.g., Lambe and Whitman, 1969; Morgenstern and Sangrey, 1978).

The infinite-slope method has been used widely in marine sediment investigations (see, for example, Almagor and Wiseman, 1977; Hampton and others, 1978; Booth and Sangrey, 1979; Keller and others, 1979; Booth and others, 1981a, 1981c; Sangrey and Marks, 1981). As in this study, its use was largely dictated by the objectives of the study along with practical considerations. Because its use is becoming commonplace, it is worthwhile at this time to review the assumptions and common limitations associated with the method. Infinite-slope stability analysis, as well as other methods of limit equilibrium analysis, only can be used to address a certain class of problem: discrete slope failure. It does not apply to other types of mass wasting nor does it account for or predict slope deformations. Moreover, several assumptions are attendant to its application. Among the more salient are:

* The lateral extent of the slide is infinite in comparison to its thickness: edge effects are insignificant.

* The sediment peak strength will be mobilized across the entire failure surface at the time of failure.

* The failure surface is a plane, and this plane is parallel to the slope surface (note that in cases where bedding plane failure is under investigation, regional dip must be equivalent to slope declivity).

* For drained analysis, pore pressures are known at the failure surface, and for undrained analysis, pore pressures measured in a triaxial test may be validly extrapolated to the field situation.

Certainly for the level of accuracy required by reconnaissance research, these assumptions are reasonable and, in fact, often necessary. However, in practice, error is introduced into the final result (the factor of safety) because these assumptions have been made.

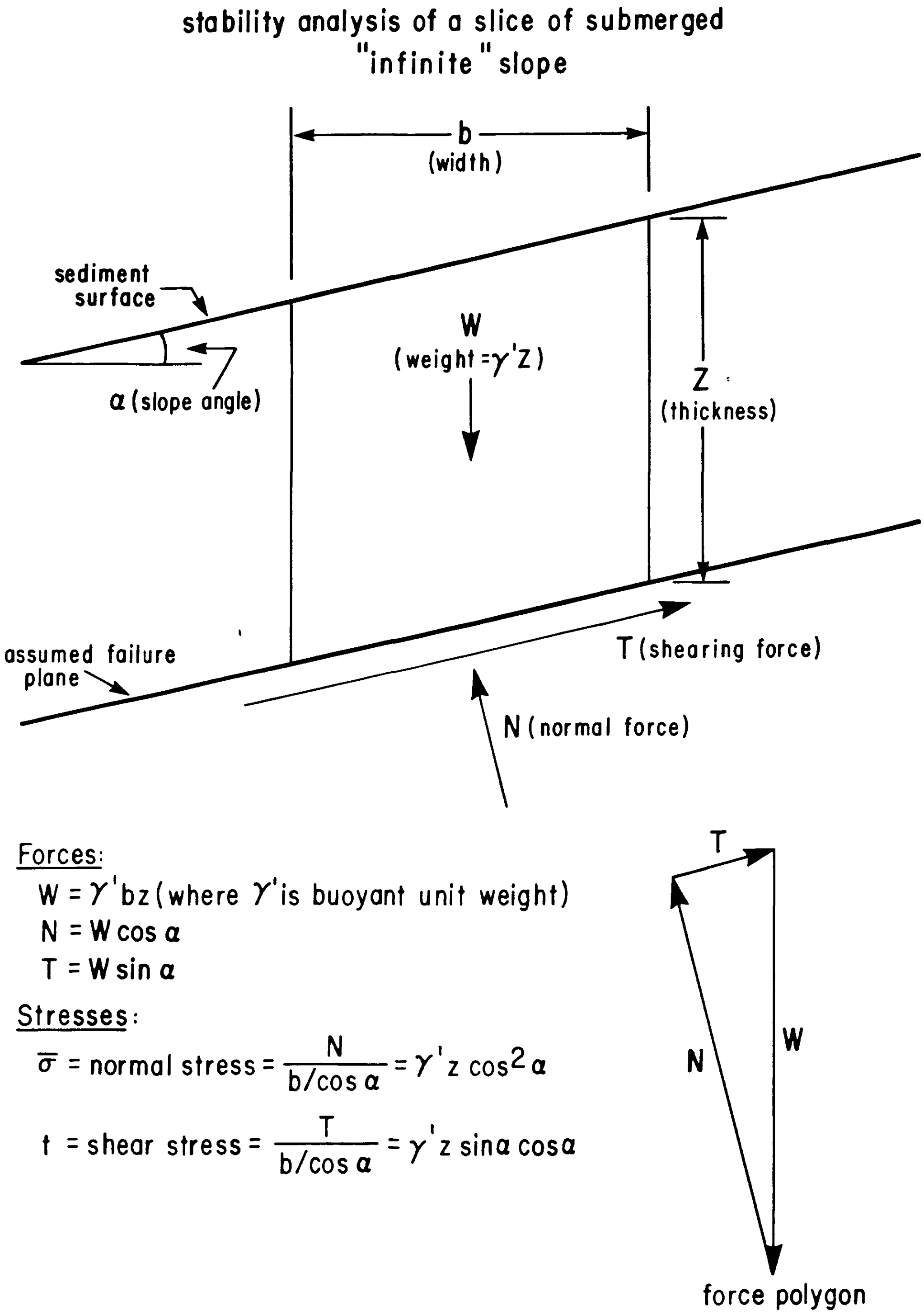

Figure 7. Infinite-slope model for stability analysis.

Constraints related to these assumptions are imposed by sampling methods and the area of investigation itself. For this study, core-site selection was biased and the cores have been mechanically disturbed to some unknown degree. Further, because core penetration is generally limited to a few meters, application of the infinite-slope model to a few tens of meters (a typical thickness of observed slide masses) requires that the sediment be homogenous or predictable with respect to measured strength properties. Geologically-related constraints are also imposed. Variable slope morphology, the presence of gassified sediments, the effect of sea-level change, as well as numerous other factors related to depositional history or in situ changes, must be taken into account in order to apply the model on a regional basis.

In light of the basic objective, which is to conduct a preliminary assessment of regional slope stability with the data available, the infinite-slope method is acceptable. However, the assumptions and limitations that go with it must be kept in mind when considering the results.

The factors of safety for static drained and undrained conditions are shown in table V. Drained conditions are traditionally assumed when instability develops over long time periods; that is, long enough to permit drainage of pore water from the plane where stresses are assumed to be concentrating (potential failure surface). Generally, this applies to conditions of moderate to slow rates of loading from sediment deposition, gradual oversteepening, and other analogous processes. Undrained conditions are assumed when instability arises over short time periods; that is, when shearing takes place too rapidly for drainage to occur, as is possible in instances of rapid undercutting or oversteepening, deltaic deposition, and dynamic loading. Rarely is drainage complete or nonexistent, so that the two types of factors of safety shown in table V represent end members for this general class of problem.

Assuming zero excess pore pressure, the slope and rise within the study area are apparently stable under static conditions. All factor of safety values are greater than one, and only four (<20% of total) have an F value less than two (PC40, PC44, PC52, PC53; table V). In each of these four, the F value was less than two in the undrained case only. For the undrained case, it is noteworthy that the widespread presence of apparently overconsolidated sediment skews the results toward higher factor of safety values because of its relatively high undrained shear strength. It is not known if the overconsolidation that is not associated with apparent erosional surfaces is representative of consolidation states farther down into the sediment column. If not, and those sediments are normally consolidated, the factors of safety would be reduced. In fact, approximately one-third of the sites would have factors of safety less than two and a few sites would be considered unstable.

Given the results of the static, no excess pore pressure case, it is instructive to consider how these results would be modified if other assumptions or conditions are imposed. Such modifications not only show the sensitivity of the factors of safety, but provide an avenue for evaluating the impact of geologic conditions or processes. Specifically, what would be the effects of dynamic loading? of excess pore pressure? of increased slope angles? of having less than peak stengths available?

Table V.

Mid-Atlantic static factors of safety

(infinite-slope model)

Core	Drained	Undrained
PC39	3.3	2.0
PC40	2.5	1.3
PC41	2.5	3.7
PC43	6.6	3.7
PC44	3.4	1.9
PC46	2.8	2.9
PC52	2.3	1.4
PC53	2.3	1.5
PC54	3.3	2.1
P14	6.4	4.5
P15	4.1	4.4
P16	4.2	3.6
P17	11.9	-
P18	8.4	7.5
P19	5.8	10.9
P20	2.2	3.6
P28	5.3	4.1
P31	3.6	5.1
P33	5.3	4.0
P34	5.8	6.9
P35	3.7	2.1
P36	7.8	4.8

Dynamic loading can occur through a variety of processes, but, inasmuch as the area of investigation is below wave base for major storms and data are lacking on internal wave forces, we have restricted our analysis to loading by earthquakes. Earthquakes may affect slope stability in two ways: by increasing shear stress through ground accelerations and by reducing shear resistance by elevating pore pressures. Only the former effect was considered in this analysis. Equations for evaluating the effects of ground accelerations have been published by Morgenstern (1967), Hampton and others (1977), and Sangrey and Marks (1981). In general, both drained and undrained stability equations may be streamlined by accounting only for horizontal accelerations (for discussion, see Booth and others, 1985b).

The results of the calculations are shown in table VI. An indication of the meaning of these results is provided by Seed and others (1975). They imply that accelerations from a 6.5 m_b earthquake would probably not exceed 5%g at a distance of 100 km from the energy source and would probably not exceed 10%g at a distance greater than 50 km from the source. Recent earthquake epicenter locations for the northeastern United States (including offshore locations) have been published by Yang and Aggarwal (1981). Some epicenters appear to be within or near 100 km of the study area, including sites near Hudson Canyon. Magnitudes determined thus far have been small, however (m_b ~3). Accordingly, only the sites of PC40, PC53, PC31A, and P35 (fig. 1) would seem somewhat vulnerable to the effects of a proximal earthquake, although several more sites would be vulnerable if quake magnitudes increased or if quakes occurred closer to the study area.

Dynamic loading, rapid deposition, artesian systems, and the presence of interstitial gas can all elevate pore pressures and, hence, reduce factors of safety. Table VI shows the excess pore-pressure values (expressed as percent of overburden pressure) that would be required to reduce static factors of safety to a value of one. Note that with the exception of a few cases (PC40, PC53), the pore pressures would have to support more than one-half of the sediment column before the effect would become important.

It is doubtful that excess pore pressures due to rapid deposition could approach the necessary values, except at the sites of PC40 and PC53, even at increased rates during lowered sea levels. For the two exceptions, deposition rates would have to have been 5 to 25 times greater before even thick sediment sections could develop the critical level of excess pore pressures; that is, from about 20 cm/1,000 y to 100-500 cm/1,000 y (based on Booth and others, 1985b). Thus, high sedimentation rates may be important locally as a cause of significant excess pore pressure, but it is unlikely that they have had an important effect regionally. Excess pore pressures due to groundwater flow would also seem incapable of causing the necessary increases on a regional basis as well. Salinity measurements made on this section of the continental margin during the USGS Atlantic Margin Drilling Project indicate a possible incursion of brackish water beneath the slope down to at least 300 m (Hathaway and others, 1979), and Robb and others (1981) present geomorphological evidence which suggests that piping or spring sapping may be occurring within a restricted area on the slope. Without additional evidence, it is assumed that any increase in pore pressure caused by an artesian system would probably be only local. Methane has been reported from direct measurements in the area (Hathaway and others, 1979) and has been tentatively identified in high-resolution seismic-reflection profiles (Hall and Ensminger, 1979). Any gas

Table VI.

Mid-Atlantic geologic conditions or changes required to bring core site to limit equilibrium (i.e., to reduce factor of safety to 1)

Core	Basic factors of safety		Ground acceleration required (%g)		Excess pore pressure required ($\%\sigma_{vo}$)		Change in slope angle (°)	
	F_d	F_u	d	u	d	u	d	u
PC39	3.3	2.0	13	22	69	79	17	-
PC40	2.5	1.3	12	3	59	32	14	5
PC41	2.5	3.7	14	25	58	73	15	-
PC43	6.6	3.7	20	20	85	84	25	-
PC44	3.4	1.9	17	26	70	80	19	-
PC46	2.8	2.9	14	13	63	65	15	23
PC52	2.3	1.4	12	11	54	53	15	21
PC53	2.3	1.5	9	2	55	26	12	4
PC54	3.3	2.1	10	10	69	69	15	18
P14	6.4	4.5	14	9	84	78	19	15
P15	4.1	4.4	11	12	76	77	16	24
P16	4.2	3.6	11	9	76	72	16	16
P17	11.9	-	17	-	92	-	28	-
P18	8.4	7.5	16	14	88	87	23	27
P19	5.8	10.9	9	19	83	91	13	-
P20	2.2	3.6	13	29	51	73	17	-
P28	5.3	4.1	17	12	81	76	23	23
P31A	3.6	5.1	6	9	72	80	9	16
P33	5.3	4.0	16	11	81	75	23	21
P34	5.8	6.9	8	10	83	85	12	16
P35	3.7	2.1	9	4	73	52	14	6
P36	7.8	4.8	19	10	87	78	27	19

F_d = Static factor of safety - drained case
F_u = Static factor of safety - undrained case
g = Gravity
σ_{vo} = Overburden stress

may increase pore pressures to the levels required to cause slope instability ($F \leq 1$) (table VI) if present in high enough concentrations. Based on seismic records, the distribution of gassified sediment is not widespread and appears to be confined to the upper slope. Finally, an occasional seismic event in the general area may also increase pore pressure, although, applying the results of a study published by Egan and Sangrey (1978), the generated excess pore pressures would probably not reach the general level required to cause instability. However, the increased shear stress (due to ground accelerations) and excess pore pressure which result from earthquakes may be a potent combination for decreasing slope stability, if magnitude, distance, and duration criteria are met.

Increased slope angles would also reduce factors of safety. Table VI shows that, in general, slope angles in the study area must be generally increased 15°-20°, although some sites (e.g., PC40, PC53, P35) would only require a small amount of additional declivity to reach limit equilibrium. Depositional oversteepening, undercutting, and tilting (in response to general tectonic or diapiric activity) may cause such a change. Keller and Shepard (1976) have investigated currents on the Continental Slope to the southwest of the study area and concluded that the velocities at the measurement site were below the threshold for grain movement. Southard and Cacchione (1972) have implied that internal waves, if present, may be capable of eroding (undercutting?) at a fairly well-defined depth over a broad region. Direct measurements of either erosional mechanism are lacking in the study area, however.

Depositional oversteepening and undercutting may be more important as local processes. The former may have occurred at the shelf edge during lowstands of the sea, but evidence of this is limited. The latter may be occurring within submarine canyons. Neither would appear to be of regional importance. Tilting through regional tectonic activity or diapirism, if occurring, has yet to produce the slope angles necessary for regional instability.

The effect of reduced strength on the factors of safety is a final point in this discussion. Static factors of safety (table VI) were computed assuming that peak strengths were available. However, the strength may be altered through strain-softening or as a result of past slope failures. Elastic rebound, dynamic loading, or creep, for example, can reduce the appropriate strength properties considerably, as implied by the sensitivities; that is, the remolded strength averages 1/5 the peak stength in these sediments. Further, jointing, which can result in the development of weak planes, can develop during elastic rebound of overconsolidated sediments. And residual friction angles, which are often manifest along failure planes, are frequently 10°-20° less than the initial friction angle for sediments of the plasticity reported here (Mitchell, 1976). What percentage of the region, if any, is appropriate for this "reduced strength" stability analysis is unknown, although possible slab-type failures have been observed. Intuitively, however, we believe that this type of analysis may be more appropriate for local areas proximal to or within canyons because of the complex morphologies, the often steeper slope angles, and the more complicated stress histories they probably represent compared to general regional conditions.

and subsequent development of weak planes or joints may also be occurring at some sites. Any of these processes or conditions mentioned may have contributed to past slope failures, particularly on a local scale. In fact, it appears that most processes or agents which may cause instability in this geologic setting have the potential to be more important locally than regionally. More focused and detailed research will be needed before the relative efficiency or future effects of the different possible causes may be evaluated because relative magnitudes, frequencies, and extents of these mechanisms have not yet been fully documented or quantified.

REFERENCES

Almagor, G. and Wiseman, G., 1977, Analysis of submarine slumping in the Continental Slope off the southern coast of Israel: Marine Geotechnology, v. 2, p. 349-388

American Society for Testing and Materials, 1982, Annual book of ASTM standards, part 19, Natural building stones; soil and rock; peats, mosses, and humis: Philadelphia, ASTM, p. 494.

Bishop, A. W., and Henkel, D. J., 1957, The measurement of soil properties in the triaxial test: London, Edward Arnold, 225 p.

Booth, J. S., 1979, Recent history of mass wasting on the upper Continental Slope, northern Gulf of Mexico as interpreted from the consolidation states of the sediment, in Pilkey, O. H., and Doyle, L. J., eds., Geology of continental slopes: Society of Economic Paleontologists and Mineralogists Special Publication no. 27, p. 153-164.

Booth, J. S., Circé, R. C., and Dahl, A. G., 1985, Geotechnical characterization and mass movement potential of the United States North Atlantic Continental Slope and Rise: U. S. Geological Survey Open-File Report 85-123, 69 p.

Booth, J. S., Farrow, R. A., and Rice, T. L., 1981a, Geotechnical properties and slope stability analysis of surficial sediments on the Baltimore Canyon Continental Slope: U. S. Geological Survey Open-File Report 81-733, 255 p.

Booth, J. S., Marks, D. L., O'Leary, D. W., and Robb, J. M., 1981b, The possible role of mass movement in the development of submarine canyon systems on the U.S. east coast Continental Slope (abs.): Geological Society of America, Abstracts with Programs, p. 413.

Booth, J. S., Robb, J. M., Aaron J. M., and Farrow, R. A., 1981c, Past and potential mass movement on the Continental Slope off the northeastern United States (abs.): American Association of Petroleum Geologists, Book of Abstracts (unnumbered).

Booth, J. S., and Sangrey D. A., 1979, Mass movement potential of recent sediments on U.S. Continental Margins (abs.): American Association of Petroleum Geologists, Book of Abstracts (unnumbered).

Booth, J. S., Sangrey, D. A., and Fugate, J. K., 1985b, A nomogram for interpreting slope stability in modern and ancient marine environments: Journal of Sedimentary Petrology (in press).

Casagrande, A., 1936, The determination of the preconsolidation load and its practical significance: Proceedings, 1st, International Conference on Soil Mechanics and Foundation Engineering, p. 60.

Casagrande, A., 1948, Classification and identification of soils: American Society of Civil Engineers Transactions, v. 113, p. 901-991.

Doyle, L. J., Pilkey, O. H., and Woo, C. C., 1979, Sedimentation on the eastern United States Continental Slope, in Doyle, L. J. and Pilkey, O. H., eds., Geology of the continental slopes: Society of Economic Paleontologists and Mineralogists Special Publication no. 27, p. 119-129.

Egan, J. A., and Sangrey, D. A., 1978, Critical state model of cyclic load pore pressures: American Society of Civil Engineers Special Conference on Earthquake Engineering and Soil Dynamics, v. 1, p. 410-424.

Embley, R. W., and Jacobi, R. D., 1977, Distribution and morphology of large sediment slides and slumps on Atlantic continental margins: Marine Geotechnology, v. 2, p. 205-228.

Emery, K. O., and Uchupi, E., 1972, Western North Atlantic Ocean: topography, rocks, structure, water, life, and sediments: American Association Petroleum Geologists Memoir 17, 532 p.

Hall, R. W., and Ensminger, H. R., eds., 1979, Potential geologic hazards and constraints for blocks in proposed Mid-Atlantic Oil and Gas Lease Sale 49: U.S. Geological Survey Open-File Report 79-264, 189 p.

Hampton, M. A., Bouma, A. H., Carlson, P. R., Molnia B. F., Clukey, E. C., and Sangrey, D. A., 1978, Quantitative study of slope instability in the Gulf of Alaska: Proceedings, Offshore Technology Conference, 10th, Houston, Texas OTC #3314, p. 2307-2318.

Hansbo, S., 1957, A new approach to the determination of the shear strength of clay by the fall-core test: Proceedings, Swedish Geotechnical Institute, Stockholm, no. 14, p. 7-47.

Hathaway, J. C., Poag, C. W., Valentine, P. C., Miller, R. E., Schultz, D. M., Manheim, F. T., Kohout, F. A., Bothner, M. H., and Sangrey, D. W., 1979, U.S. Geological Survey core drilling on the Atlantic Shelf: Science, v. 206, p. 514-527.

Keer, F. J., and Cardinell, A. P., 1981, Potential geologic hazards and constraints for blocks in proposed Mid-Atlantic OCS Oil and Gas Lease Sale 59: U.S. Geological Survey Open-File Report 81-725, 109 p.

Keller, G. H., Lambert, D. N., and Bennett, R. H., 1979, Geotechnical properties of continental slope sediments-Cape Hatteras to Hydrographer Canyon, in Doyle, L. J., and Pilkey, O. H., eds., Geology of the continental slopes: Society of Economic Paleontologists and Mineralogists Special Publication no. 27, p. 131-151.

Keller, G. H., and Shepard, F. P., 1978, Currents and sedimentary processes in submarine canyons off the northeastern United States, in Stanley, D. J., and Kelling, G., eds., Sedimentation in submarine canyons, fans, amd trenches: Stroudsburg, Penn., Dowden, Hutchinson and Ross, p. 15-32.

Kenney, T. C., 1959, Discussion: Journal of Soil Mechanics and Foundations Division, American Society of Civil Engineers, v. 85, no. SM3, p. 67-79.

Knebel, H. J., and Carson, B., 1979, Small-scale slump deposits, Middle Atlantic Continental Slope, off Eastern United States: Marine Geology, v. 29, p. 221-236.

Ladd, C. C., Foott, R., Ishihara, K., and Schlosser, F., 1977, Stress-deformation and strength characteristics: Proceedings, International Conference on Soil Mechanics and Foundation Engineering, 9th, Tokyo, p. 421-494.

Lambe, T. W., and Whitman, R. V., 1969, Soil mechanics: New York, John Wiley, 553 p.

Lambert, D. N., Bennett, R. H., Sawyer, W. B., and Keller, G. H., 1981, Geotechnical properties of continental upper rise sediments-Veatch Canyon to Cape Hatteras: Marine Geotechnology, v. 4, p. 281-306.

Malahoff, A., Embley, R. W., Perry, R. B., and Fefe, C., 1980, Submarine mass-wasting of sediments on the continental slope and upper rise south of Baltimore Canyon: Earth and Planetary Science Letters, v. 49, p. 1-7.

Manheim, F. T., and Hall, R. E., 1976, Deep evaporitic strata off New York and New Jersey-evidence from interstitial water chemistry of drill holes: Journal of Research of the U.S. Geological Survey, v. 4, p. 697-702.

McClelland, B., 1967, Progress of consolidation in delta front and prodelta clays of the Mississippi River, in Richards, A. F., ed., Marine geotechnique: Urbana, Ill., University of Illinois Press, p. 22-40.

McGregor, B. A., 1977, Geophysical assessment of submarine slide northeast of Wilmington Canyon: Marine Geotechnology, v. 2, p. 229-244.

McGregor, B. A., Bennett, R. H., and Lambert, D. N., 1979, Bottom processes, morphology, and geotechnical properties of the continental slope south of Baltimore Canyon: Applied Ocean Research, v. 1, p. 177-187.

Mitchell, J. K., 1976, Fundamentals of soil behavior: New York, John Wiley, 422 p.

Morgenstern, N. R., 1967, Submarine slumping and the initiation of turbidity currents, in Richards, A. F., ed., Marine Geotechnique: Urbana, Ill., University of Illinois Press, p. 189-220.

Morgenstern, N. R., and Sangrey, D. A., 1978, Methods of stability analysis, in Landslides: Analysis and control: Washington, D. C., Transportation Research Board, National Research Council, p. 155-171.

Nacci, V. A., Kelly, W. E., Wang, M. C., and Demars, K. R., 1974, Strength and stress-strain characteristics of cemented deep-sea sediments, in Inderbitzen, A. L., ed., Deep-sea sediments: Physical and mechanical properties: New York, Plenum Press, p. 129-150.

Olsen, H. W., McGregor, B. A., Booth, J. S., Cardinell, A. P., and Rice T. L., 1982, Stability of near-surface sediment on the Mid-Atlantic upper Continental Slope: Proceedings, Offshore Technology Conference, 14th, Houston, Tex., p. 21-35.

Olsen, H. W., and Rice, T. L., 1982, Geotechnical profiles for thirty-one sites on the mid-Atlantic upper Continental Slope: U. S. Geological Survey Open-File Report 82-841, 147 p.

Poag, C. W., 1980, Foraminiferal stratigraphy, paleoenvironments, depositional cycles in the outer Baltimore Canyon Trough, in Scholle, P. A., ed., Geologic studies of the COST No. B-3 well, United States Mid-Atlantic Continental Slope area: U.S. Geological Survey Circular 833, p. 44-66.

Robb, J. M., 1984, Spring sapping on the lower continental slope offshore New Jersey: Geology, v. 12, p. 278-282.

Robb, J. M., Hampson, J. C., Jr., Kirby, J. R., and Twichell, D. C., 1981, Geology and potential hazards of the Continental Slope between Lindenkohl and South Toms Canyons, offshore Mid-Atlantic United States: U.S. Geological Survey Open-File Report 81-600, 33 p.

Rosenqvist, I. Th., 1953, Considerations on the sensitivity of Norwegian quick clays: Geotechnique, v. 3, p. 195-200.

Sangrey, D. A., and Marks, D. L., 1981, Hindcasting evaluation of slope stability in the Baltimore Canyon Trough Area: Proceedings, Offshore Technology Conference, 13th, Houston, Tex., p. 241-252.

Seed, H. B., Murarka, R., Lysmer, J., and Idriss, I. M., 1975, Relationships between maximum acceleration, maximum velocity, distance from source and local site conditions for moderately strong earthquakes: University of California, Berkeley, Earthquake Engineering Research Center Report No. 75-17, 23 p.

Silva, A. J., and Hollister, C. D., 1979, Geotechnical properties of ocean sediments recovered with the giant piston core: Blake-Bahama Outer Ridge: Marine Geology, v. 29, p. 1-22.

Skempton, A. W., 1954, Discussion of the structure of inorganic soil: Journal of Soil Mechanics and Foundation Division, Proceedings, ASCE, v. 80, Report No. 478, p. 19-22.

Southard, J. B., and Cacchione, D. A., 1972, Experiments on bottom sediment movement by breaking internal waves, in Swift, D. J. P., Duane, D. B., and Pilkey, O. H., eds., Shelf sediment transport: Stroudsburg, Penn., Dowden, Hutchinson and Ross, p. 83-98.

Sykes, L. E., 1978, Intraplate seismicity, reactivation of preexisting zones of weakness, alkaline magmatism, and other tectonism postdating continental fragmentation: Reviews of Geophysics and Space Physics, v. 16, p. 621-688.

Terzaghi, K., and Peck, R. B., 1967, Soil mechanics in engineering practice: New York, John Wiley, 729 p.

Valentine, P. C., Uzmann, J. R., and Cooper, R. A., 1980, Geology and biology of Oceanographer Submarine Canyon: Marine Geology, v. 38, p. 283-312.

Wagner, A. A., 1957, The use of the Unified Soil Classification System by the Bureau of Reclamation: International Conference of Soil Mechanics and Foundation Engineering, 4th, London, v. 1, p. 125.

Wissa, A. E. Z., Christian, J. T., Davis, E. H., and Heiberg, S., 1971, Consolidation at constant rate of strain: Journal of Soil Mechanics and Foundation Division, ASCE, v. 97, SM 10, Proceedings Paper 8447, p. 1393-1413.

Yang, J., and Aggarwal, Y. P., 1981, Seismotectonics of northeastern United States and adjacent Canada: Journal of Geophysical Research, v. 86, no. B6, p. 4981-4998.